NESTLER

NESTLER
oNe hEalth SusTainabiLity partnership between
EU-AFRICA for food sEcuRity

Deliverable D3.2

NESTLER implementation of data aggregation protocols and AI algorithms

Authors	Th. Zahariadis, S. Bourou, N. Arvanitis, P. Athanasoulis, G. Pantelide, N. Polushkina, D. Kolev, T. Odedeyi, A. Sarelli, I.Darwazeh, A. Nchange Kouotou
Nature	Report
Dissemination	PUBLIC
Version	V1.0
Status	Final
Delivery Date (DoA)	M36
Actual Delivery Date	21/10/2025

Keywords	IoT Sensors, Remote Sensing, Multi-modal, Satellite, Drone, Environmental Monitoring, Crop Farming/Livestock/Aquaculture Monitoring, Pest Infestation
Abstract	The document explores AI applications in agriculture and environmental monitoring with the focus on precision agriculture, leveraging UAVs and remote sensing to assess crop health through vegetation indices for early pest and stress detection. It examines AI systems for animal health, including DAHMS for domestic animals using optical flow, behavior, and audio analysis, and WAMS for wild animals, detecting predator threats. It describes AI in fish health monitoring using underwater cameras and metrics to detect stress or disease. It addresses pest management in crops like cocoa and maize, using UAVs and deep learning models for real-time pest detection via mobile apps. It highlights connectivity solutions in remote agriculture, such as UAV-based mesh networks and advanced communication protocols for real-time decision-making. It focuses on satellite data insights, including crop yield estimation and meteorological integration for land monitoring.

DISCLAIMER

	Participant organisation name	***Short***	***Country***
01	SYNELIXIS SOLUTIONS S.A.	SYN	EL
02	CloudEO AG (Terminated)	CEO	DE
03	RINIGARD DOO ZA USLUGE	RINI	HR
04	EBOS TECHNOLOGIES LIMITED	eBOS	CY
05	STICHTING IDH SUSTAINABLE TRADE INITIATIVE	IDH	NL
06	ZANASI ALESSANDRO SRL	Z&P	IT
07	AGRIX TECH SARL	AGRI	CM
08	CONSERVATION THROUGH PUBLIC HEALTH	CTPH	UG
09	THE INTERNATIONAL CENTRE OF INSECT PHYSIOLOGY AND ECOLOGY LBG	ICIPE	KE
10	ETHIOPIAN INSTITUTE OF AGRICULTURAL RESEARCH	EIAR	ET
11	RWANDA AGRICULTURE AND ANIMAL RESOURCES DEVELOPMENT BOARD	RAB	RW
12	INTERNATIONAL INSTITUTE OF TROPICAL AGRICULTURE	IITA	NG
13	MANA BIOSYSTEMS LIMITED	MANA	UK
14	UNIVERSITY COLLEGE LONDON	UCL	UK
15	RINISOFT LTD	RINIS	BG
16	ADAPT IT GMBH	ADA	DE

ACKNOWLEDGEMENT

This document is a deliverable of the NESTLER project. This project has received funding from the European Union's Horizon Research and innovation programme under grant agreement № 101060762. Views and opinions expressed are however those of the author(s) only and do not necessarily reflect those of the European Union or the European Research Executive Agency, while neither the European Union nor the granting authority can be held responsible for any use that may be made of the information it contains.

Document History

Version	Date	Contributor(s)	Description
V0.1	30/10/2024	RINIS	ToC
V0.2	13/11/2024	RINIS	Updated ToC
V0.3	06/12/2024	RINIS, SYN, CEO	First Contributions
V0.4	10/01/2025	RINIS, SYN, AGRI, EBOS, UCL	Second Contributions
V0.5	14/01/2025	RINIS, SYN, AGRI, EBOS, UCL	Review and Update
V0.6	08/08/2025	RINIS	Updated ToC
V0.7	08/10/2025	RINIS	Version completed
V0.8	15/10/2025	RINIS, SYN	Update after review comments ● Section 6 has been updated
V0.9	19/10/2025	RINIS, SYN,UCL	Final Review
V1.0	20/10/2025	RINIS	Final version ready for submission

Document Reviewers

Date	Reviewer's name	Affiliation
16/01/2025	Nikos Arvanitis	SYN
16/01/2025	Temitope Odedeyi	UCL
13/10/2025	Nikos Arvanitis	SYN
13/10/2025	Temitope Odedeyi	UCL
20/10/2025	Nikos Arvanitis	SYN
20/10/2025	Temitope Odedeyi	UCL

Table of Content

Definitions, Acronyms and Abbreviations

ADDF	Average Diving Depth of Fish
ADS	Anomaly Detection Service
AI	Artificial Intelligence
ANN	Artificial Neural Network
CIG	Chlorophyll Index Green Channel
CIR	Chlorophyll Index Red Edge Channel
CLMS	Copernicus Land Monitoring Service
CNN	Convolutional Neural Networks
DAHMS	Domestic Animal Health Monitoring system
Deep SORT	Simple Online and Real-time Tracking
FAPAR	Fraction of Absorbed Photosynthetically Active Radiation
FFDS	Fish Farm Dataset
GDPR	EU General Data Protection Regulation no. 2016/679
GIBS	Global Imagery Browse Services
GNDVI	Green Normalized Difference Vegetation Index
HAAT	Hen Automated Annotation Tool
IoT	Internet of Things
KNN	k-Nearest Neighbours Algorithm
LST	Land Surface Temperature
MOT	Multiple Object Tracking
NDRE	Normalized Difference Red Edge Index
NDVI	Normalized Difference Vegetation Index
PM	Project Manager
PMT	Project Management Team
RSHF	Reference Speed of Healthy Fish
ROI	Regions Of Interest
TL	Task Leader
TM	Technical Manager

UAV	Unmanned Aerial Vehicle
VI	Vegetation Indices
WAMS	Wild Animal Monitoring System
WP	Work Package
WPL	Work Package Lead
YOLO	You Only Look Once

List of Figures

List of Tables

Executive Summary

This document consists of the Deliverable "D3.2: NESTLER implementation of data aggregation protocols and AI algorithms of the European Horizon Europe project "NESTLER: oNe hEalth SusTainabiLity partnership between EU-AFRICA for food sEcuRity".

Deliverable D3.2 focuses on implementing data aggregation protocols and AI algorithms across four subsystems - crop monitoring, animal health monitoring, aquaculture monitoring, and pest detection.

D3.2 offers a detailed exploration of:

1. Animal Health Monitoring: Development of AI systems (DAHMS and WAMS) to monitor health and detect threats in domestic and wild animals.
2. Aquaculture Monitoring: Use of underwater cameras and AI for fish health analysis, focusing on key metrics like Reference Speed of Healthy Fish (RSHF) and Average Diving Depth of Fish (ADDF).
3. Pest Detection: Implementation of UAV-based remote sensing and deep learning models for real-time pest identification in crops like cocoa, mango, maize, and coffee.
4. Last-Mile Connectivity: Innovative solutions for real-time data transmission using UAV-based mesh networks and advanced communication protocols.
5. Utilization of IoT devices, UAVs, and AI to optimize crop yield and identify early pest infestations using vegetation indices like NDVI and NDRE.
6. Deployment of IoT sensors and advanced AI algorithms for data-driven decision-making.
7. Integration of satellite imagery and GIS data for crop yield predictions and environmental monitoring.
8. Use of machine learning models like YOLO and CNN for animal and pest behaviour analysis.
9. Addressing connectivity issues in remote areas using mesh-in-the-sky technology.
10. Developing cost-effective and scalable AI solutions adaptable to diverse agricultural environments.

The objective of this deliverable is to analyse various IoT sensors and devices employed in environmental and crop farming monitoring, including those used for measuring crop quality. Additionally, it defines the parameters, devices, and techniques utilized in livestock and aquaculture monitoring. Furthermore, it presents the remote sensing solutions, which are satellite and drone imagery, used in the NESTLER project, along with the methods and techniques for extracting information from these sources.

1. Introduction

The successful integration of a subsystem into the NESTLER platform is evaluated based on the accuracy, completeness, and relevance of the data transferred from the subsystem to the platform. These key parameters directly influence the selection and configuration of the data exchange protocols. Such protocols must encompass aggregated data from all sensors, information sources, and analytical systems. The information consolidated on the platform should be comprehensive enough to support decision-making processes and facilitate user notifications in an intuitive format.

The selection and design of these data exchange protocols are determined by the type of data collected from sensors and the algorithms used to analyse that data. In this context, protocols refer not to traditional network-level communication protocols, but to logical data integration protocols that standardize and formalize information from disparate sources into a unified, interoperable format. This approach ensures the scalability of the solution, making it adaptable for farms of any size or complexity.

In the NESTLER project, the primary information sources are grouped into the following subsystems:

- Agriculture monitoring subsystem
- Domestic and wild animals monitoring subsystem
- Aquaculture monitoring subsystem
- Insect monitoring subsystem

The current challenges include the inability to consistently monitor the health of animals and the large-scale detection of insect swarms, both of which represent significant risks to agriculture and livestock. The NESTLER system addresses these challenges by integrating IoT devices, AI-driven analytics, and cloud computing, providing a comprehensive, real-time monitoring solution capable of addressing gaps in existing systems.

1.1. NESTLER Subsystems Overview

1.1.1. Crop Monitoring Subsystem

The Crop Monitoring Subsystem is an integral part of the NESTLER project, designed to leverage cutting-edge technology for sustainable agricultural practices. This subsystem focuses on the deployment and utilisation of Internet of Things (IoT) devices to measure and collect critical environmental data. These devices monitor both soil and atmospheric conditions, capturing parameters such as temperature, humidity and soil moisture. The primary objective is to create data-driven models that optimise crop yield and growth conditions by identifying environmental variables that significantly influence productivity. By integrating this information, the subsystem enables precision agriculture practices, reducing resource wastage and improving sustainability.

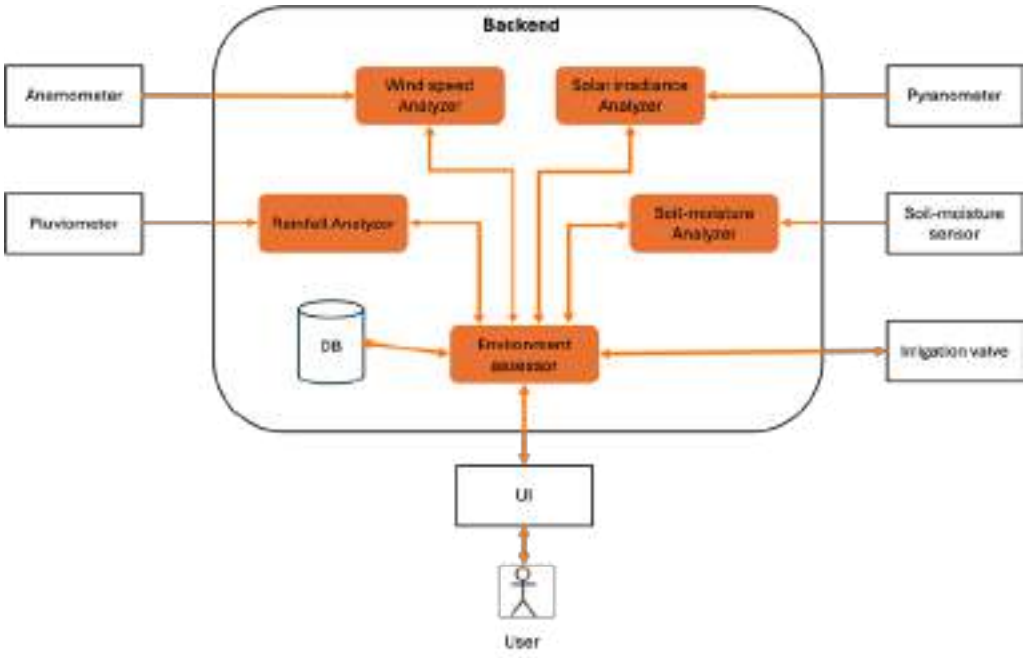

Figure 1: Crop monitoring subsystem layers diagram

1.1.2. Crop Quality Measuring Subsystem

The crop quality subsystem centres on the design and validation of a handheld device developed to measure postharvest crop quality, with an initial focus on cassava — a tropical root crop of high nutritional, industrial, and commercial significance in sub-Saharan Africa. The device provides a rapid, non-destructive, low-cost, and user-friendly method for assessing crop quality directly in the field. By generating real-time insights, it empowers farmers, industrial processors, and plant breeding researchers to make informed decisions on the most suitable uses of harvested crops, as well as appropriate sales channels. This capability also targets the reduction of postharvest losses by improving logistical coordination between producers and buyers.

The handheld device is equipped with Bluetooth Low-Energy (BLE) modules, enabling seamless data transfer to mobile phones used by stakeholders engaged in the pilot phase. Each measurement includes crop quality data alongside contextual metadata (e.g., geolocation, timestamp, user ID, device ID). Once within range of local mobile network coverage, the mobile application automatically synchronises the stored data with the NESTLER cloud database. This design choice avoids the need for dedicated or specialised connectivity infrastructure, thereby enhancing both the scalability and commercial viability of the subsystem.

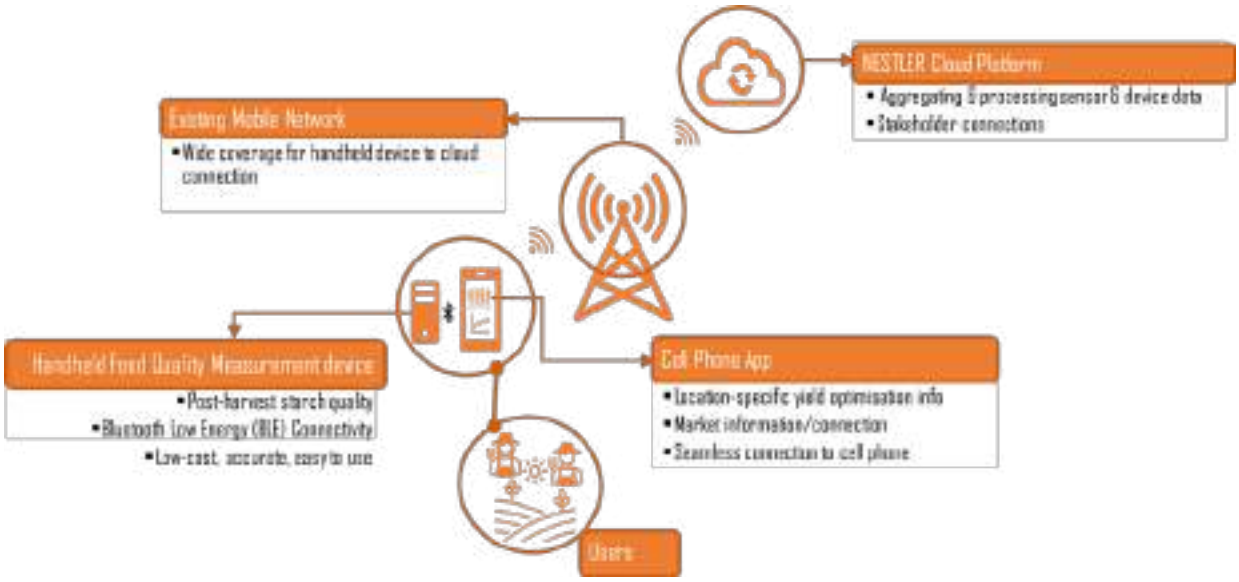

Figure 2: Overview of the crop quality measurement subsystem, illustrating its core functions and integration pathway from handheld device users to the NESTLER platform

Figure 3: Prototype crop quality measurement device featuring an OLED display and a 5-LED traffic-light indicator system for intuitive visual reporting of crop quality

The accompanying mobile application manages the retrieval, visualisation, and archiving of data from the handheld device before securely uploading it to the NESTLER platform. Through this mechanism,

the crop quality subsystem integrates seamlessly into the wider NESTLER ecosystem, leveraging readily available mobile networks to ensure accessibility, interoperability, and impact across diverse agricultural contexts. The crop quality measurement device connects wirelessly to a mobile application via Bluetooth, enabling seamless data transfer, real-time visualisation of results, and integration with broader digital platforms for analysis and decision support.

Figure 4: The crop quality measurement device

1.1.3. Animal Health Monitoring Subsystem

The Poultry Health Monitoring System and Wildlife Monitoring System use AI and IoT devices to monitor animal health and behaviour. By analysing visual and audio data, these systems detect abnormalities, assess risks, and provide actionable insights for proactive flock management and wildlife threat assessment.

1.1.3.1. Poultry Health Monitoring System

The following paragraphs describe the key components of the NESTLER poultry health monitoring system.

The Poultry Health Monitoring System uses multimedia data and AI to detect early signs of diseases in poultry flocks. By focusing on visual and acoustic parameters, the system identifies abnormalities in chickens' behaviour and physical appearance. Iota devices such as cameras and microphones capture essential data for analysis. This enables proactive health monitoring, ensuring timely intervention and optimal flock management.

System Layers: The system is organized into three key layers - Data Collection, Data Analysis, and Decision-Making as shown in Figure 5. The Data Collection Layer gathers visual and audio data using IoT

devices like cameras and microphones. The Data Analysis Layer processes the data using AI modules, including behaviour, appearance, and vocalization analysers. Finally, the Decision-Making Layer applies analytics to generate actionable insights, enabling health predictions for the poultry flock.

Monitoring Parameters: Monitoring focuses on two primary data types - visual and audio. Visual data involves tracking individual chickens for behavioural patterns, physical markers, and anomalies such as posture or feather condition. Audio data assesses vocalizations to identify stress or health issues, though challenges like noise interference exist. Together, these parameters provide a comprehensive understanding of flock health and behaviour.

NESTLER Project Key Metrics: The NESTLER project defines critical metrics to monitor poultry health at both the flock and individual levels. Key parameters include flock movement consistency, measured through optical flow analysis, and individual behaviours such as feeding, sleeping, and posture changes. Vocalization analysis is also performed to detect anomalies in sound frequencies and patterns. These combined metrics enable the system to assess overall flock health effectively.

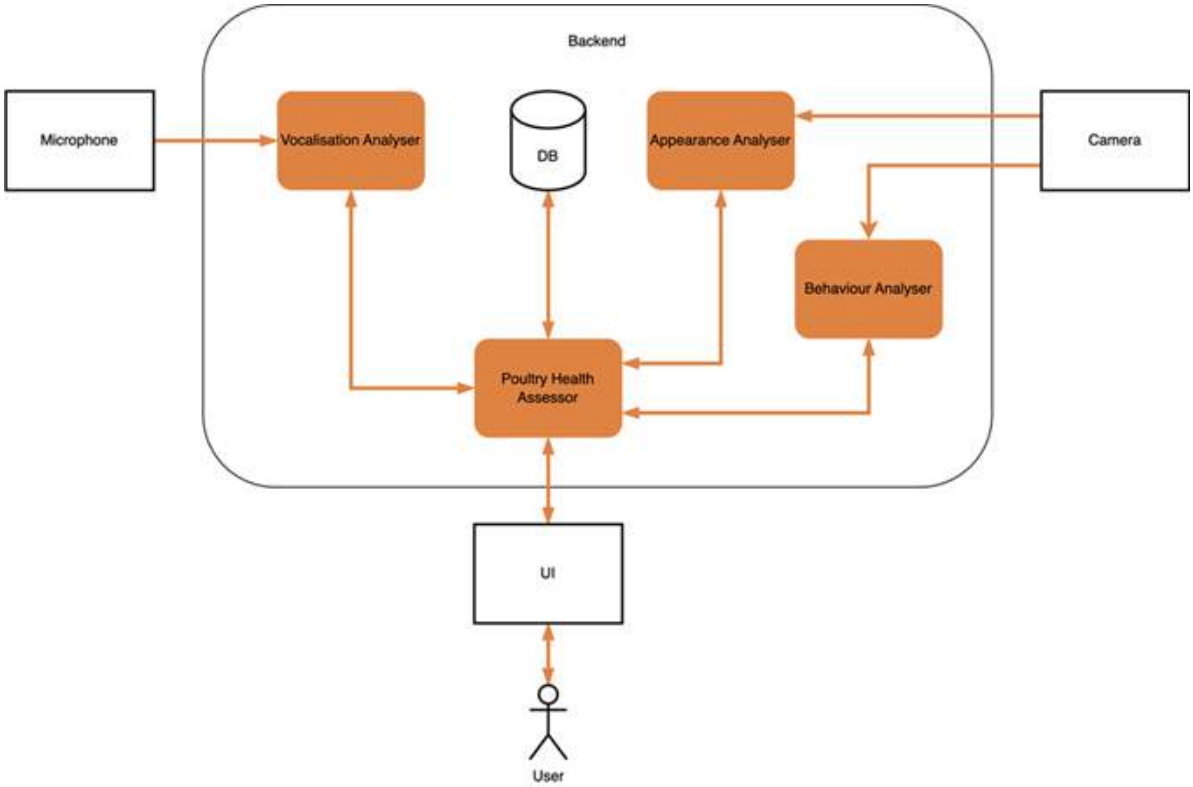

Figure 5: Poultry Health Monitoring System layers diagram

Sensors and Hardware: Reliable sensors and computing hardware are vital for continuous health monitoring. High-resolution Hikvision IP cameras with built-in microphones capture visual and audio data, while a RiniSoft server processes and analyses the collected information. The hardware is selected for cost-effectiveness, durability, and 24/7 operation. Together, these components ensure robust, real-time health assessments.

Behaviour Analysis: This focuses on identifying flock-wide and individual activity patterns using computer vision methods. YOLO models detect chickens in video frames and classify their actions, while optical flow maps flock movement and highlights anomalies. Day and night activity comparisons help identify over activity, underfeeding, or abnormal patterns. This method provides insights into flock health without tracking every individual bird.

Appearance Analysis: Appearance analysis examines chickens' physical features to detect signs of illness. Using the DINO v2 self-supervised model, visual features are extracted from video streams to identify anomalies. While labelled datasets for diseased chickens are limited, unsupervised methods help pinpoint abnormalities. This approach allows for the detection of subtle physical changes indicative of health issues.

1.1.3.2. Wildlife Monitoring System

The Wildlife Monitoring System is designed to detect and classify various types of wildlife to assess potential risks they may pose to domestic animals. The system can identify wildlife both in the air and on the ground and classifies them as either dangerous or safe. The hazard assessment process considers multiple factors. While some wild animals, such as antelopes or vultures, may not directly threaten livestock, they can serve as carriers of contagious diseases and parasites. If the system detects persistent routes or locations where such wildlife congregates or travel, those areas can be flagged as potentially hazardous to livestock.

System Layers: The system is structured into three key layers - Data Collection, Data Analysis, and Decision-Making. The Data Collection Layer gathers visual and audio data through Iota devices, such as cameras and microphones. The Data Analysis Layer processes the collected data using AI modules, including behaviour analysers, appearance analysers, and vocalization analysers.

Monitoring Parameters: These are the vector of movement direction, measure of movement, and points of attraction of objects. Secondary parameters consist of the approximate size, type of movement, and the presence of specific features.

NESTLER Project Key Metrics: Key parameters include movement consistency, measured through optical flow analysis, and frequency of detection in different times of the day for various animal classes. These combined metrics enable the system to assess the most vulnerable parts of the farm and allow for prompt counter-action from the farmers.

Sensors and Hardware: The same cameras used to monitor domestic animals are also employed for wildlife monitoring. This unification significantly reduces both implementation and operational costs.

Detection and Classification Analysis: The cameras used in the project facilitate surveillance across two environments: air and ground. Due to the near-opacity of water in rivers and lakes, the water surface is treated as equivalent to the ground surface. The algorithms for detecting objects on the water surface are identical to those used for ground-based object detection.

In the air environment, the system detects and classifies only birds. Classification is based on identifying specific movement trajectories and analysing wing motion patterns.

For the ground surface, the detection and classification of animals involve identifying moving objects and comparing them to skeletal models on which the neural network has been trained. This method effectively filters out non-fauna elements, such as moving grass, branches, or other irrelevant objects within the scene.

Once objects are detected and recognized, their movement trajectories within the sensor's field of view are analysed. Based on these trajectories, as well as the speed of movement, approximate size, and specific features of the objects, a decision is made regarding the level of threat to livestock.

1.1.4. Aquaculture Monitoring Subsystem

The Aquaculture Monitoring System (AMS) is designed to ensure the health and well-being of fish populations by analysing multimedia data. It operates through three key layers: data collection, analysis, and decision-making. Underwater cameras are used to capture fish movement and behaviour, while AI algorithms analyse the data to detect health anomalies. The system enables proactive health monitoring, ensuring early intervention and sustainable aquaculture management.

System Layers: The system comprises specialized modules for analysing fish behaviour and health. The Behaviour Analyser examines flock-wide mobility using optical flow, while the Appearance Analyser assesses individual fish health markers. The Fish Health Assessor Module integrates and interprets data to predict overall flock health. AI methodologies, including statistical models, CNNs, and Deep SORT, are applied for fish detection, tracking, and anomaly detection, ensuring precise and reliable results.

Monitoring Parameters: Effective monitoring of fish health relies on video-based analysis of key parameters. These include object detection to track fish behaviour, linear dimensions for growth monitoring, and location tracking to map spatial movements. Additionally, water transparency is assessed to evaluate environmental quality. Computable parameters such as average speed and trajectory tracking help identify changes in behaviour, offering insights into the flock's overall health and detecting early stress indicators.

IoT Sensors and Devices: The aquaculture monitoring system utilizes non-invasive sensors adapted to the aquatic environment. Unlike poultry systems, audio sensors are excluded, focusing solely on video-based monitoring. High-resolution cameras are employed to track fish movement and analyse behaviour in real-time. Data processing is conducted on robust computing hardware, ensuring reliable and efficient system performance. This setup is cost-effective, durable, and suitable for continuous operation in fish farms.

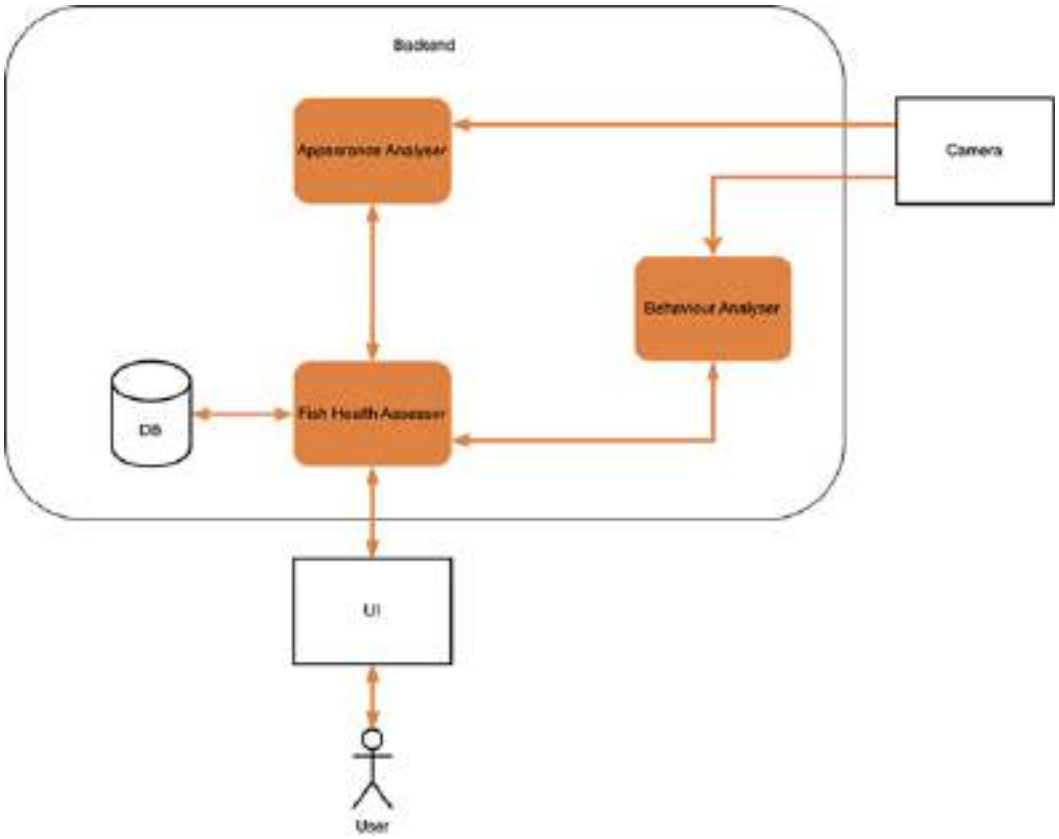

Figure 6: Aquaculture Monitoring Subsystem layers diagram

NESTLER Project Key Metrics: The fish monitoring system focuses on two critical health parameters: Reference Speed of Healthy Fish (RSHF) and Average Diving Depth of Fish (ADDF). RSHF measures the swimming speed of healthy fish, helping detect stress, infections, or parasites when speeds decrease. ADDF monitors diving depth, identifying gastrointestinal issues through abnormal swimming patterns. By continuously analysing these parameters, the system enables early detection of health issues, ensuring timely intervention and improved fish welfare.

Fish Farm Dataset (FFDS): Developing a robust AI model for aquaculture requires high-quality video datasets tailored to specific fish species. Data is collected for three age groups - fry, juveniles, and adults-with each population containing 60-100 fish of similar age. The dataset focuses on visual analysis within the constraints of water transparency. Guided by the Central Limit Theorem, sufficient data ensures reliable AI training and accurate health predictions for fish flocks.

1.1.5. Pest Detection and Classification Subsystem

The Pest Detection and Classification Subsystem is a component of the NESTLER project which harnesses advanced technologies to promote sustainable agricultural practices. The main objective is to create data-driven models that enable farmers to take targeted control measures, reducing the usage of chemical pesticides and minimizing environmental impact. The system supports precision agricultural practices, optimizing crop yields and reducing economic losses. Leveraging a UAV multispectral camera, the system monitors the field vegetation for possible changes caused by pests. If

significant changes are detected as an early warning, then on-field analysis takes place by the developed mobile application that enables farmers to report pest outbreaks and receive personalized recommendations for integrated pest management strategies, facilitating a proactive and collaborative approach to pest control. Finally, the system includes a mobile application that enables farmers to report pest outbreaks and receive personalized recommendations for integrated pest management strategies, facilitating a proactive and collaborative approach to pest control.

1.2. Intended Audience

The intended audience for this deliverable is diverse, encompassing professionals and stakeholders in agriculture, environmental science, and technology. It is particularly valuable for agricultural technologists, environmental scientists, and Iota specialists seeking to integrate advanced sensor and remote sensing technologies into their work. The document is also relevant for policymakers and development practitioners involved in shaping and implementing sustainable agricultural practices and environmental monitoring policies. Furthermore, it serves as a critical resource for academics in these fields, offering comprehensive insights into the latest technological advancements and their practical applications. Finally, this report has been developed within the framework of WP3 and is also highly relevant for WP4, WP5, and project partners, supporting their collaborative efforts and objectives.

1.3. Relations to other activities

This deliverable is primarily aligned with all the tasks of WP3 “Remote Sensing Technologies and Multi-Modal Data Aggregation”. The overarching objective of WP3 is to develop technologies with remote sensing capabilities and to design and IoT sensors and devices for monitoring environmental variables and crop quality. WP3 aims to develop the key modules of NESTLER platform that enable its main functions. Additionally, WP3 focuses on developing methods for multi-modal data aggregation.

The data sources outlined in this deliverable play a crucial role in supporting the formulation of AI algorithms and automated methods within WP4, such as algorithms for assessing the impact of external weather conditions on agricultural farming and evaluating crop yield quality. Finally, this document provides valuable input for future integration and validation activities, as well as for the preparation of pilot implementations under WP5.

1.4. Document Overview

The rest of the document is divided into the following sections:

- ***Section 2*** focuses on developing AI algorithms for precision agriculture, utilizing UAV and remote sensing imagery for crop health assessment. It explains vegetation indices like NDVI and NDRE for early-stage pest and stress detection. The chapter also discusses sensor integration and the data flow architecture for real-time monitoring.
- ***Section 3*** describes AI-driven systems for monitoring the health of domestic and wild animals. It includes the Domestic Animal Health Monitoring System (DAHMS), which employs optical flow, behaviour analysis, and audio monitoring, and the Wild Animal Monitoring System (WAMS), which detects threats from predators using advanced detection models like YOLO.

- ***Section 4*** covers methods for monitoring fish health and behaviour using underwater cameras and AI algorithms. It outlines key metrics like average swimming speed and diving depth to detect stress or disease. Integration of video-based analysis and a robust dataset for developing models is also detailed.
- ***Section 5*** highlights the use of multispectral imagery and UAVs to monitor pest infestations in crops. The chapter introduces algorithms for pest detection and classification in crops such as tomato, cocoa, mango, maize, and coffee, leveraging deep learning models and mobile applications for real-time identification and management.
- ***Section 6*** details the deployment and initial findings of the Insect Traps Network Subsystem – a core technological solution within the NESTLER project designed to combat the spread of zoonotic diseases (diseases transmitted from animals to humans). It emphasizes that these diseases are complex, driven by factors like climate change, habitat loss, and increased human-wildlife contact, particularly in Africa. The approach is multidisciplinary, combining technology with expertise from ecologists, veterinarians, and public health experts.
- ***Section 7*** describes how innovative solutions like UAV-based mesh networks, the Mesh-in-the-Sky architecture, and advanced communication protocols, address connectivity challenges in remote agricultural areas to enable real-time data collection and decision-making.
- ***Section 8*** focuses on extracting insights from satellite data, including crop yield estimation algorithms and integration of meteorological measurements. This chapter details the use of remote sensing technologies for land monitoring and agricultural decision-making.
- ***Section 9*** provides a summary of key findings and reflects on the implications of these technologies for future agricultural and environmental monitoring practices.
- ***Section 10*** contains the list of references.

2. AI for Agriculture Monitoring Subsystem

2.1. Agriculture Monitoring Algorithm Development and Validation

Developing and validating algorithms for agriculture monitoring is a critical step in leveraging technology to optimise crop production and resource management. These algorithms are designed to process and analyse diverse data streams, including soil conditions, atmospheric parameters, and UAV and remote sensing imagery. The aim is to generate actionable insights that support precision agriculture practices and enhance decision-making at the farm and supply chain levels.

The NESTLER Agriculture Monitoring Subsystem also has the role of an alert for possibly pest or disease presence. This subsystem works in collaboration with Pest Recognition Subsystem (see Chapter 5). A UAV able to capture multispectral imagery flies over a field to monitor crop changes. A multispectral camera for the UAV imagery is essential to extract Vegetation Indices related to crop health such as NDVI and NDRE. In particular, NDRE is more effective than NDVI in revealing crop health issues in earlier stages. To decide whether a NDRE pixel value indicates crop vegetation issues due to pests or diseases, some thresholds have been set.

2.2. Agriculture Monitoring Implementation

The development process starts with data acquisition, incorporating inputs from IoT sensors, drones, and satellite imagery. Machine learning and statistical models are then utilised to identify patterns, predict crop performance, and evaluate environmental factors influencing productivity. Key considerations during the development phase include scalability, cost-effectiveness, and adaptability to various agro-ecological zones. The sensors deployed are rugged, solar-powered devices capable of transmitting collected field data in real time via existing network infrastructure.

2.3. Agriculture Monitoring Sensors Integration and Data Flow

The integration of agriculture monitoring sensors and the design of an efficient data flow architecture are fundamental to achieving real-time, accurate, and actionable insights for precision agriculture. This process involves the seamless connection of diverse IoT-enabled sensors to capture critical parameters such as soil and atmospheric moisture, temperature, atmospheric humidity, and light intensity.

At the core of the system is a robust sensor network designed for scalability and adaptability to different agro-ecological zones. Sensors are strategically deployed across monitoring sites to ensure comprehensive data collection, with redundancy measures in place to minimise data loss. These sensors, often solar-powered for sustainability, communicate existing cellular infrastructure to a centralised gateway, which aggregates the data.

The data flow architecture follows a well-defined pipeline to ensure minimal latency and high reliability. Sensor data is transmitted in real time to cloud-based platforms for storage, processing, and analysis. Edge computing is incorporated at gateway nodes for preliminary processing, reducing bandwidth

usage and enhancing response times. The processed data is then fed into machine learning models for yield prediction, crop health assessment, and environmental monitoring.

This integration framework not only facilitates real-time monitoring but also supports long-term data archiving, enabling historical analysis and predictive modelling. By ensuring the interoperability of sensors and maintaining a streamlined data flow, this subsystem provides the foundation for scalable, data-driven solutions that empower farmers and agricultural stakeholders.

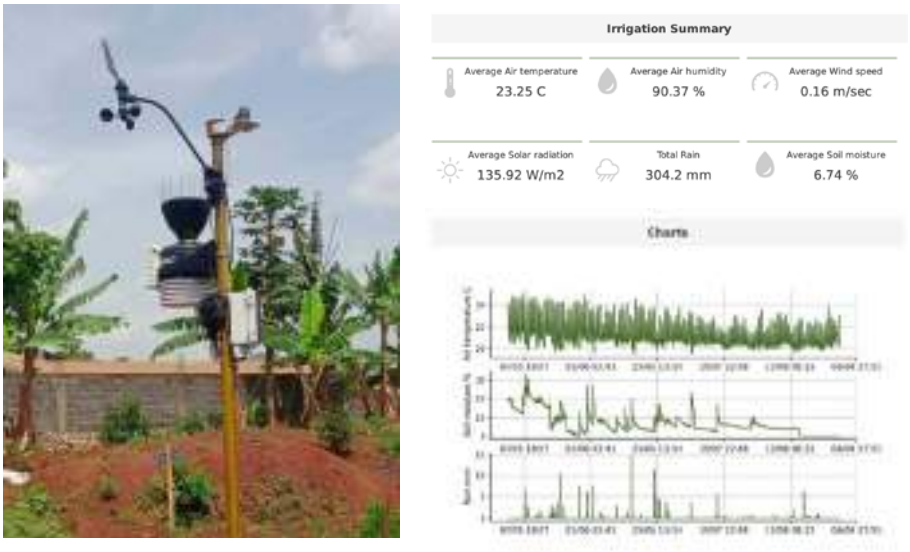

Figure 7: Agriculture monitoring sensors implemented in a pilot site in Cameroon

3. AI for Animal Health Monitoring Subsystem

3.1. Domestic Animal Health Monitoring

Domestic Animal Health Monitoring system (DAHMS) is designed to analyse video feed from the farm, detect anomalies of the behaviour of domestic animals, and raise early warnings. Within the NESTLER project, the system was tailored to the behaviour analysis of poultry.

3.1.1. Domestic Animal Monitoring Algorithm Development and Validation

The main functions of DAHMS are as follows.

- Creation of a statistical profile that describes typical flock activity patterns. This statistical profile is recorded incrementally for different times of the day and different locations in the farm. The statistical activity profile incorporates overall activity-based patterns recognition, offering a robust baseline for subsequent anomaly detection.
- Identification of abnormal activity level of the flock. This function relies on the statistical activity profile and operates as an anomaly detector. These abnormalities can signal potential health issues, stress factors, or environmental disturbances. By continuously monitoring real-time data and comparing it to the statistical baseline, it ensures timely alerts for anomaly early recognition.
- Creation of a statistical behaviour profile of the flock. This function relies on the visual appearance of each individual chicken and its activity in a given moment of time. Key indicators include individual pose and activity estimation. This profile enables the assessment of the overall distribution of activity types among flock members during daytime ensuring consistency on a daily basis.
- Identification of the persistent abnormal behaviour pattern. This function relies on the statistical behaviour profile as the baseline and generates timely alerts when anomalous patterns in the distribution of chicken behaviour are detected during the day.
- Identification of respiratory diseases. DAHMS includes functionality for automatically detecting vivid signs of respiratory diseases within the flock, by regularly analysing and classifying spectrograms of the audio stream segments.
- Identification of significant visual anomalies in chicken appearance. This function enables an automatic detection of individual chickens exhibiting abnormal physical features, which may indicate health issues, injuries, or other conditions requiring prompt attention and interventions. DAHMS produces specific alerts for these cases with sample images to provide context for detected anomalies.

Above-mentioned functions are implemented using the following AI techniques and indicators.

- Optical flows for activity analysis. Activity levels are quantified by analysing statistical features of movement intensity within the observed frame, including mean, variance,

skewness and kurtosis. These statistical measures capture average intensity, variability, asymmetry, and extreme deviations in motion, providing a comprehensive measure of the flock's overall activity and coherence.

- Chicken pose estimator and behavioural models based on Deeper Cut fine-tuned model for skeleton recognition and custom RNN for action recognition.
- YOLOv11 for individual chicken detection and DinoV2 model for appearance feature extraction and classification.
- Random forests for spectral analysis of respiratory diseases.
- Custom time series anomaly detection model based on KNN.

In the domain of algorithm development, an automated annotation tool, referred to as the Hen Automated Annotation Tool (HAAT), was designed and implemented to facilitate precise and efficient labelling of large-scale datasets for poultry behaviour analysis.

HAAT is a multi-platform desktop solution that provides tools for labelling sequential datasets. It works with poultry video fragments and includes pre-processing utilities, such as rescaling and framerate modification. Labelling is performed in two steps: multi-object per-frame pose annotation and per-object action labelling for video sequences. The application uses mouse and key bindings to provide advanced control schema for quick access to various functionalities, e.g. arbitrary frame scaling, forward and backward time-shifts and simple modification of any existing label.

In pose labelling mode, simultaneous multi-object annotation is performed based on pre-described pose graph configurations. To accelerate high frame rate video processing, two techniques are used. The first one is an adjustable body part position interpolation that utilizes generally low poultry movement activity level to automatically create annotations between two manually labelled frames within the specified time range; special quality control functionalities are used to quickly validate and correct created annotations. The second technique incorporates pose estimation neural networks to build predictions of body part locations; these predictions form the first estimate of frame annotations for users to manually correct. Designed filters that are applied to network results consider spatio-temporal characteristics of pose graphs to minimize false detections and labelling corruption. Joint application of both techniques gives a solution to controllable automatic prediction capable of recognizing significant pose changes without labelling quality loss.

Pose annotations form an additional input source for the action labelling step. Similarly, to pose labelling, automation tools are used to increase performance. Instead of interpolation, an adjustable clipping functionality is proposed that allows to set per-object action labels not for one frame, but for the selected time range in one click. Clip replays and time range modifications provide reliable forward and backward navigation over video sequences. Action recognition network is used based on pose annotations to create initial action labelling for all the recognized objects on the whole video sequence. Post-processing algorithms are applied to initial labels to create more continuous action sequences.

Using the annotated data, a sophisticated model pipeline integrating pose estimation and action recognition frameworks was developed and trained to achieve high accuracy in detecting and classifying key behavioural patterns. Additionally, rigorous optimization of model hyper parameters and

architectures was conducted to enhance computational efficiency, improve generalisability, and ensure scalability for deployment in applied research and practical settings.

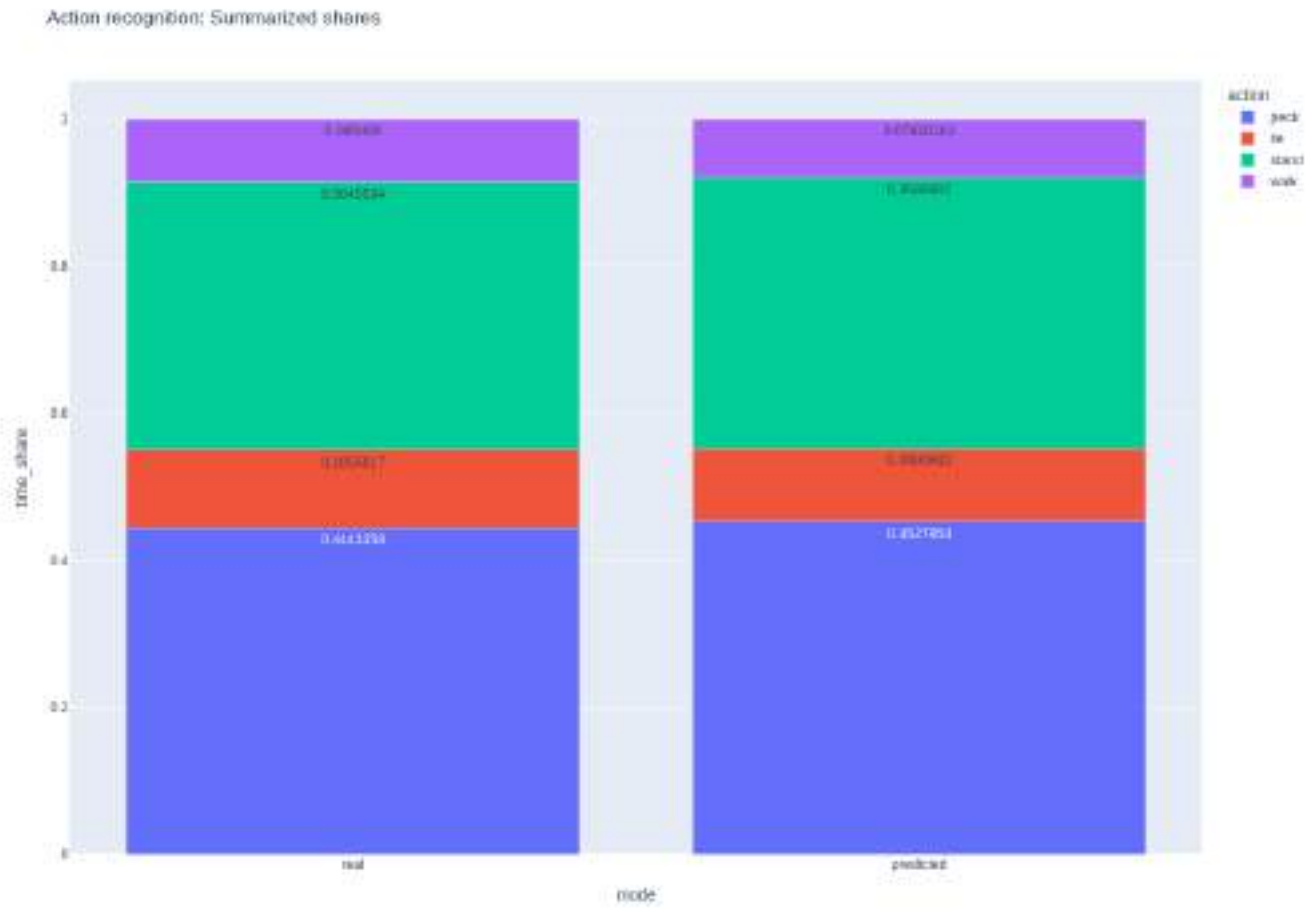

Figure 8: Action Class Distribution (ground truth vs. predicted)

The objective was to compute and analyse the class-wise detection performance of a system by summing the total number of detections for each class across the entire dataset. This analysis involves two distinct components: the detections produced by the model and the ground-truth annotations (mark-ups) provided as a reference. For each class, the fraction of total detections attributed to that class, termed the action fraction, is calculated separately for the model's detections and the ground-truth annotations. These fractions are then compared to assess the alignment between the model's detection distribution and the true distribution as defined by the ground-truth data. This comparison provides insights into the model's performance, particularly its ability to detect and proportionally represent the occurrence of each class accurately.

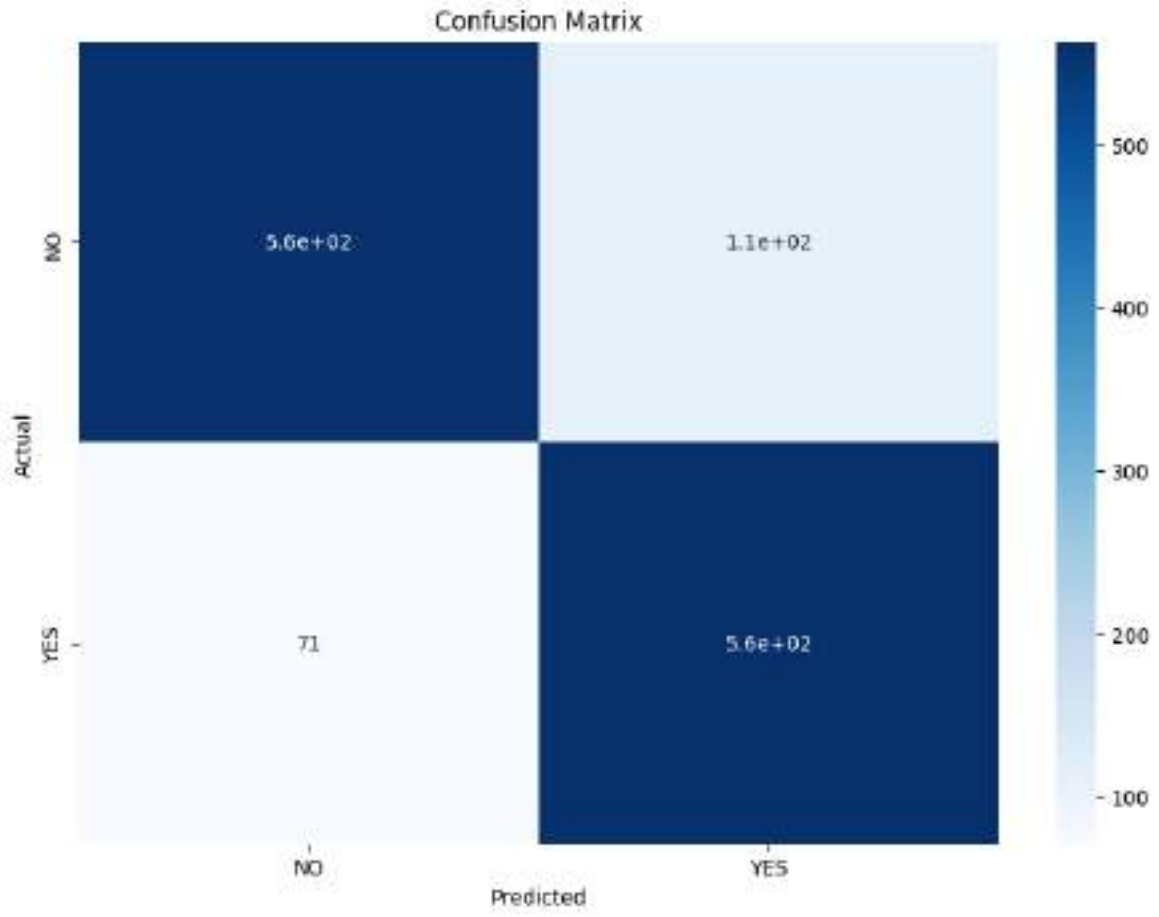

Figure 9: Action Classification Confusion Matrix

Here's a detailed and formal description of the action recognition classes for chicken behaviour:

1. **Peck**: This class represents the action of the chicken using its beak to interact with the environment, typically associated with feeding behaviour. It includes actions such as pecking at the ground, feed, or objects.
2. **Stand**: This class captures the stationary upright posture of the chicken where it remains on its legs without significant movement. It indicates a resting or observational state while maintaining balance.
3. **Lie**: This class denotes the posture where the chicken is positioned with its body in contact with the ground, often indicative of resting or sleeping behaviour. The legs are usually tucked under the body, and the chicken appears stationary.
4. **Walk**: This class encompasses the locomotion behaviour where the chicken moves by sequentially lifting and placing its legs. It is characterized by deliberate movement across the environment, typically at a slow or moderate pace.

These action classes are fundamental for recognizing and analysing chicken behaviour in various contexts, providing insights into their activity patterns and well-being.

The whole action recognition pipeline was finally formalised. The provided Figure 10 outlines a pipeline designed for pose detection, tracking, and action recognition to analyse chicken behaviour. The process begins with input images being processed with a model (ANN based on DeeperCut architecture). This network identifies key points of chickens within each input frame, outputting a set of these points that represent different body parts.

Each key point has its own signature allowing them to be combined into “skeletons”, which serve as a simplified representation of the chicken’s poses. To maintain consistency of tracking across frames, as the static pose is not sufficient for action recognition, a Multiple Object Tracking (MOT) algorithm assigns track IDs to the skeletons, allowing each individual chicken to be tracked through time. The result of this stage is a set of skeletons for each frame, linked by a consistent ID.

After tracking, additional features are extracted from each skeleton. For instance, a separate feature is used to estimate the likelihood that a chicken is laying down by checking if leg key points are absent or positioned near the ground. A cache buffer accumulates a sequence of these skeletons with the same track ID to maintain a history for each tracked chicken.

Dynamic actions, such as walking or pecking, are identified using a RNN, which outputs tags for these behaviours. Static actions, like standing or lying, are determined through fuzzy logic, which marks the pose of the chickens.

In the end, after post-processing the set of labels of the action chicken classes is produced and transferred to another module for the more general analysis.

The normalised simplified structure of the chicken is shown in Figure 11. It consists of 5 key points: head, tail, centre, left and right leg. Key point detection model was trained on the custom dataset, which includes auto generated synthetic data using Blender rendering engine and semi-manually annotated real data from Sliven bio laboratory through the developed HAAT.

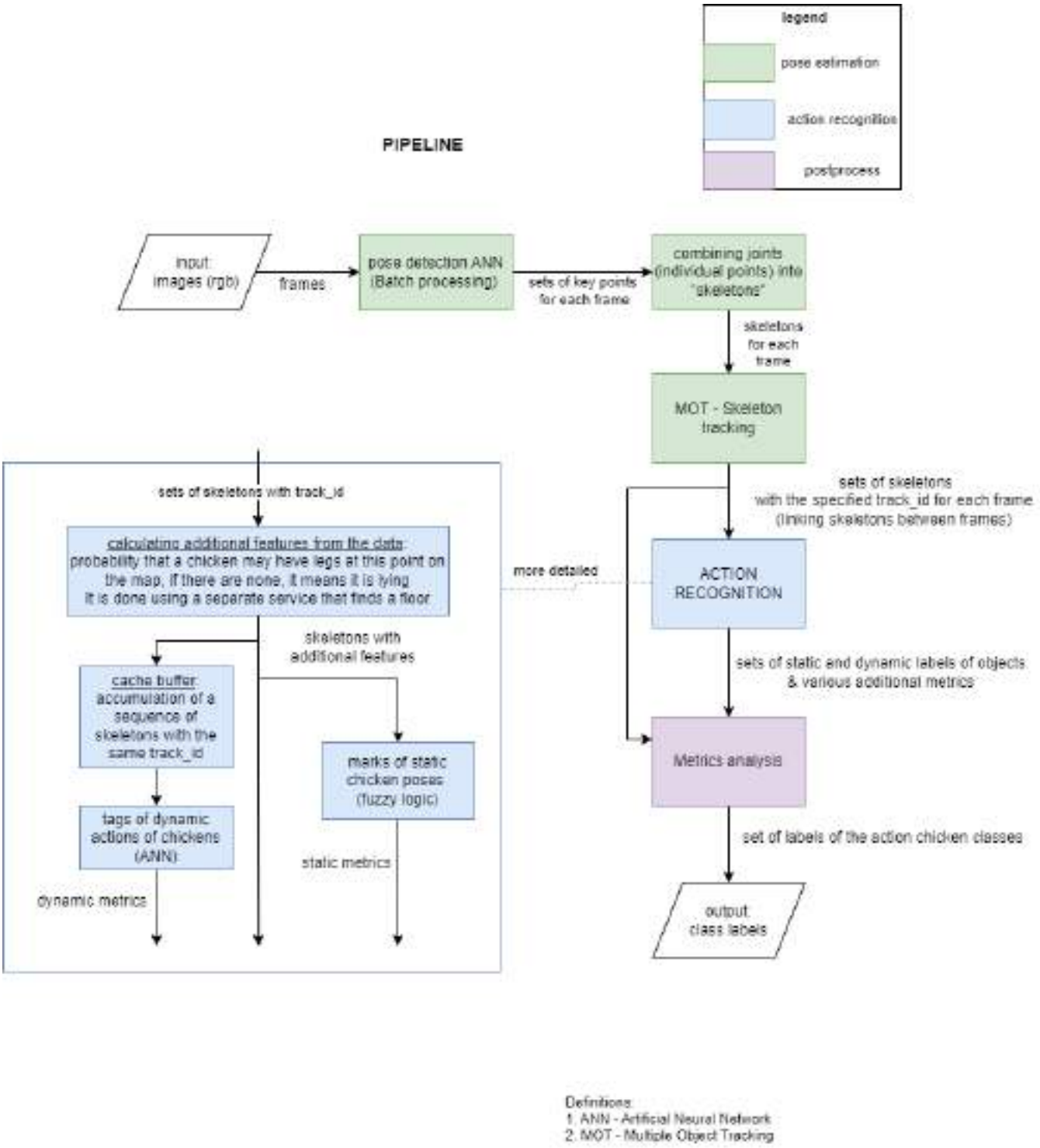

Figure 10: Action Recognition Pipeline

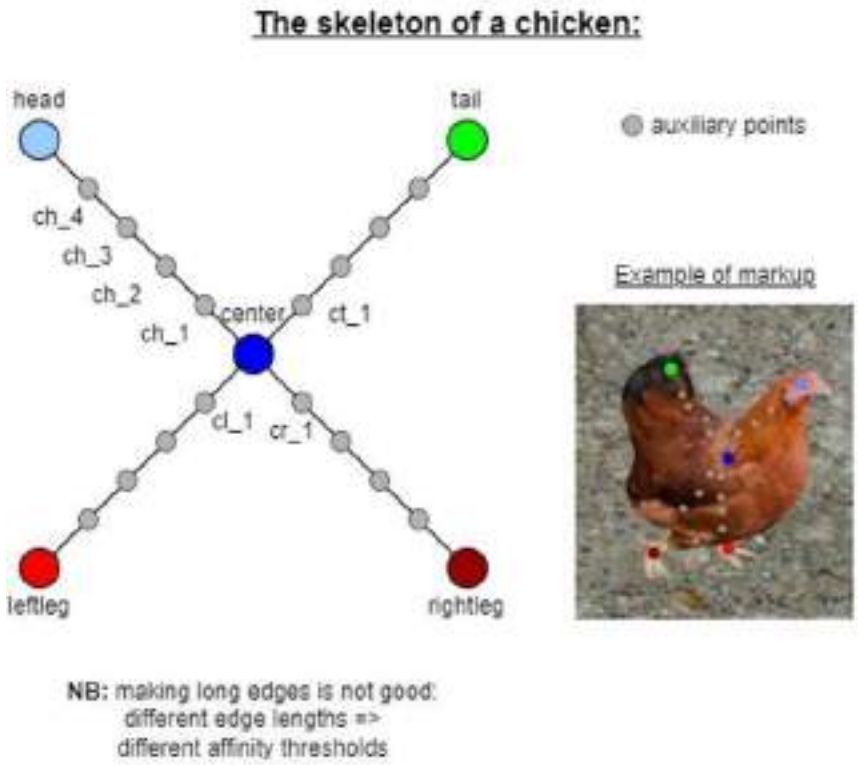

Figure 11: Simplified Chicken Model for Pose Estimation

Algorithm for adaptive detection of floor area in video stream based on chicken pose detector

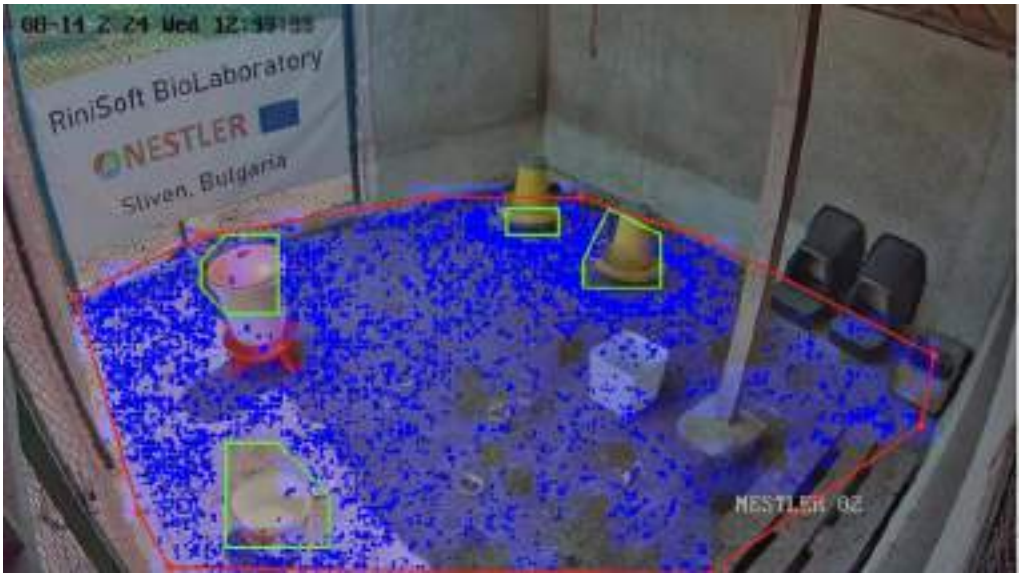

Figure 12: Floor Polygon by Leveraging Chicken Leg Recognition

This process involved detecting and analysing the positions of chicken legs within a visual frame and using these positional data points to infer and delineate the spatial boundaries of the floor area. The approach required integrating pose estimation techniques to accurately identify leg positions and applying geometric principles to construct a precise polygon representing the floor. This methodology is instrumental in creating spatial mappings and further applications in behavioural analysis and environmental interaction studies.

Example frames for several cameras with an activity heat map overlaid are shown in Figure 13. The map is computed from dense optical flow; per-pixel motion magnitude is accumulated over a sliding time window, smoothed, and normalised. Colours encode relative activity, with red indicating persistent, high-intensity motion. The visualization highlights movement routes and interaction hotspots (e.g., around feeders/drinkers) while cooler regions correspond to resting or lying areas.

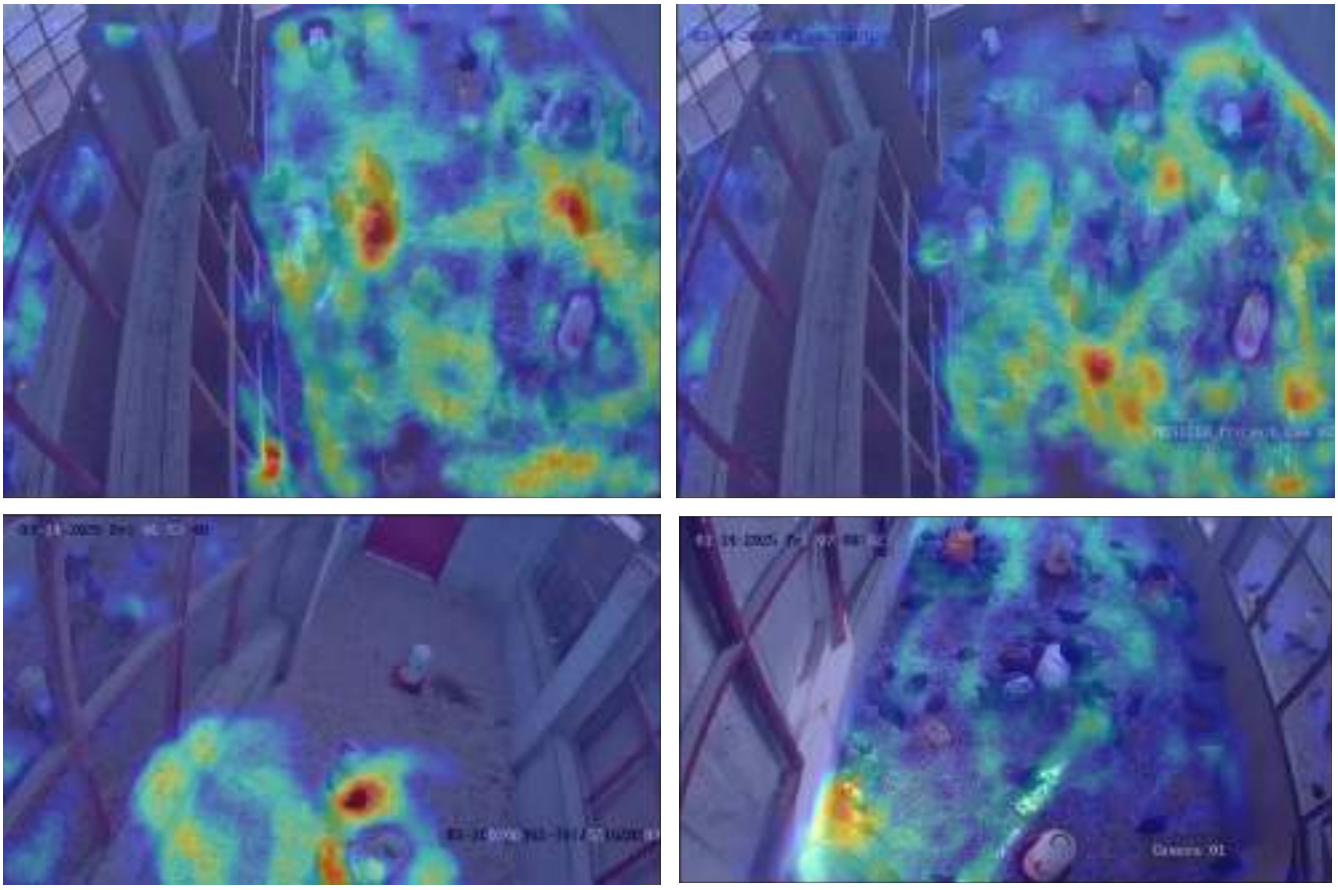

Figure 13: Movement Heat Maps

These heat maps are used to incrementally build the statistical activity profile per camera and time-of-day, derive stable zones of interest and refine the floor mask, and trigger early warnings when atypical patterns emerge — such as abnormal crowding or uniformly depressed activity. Summary statistics of the flow field (mean, variance, skewness, kurtosis) computed from these maps feed the anomaly detector and support flock-level behaviour analysis.

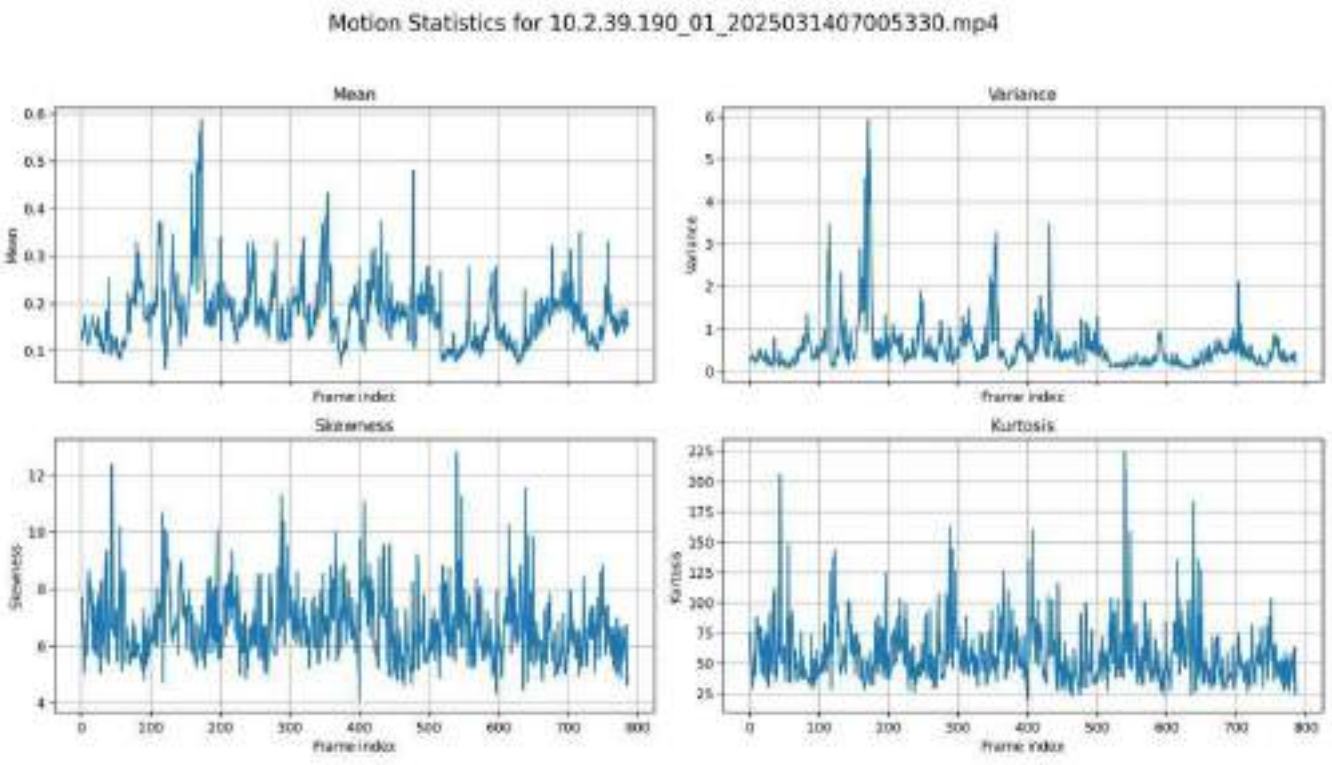

Figure 14: Motion Statistics

Figure14 presents the four primary statistical metrics (mean, variance, skewness, kurtosis) computed for each consecutive frame pair based in the optical flow field. These descriptors jointly form the statistical profile of flock mobility over time. The accumulated metrics enable the extraction of stable activity patterns and support anomaly detection during system operation, such as deviations from expected movement dynamics.

3.1.2. Domestic Animal Monitoring Implementation

The infrastructure modules and separate components of DAHMS were implemented. The AI modules system has a layered design that connects different components for metric generation, metric analysis, anomaly detection and reporting.

The architecture implies two parallel processes: generation of metrics with storage in the database and analysis of read from database metrics with individual pipelines and aggregation. Every metric - Optical Flow, Behaviour, Appearance, and others, is produced by generators. Metric generators produce metrics based on multimedia data coming from sensors via a request from the core scheduler. These modules produce metrics and metadata using the described above models and save them into two separate databases: MetricMetaStorage and TimeSeriesData. MetricMetaStorage stores metadata like floor polygon, zones of interest of the chickens and so on. These pieces of information facilitate and improve further predictions. TimeSeriesData is a column database that stores the temporal data over time.

The anomaly detection service (ADS) is the central component of this architecture, responsible for analysing the metrics and detecting anomalies. It starts by initialising management, which involves parsing and aggregating the stored data from the MetricMetaStorage and TimeSeriesData. ADS then generates comprehensive summaries or statistical profiles and representations of the metrics over different time intervals. Then, the aggregated temporal data with sufficient history context is processed through a custom anomaly detector. If needed, Anomaly Model Updater ensures that the ADS models stay updated based on the aggregated information.

The anomaly detection system outputs its results into the ADS Aggregates Storage, which stores the aggregated anomalies and their metadata. Once all aggregations are complete, the system triggers an Anomaly Decider. This component takes the weighted sum of anomalies detected across all intervals for a fixed time period and makes decisions regarding the presence of anomalies. If anomalies are found, Anomaly Decider can produce either prompt alert or schedule a report generation.

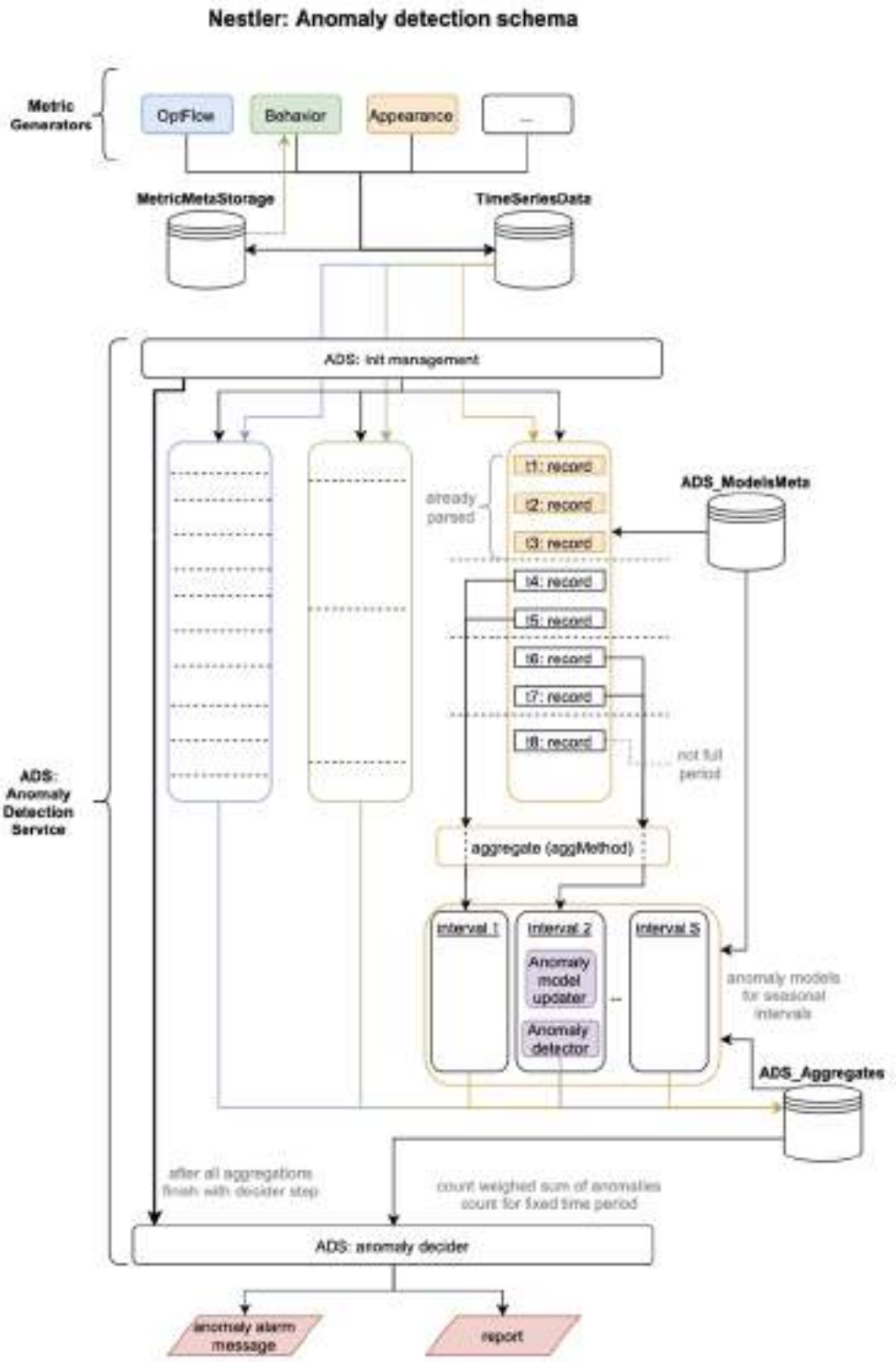

Figure 15: Analytics Modules Data Flow Diagram

3.1.3. Sensors Integration and Data Flow

In order to integrate sensors with smart AI modules of DAHMS and provide stable multimedia feeds the following infrastructure platform was partially implemented.

The platform comprises multiple key components, each responsible for specific aspects of data handling and processing, working together to provide seamless and secure service. DAHMS provides a specific interface for every metric analysis pipeline as an Analytic Service interface and requests multimedia data from sensors via the StreamCenter module.

The video streams originate from multiple IP cameras. These feeds are processed by the QNESTLER system, which consists of several interconnected modules, Streamcenter, NGINX, Analytic Services and Control module.

The StreamCenter module is responsible for the initial reception and processing of the video stream. It includes a Restreamer, which functions as a proxy server for managing the broadcasts and ensuring the consistent flow of the media streams. The incoming video feeds are temporarily stored and archived in a specific storage to allow for buffering or delayed processing. The Framer component ensures DAHMS get the multimedia content in the appropriate and optimal format, allowing metric generator modules to request for a specific resolution, framerate, etc.

The Analytics module is responsible for the analysis of multimedia content and consists of the Metric Generator services, Metric Analysis Services, ADS, and multiple metric and metadata storages.

The Control module is tasked with providing administrative and configuration services for the QNESTLER system as well as providing the actual processed data to the Main NESTLER Platform backend, encapsulating all the sophisticated logic and non-aggregated metrics, acting as a bridge between the data collection and processing activities and the backend. The control module also oversees user authorisation, ensuring only authorised users and services have access to specific parts of the system, thus maintaining a secure operational environment.

Additionally, the NGINX module plays a vital role in managing communication between the various components. It handles secure routing, load balancing, and proxy services, enabling the system to scale effectively while maintaining high availability.

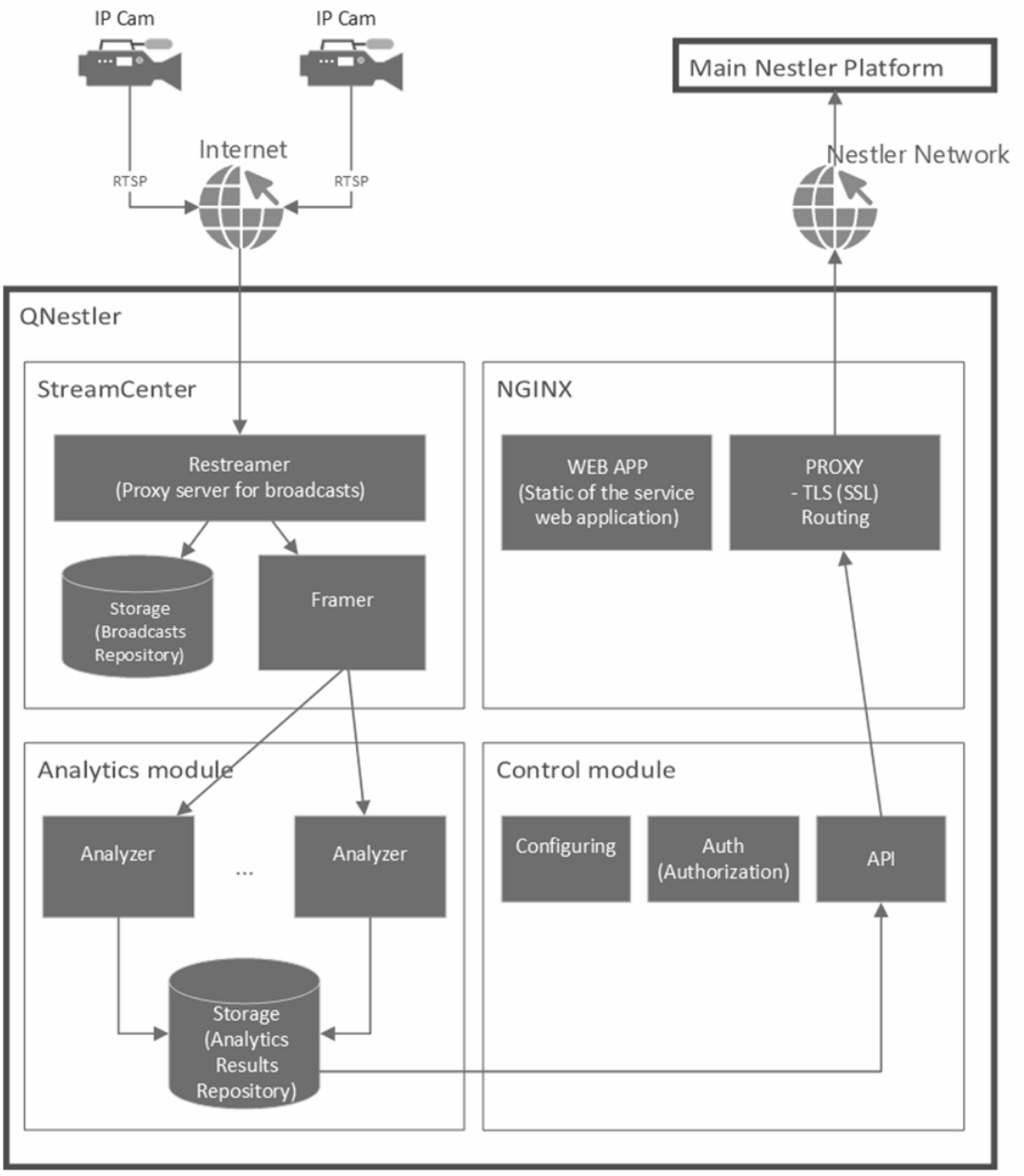

Figure 16: Infrastructure Data Flow Diagram

3.1.4. Analysis of Poultry Video Data

In the last six months of the project, we processed and annotated videos from the Muhanga Poultry Experiment Pilot (P.RWA.1).

Figure 17: Muhanga Poultry Experiment Pilot (P.RWA.1)

Several dozen video recordings were received and used for manual annotation of key points of interest on chicken bodies. These annotations were utilized in the fine-tuning process of our skeletal detection model for chickens. The videos were recorded during late morning (around 10:00) with a fixed overhead camera setup at a frame rate of 25 FPS and resolution of 1920×1080. The annotated key points include the head, body centre, tail, and leg joints, which are essential for accurate skeleton reconstruction.

Additionally, these video recordings were used for a preliminary test run of our mobility analytics system through statistical analysis of optical flow. We employed four primary statistical metrics of the absolute values of motion vectors per video frame: mean, variance, skewness, and kurtosis. These four metrics were selected because they provide complementary insights into motion distribution: the mean captures the overall activity level, variance reflects the heterogeneity of motion, skewness indicates asymmetry associated with localized bursts of movement, and kurtosis highlights the occurrence of extreme motion events, such as sudden jumps or aggressive interactions.

Unfortunately, the videos were acquired approximately once every two days and had a maximum duration of 1.5 hours. This limited the ability to identify daily mobility patterns. Consequently, these videos were only sufficient to verify the overall functionality of the metric collection pipeline, but not for comprehensive behavioural analysis.

The Figure 18 presents the temporal dynamics of the main statistical metrics throughout a single 30-minute video recording.

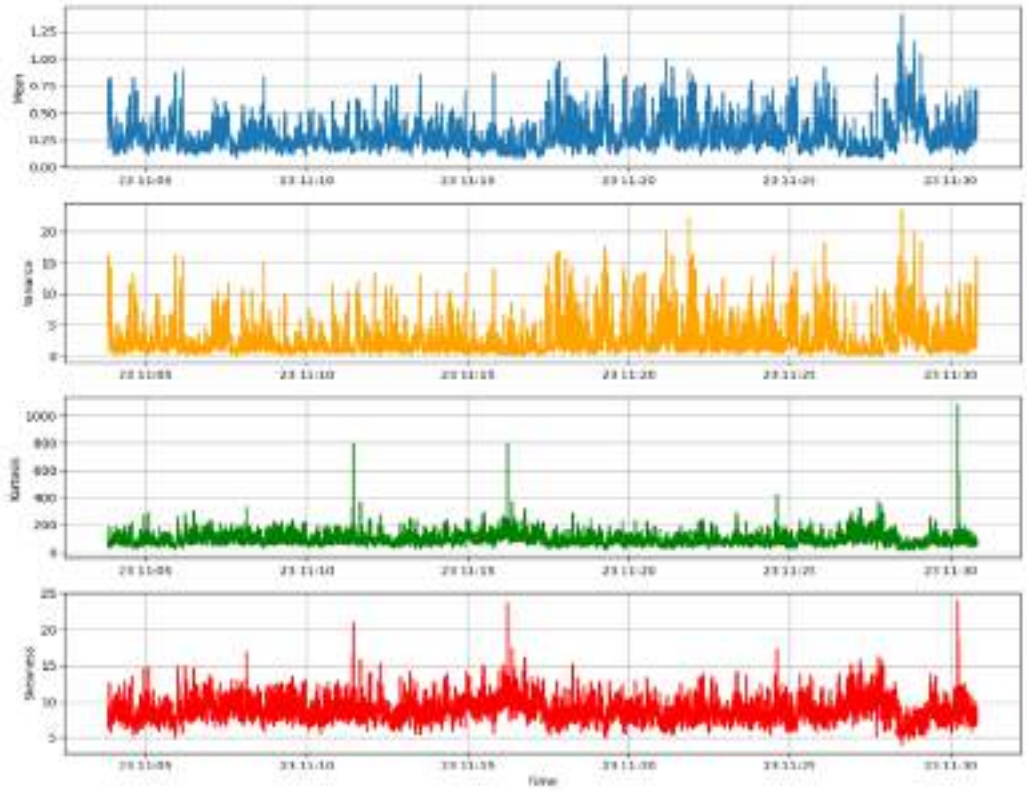

Figure 18: Statistical metrics of chicken mobility during a 30-minute recording

Prolonged optical flow analysis of the video data enabled the identification of zones of interest for the chickens, primarily located around feeders and drinkers, which is explained by the high level of mobility observed in these areas. Additionally, we were able to detect zones of minimal mobility, such as walls and overhead structures. This, in turn, allowed for a semantic segmentation of the environment into distinct regions:

- Floor area – regions of moderate mobility;
- Walls and overhead structures – regions of minimal mobility;
- Feeders and drinkers – regions of highest mobility.

The method we applied for this semantic segmentation involves cumulative aggregation of optical flow matrices across all frames into a single normalized matrix. The aggregation process is mathematically equivalent to summing the magnitude of motion vectors across all frames followed by min-max normalization to produce a spatial probability distribution of activity. This resulting heat map can be thresholded to classify regions into distinct semantic categories and potentially used for real-time monitoring of flock distribution. This approach proved to be effective across all provided videos, even when recorded from multiple camera angles.

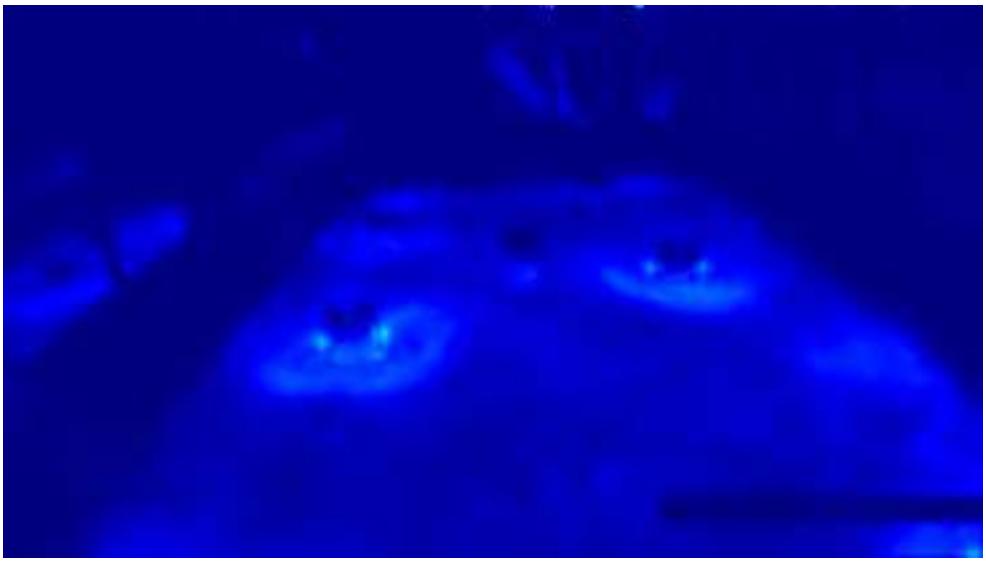

Figure 19: Heat map of chicken activity

The video recordings were also used to test the developed chicken activity detection model. The fine-tuning process of the skeletal detection model is still ongoing; however, after adjusting the camera angle to a lower perspective at our request, the chickens' legs became more distinguishable to the model. This improvement resulted in higher accuracy of the chicken activity detection model.

Figure 20: Chicken action recognition

3.2. Wild Animals Monitoring

The content of this section describes the Wild Animals Monitoring system (WAMS), which is designed to automatically detect and classify predators around a farm's perimeter. The system uses advanced machine learning and computer vision, with a YOLOv11-based model at its core. This model is trained to classify animals into three categories: land predators, bird predators, and non-predators. Specialized models were developed to work with both colour and black-and-white images, and a unique algorithm was created to detect vultures by analysing their characteristic circular flight patterns. The section also details the system's implementation, including the use of microservices to process camera feeds, track objects, and trigger alerts when a predator is detected within a defined region. The models were trained using a newly created, open-source dataset of annotated wildlife images from Bulgaria and Uganda.

3.2.1. Wild Animals Monitoring Algorithm Development and Validation

Predator detection around the perimeter of the farm

The research aimed to classify various animals into three distinct categories using a machine learning model. The identified classes were:

1. Land predators
2. Bird predators
3. Non-predators

Methodology:

1. **Data Collection:**
    - The dataset was curated from open-source repositories to ensure diversity and representativeness across the three identified classes.
    - Images were pre-processed and labelled accordingly to align with the categories of interest.
2. **Class Definition:**
    - **Land Predator:** Terrestrial animals exhibiting predatory behaviour, such as Canidae (dogs, wolves, foxes, etc.) and Cervidae (deers), Peleinae (roe deers).
    - **Bird Predator:** Avian species that hunt other animals, such as Avian species that hunt other animals, such as Aquila (eagles) and Neophron (vultures).
    - **Non-Predator:** Animals that are not categorized as predators, spanning a wide range of species without predatory traits.
    - The classification network was designed as a flexible model, allowing the addition of any bird species, provided a suitable training sample is available.

3. **Model Training:**

    - The YOLOv11 (You Only Look Once, version 11) model was selected due to its efficiency in real-time object detection tasks.
    - The model was trained using the curated dataset with images classified into the three defined classes.
    - Hyper parameter tuning was conducted to optimize the model's performance, and techniques such as data augmentation were applied to improve robustness.

Development of the algorithm using YOLOv11

The development process aimed to utilize the YOLOv11 model to create robust detection models tailored for specific classification tasks. The primary focus was on detecting and distinguishing predators (land and bird predators) from non-predators using both colour and black-and-white data inputs.

As a result, three specialized models were developed:

1. **Land Predator Detection Model (Colour Version):**

    - **Input:** Colour images.
    - **Classes:**
        - **Land Predator:** Identifies terrestrial animals exhibiting predatory traits.
        - **Not Predator:** Includes all other animals that are not classified as land predators.
    - **Purpose:** To leverage colour-based features in images to enhance the detection of land predators, capitalizing on visual cues such as fur patterns and environmental context.
2. **Land Predator Detection Model (Black-and-White Version):**

    - **Input:** Grayscale images.
    - **Classes:**
        - **Land Predator:** Similar to the RGB (colour) version, this class includes terrestrial predatory animals.
        - **Not Predator:** Non-predatory animals.
    - **Purpose:** Designed to test the model's ability to distinguish land predators using only structural and textural features in the absence of colour information.
3. **Bird Predator Detection Model (Colour Version):**

    - **Input:** Colour images.
    - **Classes:**
        - **Bird Predator:** Focuses exclusively on detecting avian species that exhibit predatory behaviour.
    - **Purpose:** To identify bird predators using colour-based features that are particularly critical for avian recognition, such as feather patterns and coloration.

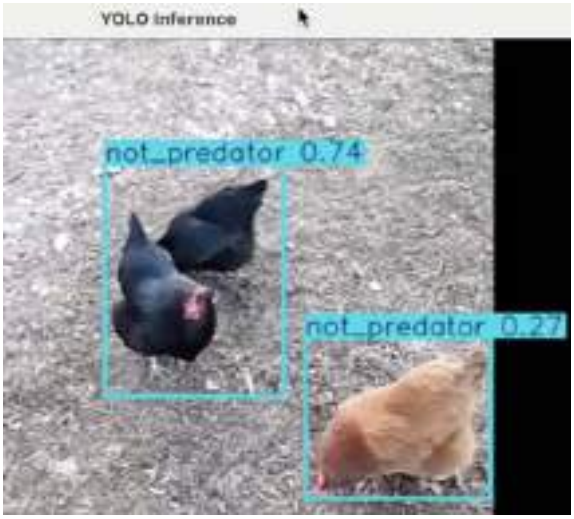

Figure 21: Detection of Poultry

Figure 22: Detection of Land Predators

Figure 23: Detection of Bird Predators

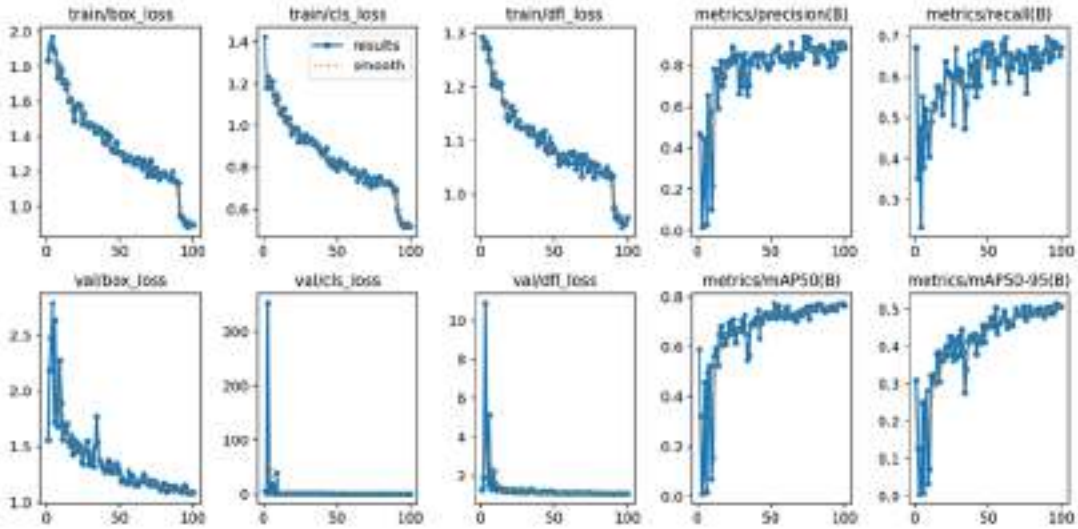

Figure 24: Training Results – Air Model

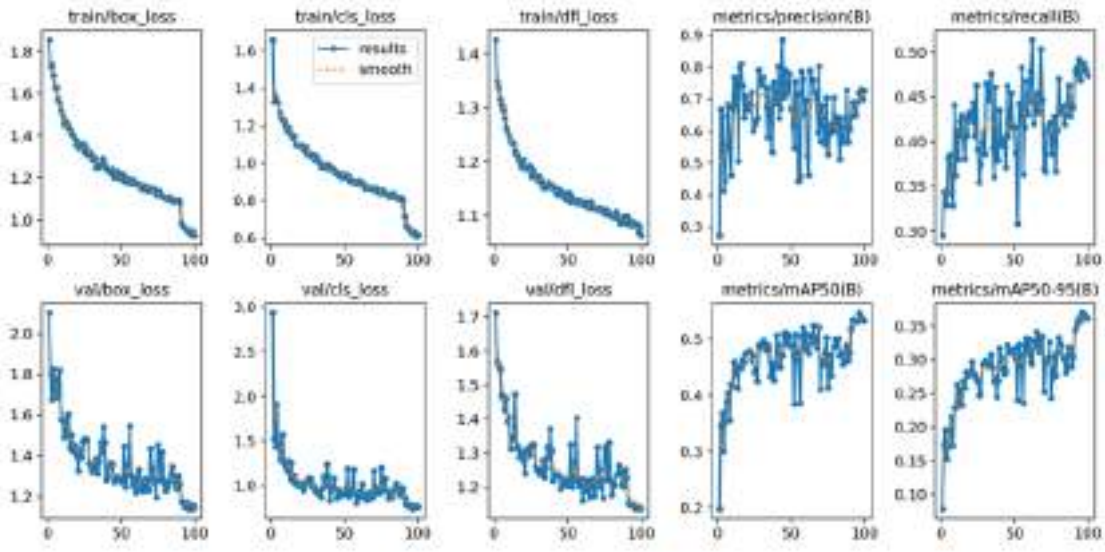

Figure 25: Training Results – Land Model

Detection of Vulture Movement Using Curl Analysis

The objective of this study was to develop an algorithm capable of detecting the characteristic circular movement of vultures, captured by an overhead camera, by leveraging the curl of the optical flow vector field.

Database Collection:

- A comprehensive dataset of videos containing various types of motion was assembled.
- The dataset included sequences with linear, elliptical, and circular motion patterns to provide diverse training and evaluation data.

Optical Flow Analysis:

1. The behaviour of the optical flow was analysed across different video samples to detect regions exhibiting elliptical or circular trajectories.
2. Optical flow was represented as a vector field indicating the motion of objects between consecutive frames.
3. It was discovered that the curl of the optical flow field serves as a robust mathematical descriptor of circular motion.

Curl: Measures the rotation or circulation within the vector field, effectively highlighting areas with rotational or elliptical dynamics.

The algorithm was developed based on insights from the research phase, consisting of the following key steps:

Optical Flow Calculation

Motion between consecutive frames was estimated using optical flow techniques (e.g., Farneback, Lucas-Kanade). Optical flow vectors were computed to capture the direction and magnitude of object movements.

Curl Calculation

The curl of the optical flow vector field was calculated to identify areas with rotational or circular motion. This step enabled the detection of regions where the motion pattern resembled an elliptical trajectory, characteristic of vulture flight.

Ellipse Approximation and Trajectory Analysis

Areas with significant curl were subjected to further processing to approximate their motion paths as ellipses. Linear motion trajectories were excluded from consideration to minimize the likelihood of false positives. The remaining trajectories were analysed and classified based on their geometric properties, including eccentricity and orientation. Only those trajectories that exhibited circular or near-elliptical shapes were retained, as these matched the characteristic flight behaviour observed in vultures.

Figure 26: Detection and identification of zebras and elephants in the wild environment

The trained predator/non-predator classifiers are encapsulated in a separate microservice. The service subscribes to the perimeter camera and sky-facing camera streams, performs detection and multi-object tracking, and evaluates each track against configurable regions of interest (ROIs). These zones are defined as two-dimensional polygons located in the image plane.

When a predator is observed within the ROI, the service computes the risk score. Exceeding a zone specific threshold triggers an event that includes snapshot and ROI identifiers. To reduce false alarms, alerts are gated by temporal smoothing (N-frame confirmation).

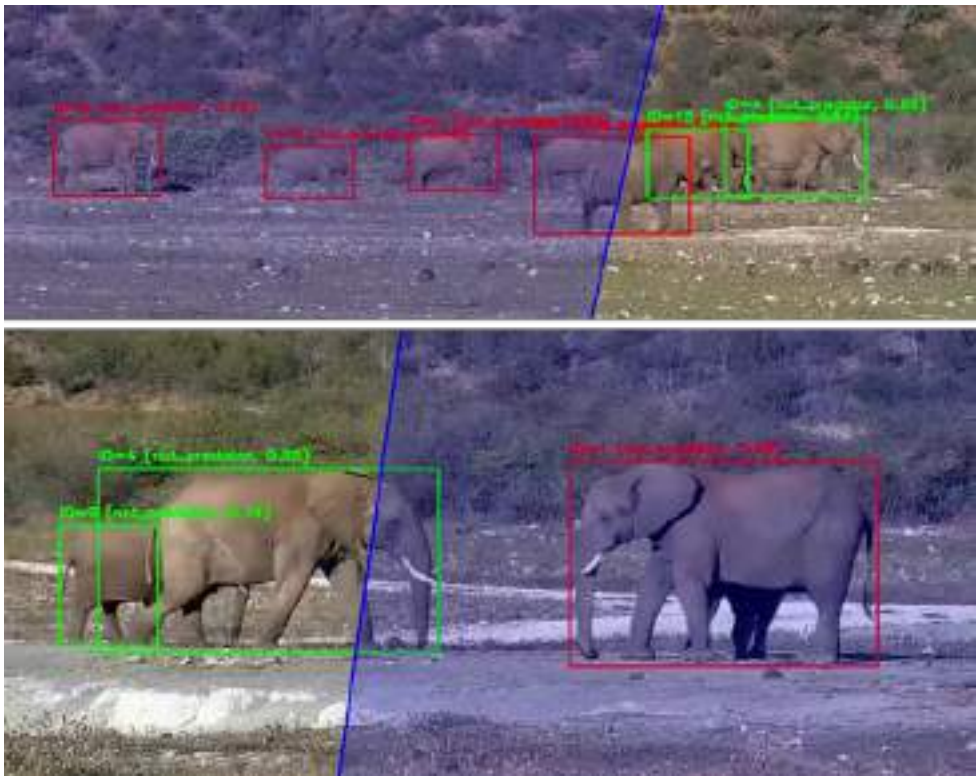

Figure 27: Line-crossing detection for harmful predators

3.2.2. Wild Animals Monitoring Implementation

The infrastructure modules and separate components of WAMS were implemented at this stage of the project. The AI modules system has the same layered design and architecture as described in 3.1.2. The only distinction of the developed modules for monitoring predator activity is the implementation of Metric Generator Services and the set of selected metrics generated by these services: number of cases of characteristic predatory birds' movements detected, number of ground predators detected.

The same infrastructure platform described in section 3.1.3 is also used to provide video feeds for AI modules analysing wild animals' activity. To generate the predator activity metrics, multiple perimeter cameras and one camera directed at the sky above the open area of the poultry yard are required per chicken farm. The rest of the architecture – Streamcenter, NGINX, the Control Module, and specific subsystems of the Analytics module, such as the Metric Analysis Service and the Anomaly Detection

Service – remains largely unchanged. These components have only been updated to ensure compatibility with the new Metric Generator Services.

3.2.3. Wild Animal Recognition Video Dataset

This dataset contains annotated wildlife images collected in three national parks in Uganda (Kibale National Park, Queen Elizabeth National Park, and Bwindi Impenetrable National Park) between February and June 2025. The images were captured using a Canon EOS M50 MK II and an iPhone 12 Pro Max (12MP Ultra-Wide, Wide, Telephoto, Night, HDR, ProRAW). Annotation was performed using bounding boxes and class labels, with outputs provided in COCO/YOLO-compatible JSON and TXT formats. It includes key species such as elephants, chimpanzees, mountain gorillas, hippopotamuses, Uganda kob, and warthogs. All images are annotated with bounding boxes and class labels in COCO/YOLO-compatible formats. The dataset includes 9 videos, 1,173 frames, and 3,909 bounding boxes. It is intended to support the development and benchmarking of wildlife detection and classification models, as well as research on AI for environmental monitoring and sustainability.

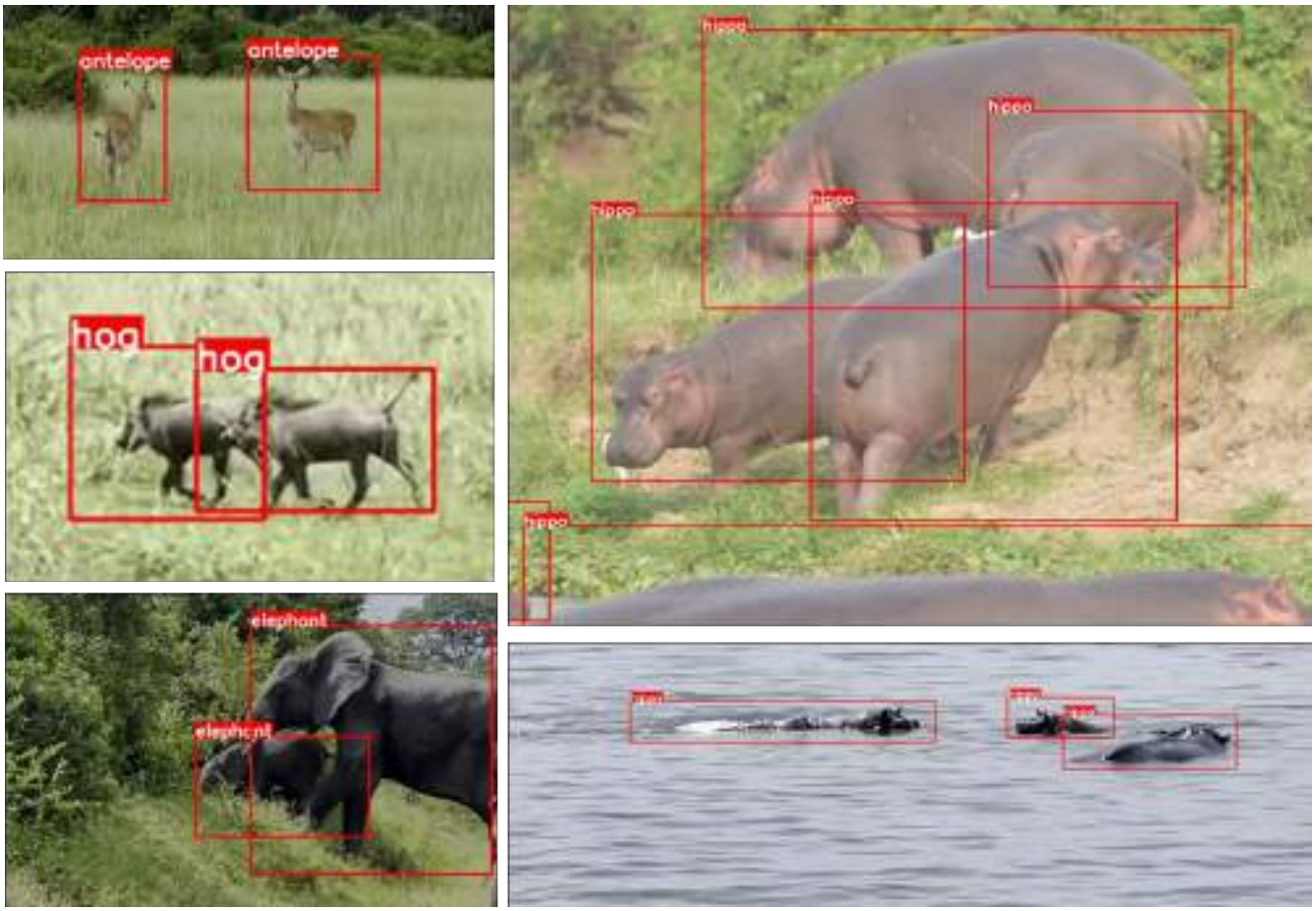

Figure 28: Examples of the annotated images

The annotated images have been published as an open-source dataset on https://zenodo.org/records/17036940.

All data were collected in line with ethical wildlife observation practices. No animals were disturbed, trapped, or manipulated, and camera traps were deployed in accordance with park regulations to minimise disturbance. All necessary permits for photography and data collection were obtained from relevant authorities. The dataset contains no personal data or identifiable human subjects, ensuring full compliance with EU data protection (GDPR) requirements.

4. AI for Aquaculture Monitoring Subsystem

4.1. Aquaculture Monitoring Algorithm Development and Validation

As it was outlined in the deliverable D3.1, one of the key priorities in aquaculture monitoring is the use of video cameras to evaluate the health and well-being of fish stocks in fish farms. This technology is particularly critical for monitoring fish species deemed strategically important for food security in the project countries. Notably, most of these species are 'bottom-dwelling,' meaning they typically inhabit the lower layers of a water body when in normal health.

During the initial phase of the project, it was not possible to access video streams from fish farms in Africa. To validate the chosen methodologies and algorithms under similar conditions, an alternative approach was employed: testing the systems with another bottom-dwelling species, the sturgeon. This allowed for preliminary evaluation of the techniques and ensured their robustness.

In subsequent stages, the neural networks and AI systems were adapted to process video footage obtained directly from fish farms raising Nile tilapia. Analysis of the results demonstrated no significant differences in the behaviour patterns of various bottom-dwelling fish species within the same biocoenosis, confirming the adaptability of the approach across different species under similar ecological conditions.

At the second stage of the project a comprehensive analysis was conducted on a dataset comprising 275,000 video fragments recorded over a period of five days. The focus was to understand fish activity patterns within a defined aquatic region. Each video fragment was thoroughly reviewed to identify and quantify fish presence.

To visually represent fish activity, heat maps were created for each day. These maps categorized fish presence into three distinct levels - low, medium, and high - along with a summary map displaying total presence across all levels.

- **Methodology:** A fish was considered to have entered a specific region if its bounding box intersected with that area. This precise detection method ensured accurate localization of fish movements and interactions with the environment.
- **Purpose:** These heat maps serve as a tool to identify areas of varying fish density, providing insights into behavioural and environmental factors influencing fish distribution.

Day 1 Summary Example

- **Records Analysed:** A total of 25,574 records were reviewed during Day 1.
- **Duration of Analysis:** 8 hours and 17 minutes.

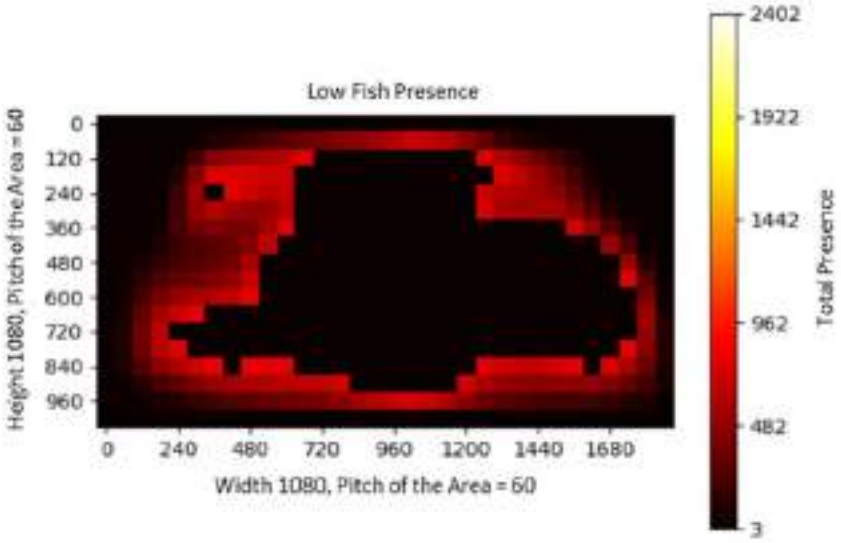

Figure 29: Low fish presence

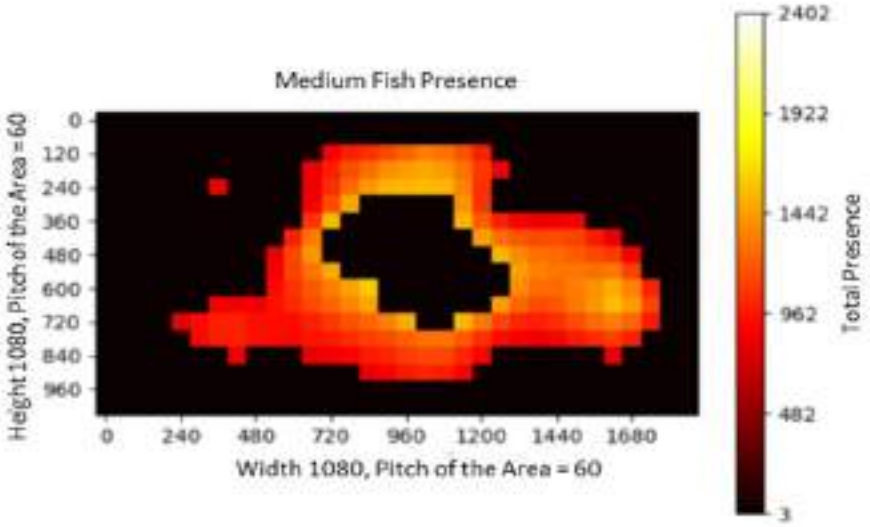

Figure 30: Medium fish presence

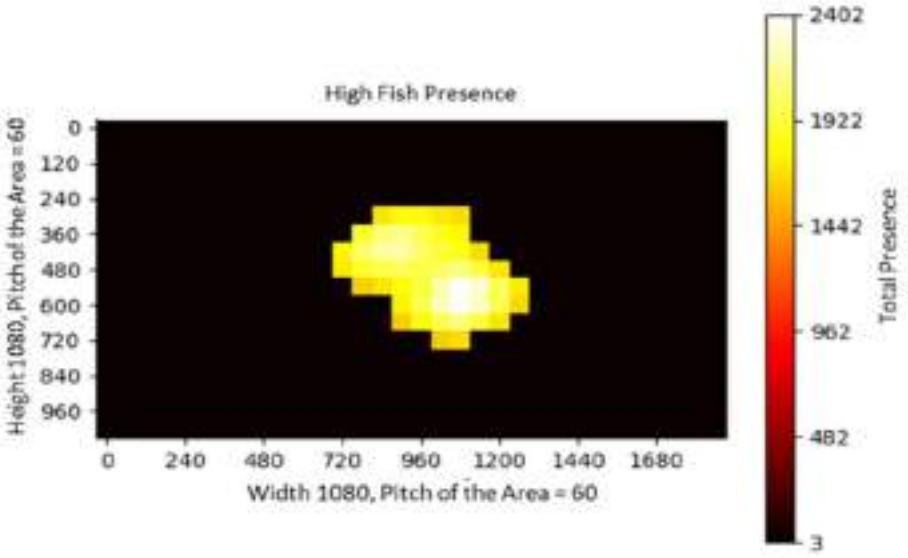

Figure 31: High fish presence

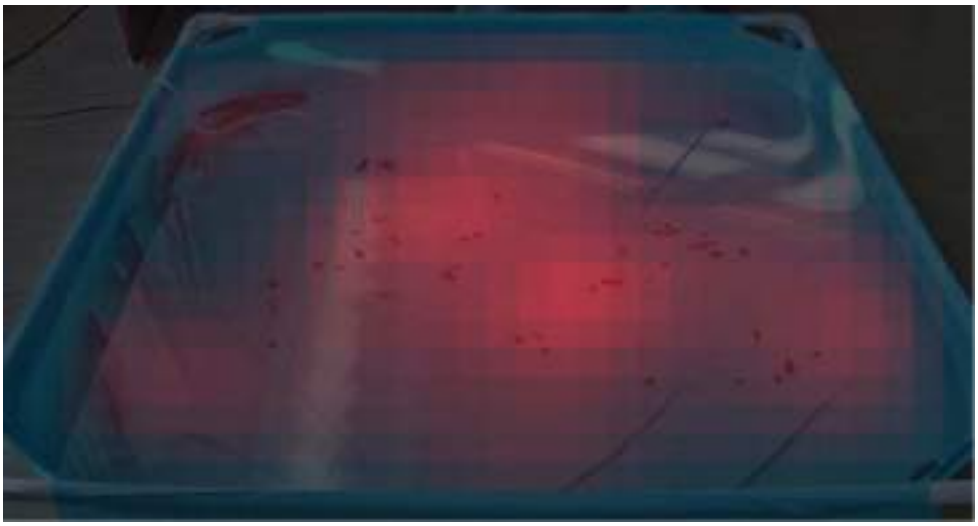

Figure 32: Heat map overlay on the pool image

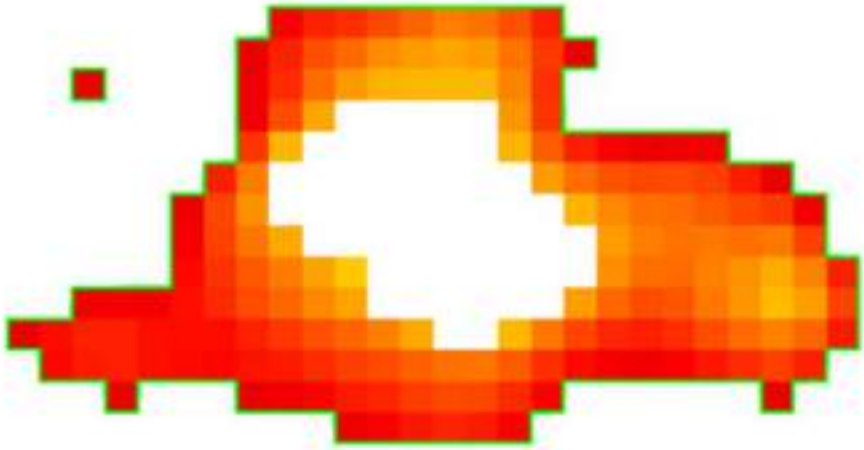

Figure 33: Example of boundary marking (Medium Presence, 50 Points)

Figure 34: General heat map visualization by boundaries (151 points)

4.2. Aquaculture Monitoring Implementation, Sensors Integration and Data Flow

The infrastructure modules and separate components of AHMS were implemented. The AI modules system has the same layered design and architecture as described in 3.1.2. The only distinction of the developed modules for monitoring the health of aquaculture, particularly fish, is the implementation of Metric Generator Services and the set of selected metrics generated by these services: optical flow (statistical distribution over time and space) and fish activity, categorized into three classes: idling, movement, and feeding.

The same infrastructure platform described in section 3.1.3 is also used to provide video feeds for AI modules analysing fish activity. To generate the activity metrics, a single camera is used for the water tank, assuming good lighting conditions and water transparency. The rest of the architecture – Streamcenter, NGINX, the Control Module, and specific subsystems of the Analytics module, such as the Metric Analysis Service and the Anomaly Detection Service – remains largely unchanged. These components have only been updated to ensure compatibility with the new Metric Generator Services.

5. AI for Pest Identification Subsystem

5.1. Pest Identification Algorithm Development and Validation

A variety of biotic and abiotic factors such as crop diseases, insects, weeds affect about 40% of agricultural productivity worldwide [1]. Facing pest infestation in crop cultivation especially at its early stages is important to eliminate the negative effects of it on crop productivity and food security [2]. To increase crop yield and crop quality farmers make use of pesticides. But the continual use of pesticides is costly and also can be harmful due to environmental pollution and potentially hazardous diseases, such as cancer [3].

Developing pest infestation identification models can be a rather complicated task considering the difficulty of creating a dataset for this purpose; since pests are very small and cannot be easily captured on an image, many of them look alike with each other and there is a big variety of them. Despite the aforementioned problems that may arise, pest identification models are a useful tool on recognising the presence of pests on a crop at its early stages and prevent further infestation of the plant. Therefore, pest identification through advanced deep learning methods at its early stages is essential to control their population, apply any treatment needed and understand the conditions that they occur [4]. Deep learning classification and detection models, like those utilized here, learn features of an image, particularly in this case features of pests [5], by processing training data and learning to differentiate among them.

However, it is rather difficult and time consuming to inspect crops one by one using such deep learning vision models as mentioned above. To address this difficulty, remote-sensing monitoring with multispectral imagery captured from a UAV over a field, is performed as a monitoring module to identify vegetation changes that are highly possible to have been caused by pests and playing the role of an early warning to the farmers. UAV is capturing georeferenced images that enable farmers to visit the specific vegetation and inspect the crop with the mobile application to perform pest recognition, and verify the presence of pests.

5.1.1. Remote-Sensing Crop Monitoring for Pest Infestation

An analysis is carried out on images captured from a UAV equipped with a multispectral camera. The images are included in a publicly available dataset of aerial photographs acquired with UAV equipped with a multispectral (Green, Red and Near-infrared channels) camera for cherry tomato (Solanum lycopersicum var. cerasiforme) monitoring [6].

Authors of the dataset used a DJI Phantom 4 Pro UAV to capture aerial images over a cherry tomato field in Navolato of Mexico. Their UAV was equipped with a Mapir Survey 3W multispectral camera of 3 multispectral channels (Green, Red, Near-Infrared). The spatial resolution of the multispectral camera is very good, at a level of 1.83 cm/pixel. Starting from mid of October 2021 till 23 of January 2022, seven photogrammetric UAV flights were carried out.

The aim of the dataset was to assess the growth stage of cherry tomatoes, their stress levels and their overall health and this is the reason that we selected it to apply the analysis for the pest identification experiments. The procedure that we followed with the specific dataset gives us experience and useful insights for carrying out a similar procedure to real conditions. As the authors of the dataset declare, two treatments were applied to the crops, and no stress was induced to them.

However, it should be mentioned that independently of the stress levels present in the crops of the dataset, and despite the fact that there is only a small level of stressed areas on the crops, this is the approach that we would follow to identify pest presence at an early stage in real-field conditions or in a dataset captured by us for crop stress detection, and resulting in notifying a farmer with an early warning.

After acquiring the multispectral images from the photogrammetric flights, image processing methods were applied to get the orthomosaics and a binary mask that distinguishes soil and any non-vegetation areas from the rest of the planted area of the tomato field. This binary mask helps us better define the thresholds of each vegetation index used without considering the soil. Specifically, for the assessment of the stress levels of the crop, we extracted two vegetation indices, relative to crop stress identification, given the available multispectral channels of the dataset's camera, which are Green Normalized Difference Vegetation Index (GNDVI) and Soil Adjusted Vegetation Index (SAVI). The formula to compute each of these two VIs are the following:

$$GNDVI = (NIR - GREEN)/(NIR + GREEN)$$

$$SAVI = (NIR - RED)/(NIR + RED + L) * (1 + L)$$

where in the SAVI equation L is a canopy background adjustment factor usually set to 0.5 (and this was also the value of L in our experiments). The visualizations of GNDVI and SAVI indices at two different growth stages of cherry tomato are presented at Figure 35 and Figure 36.

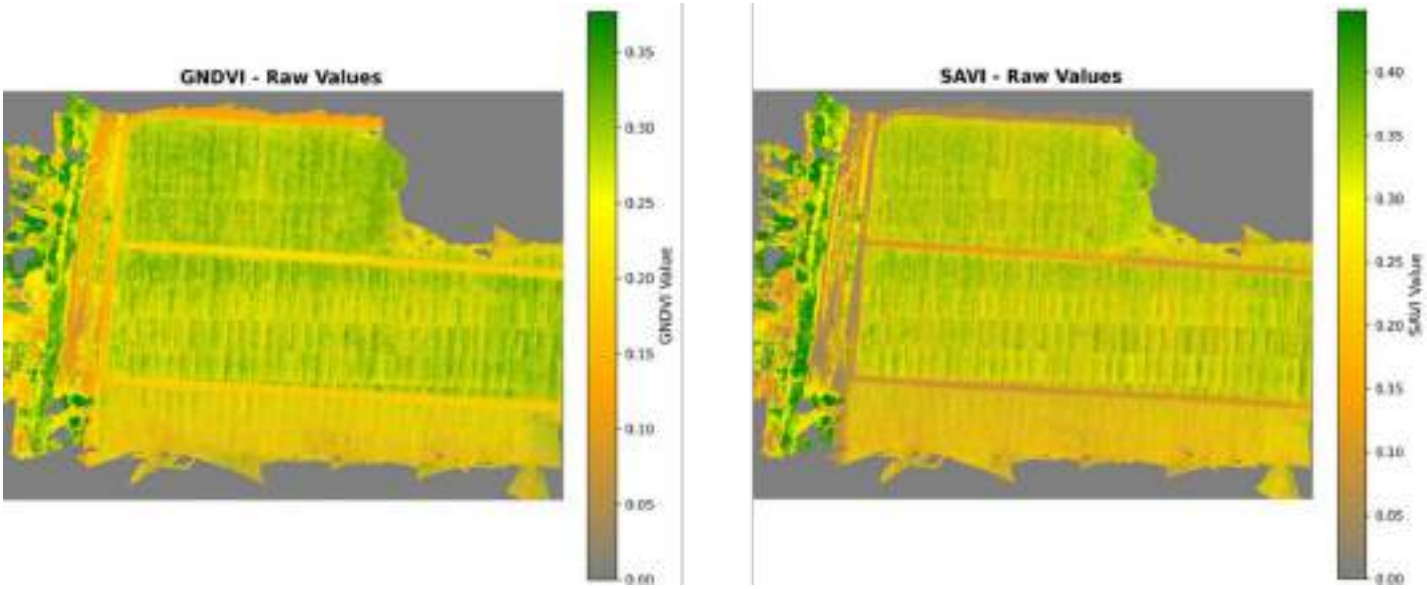

Figure 35: Visualization of GNDVI (at the left) and SAVI (at the right) over a field with cherry tomatoes. The growth stage of cherry tomato is flowering

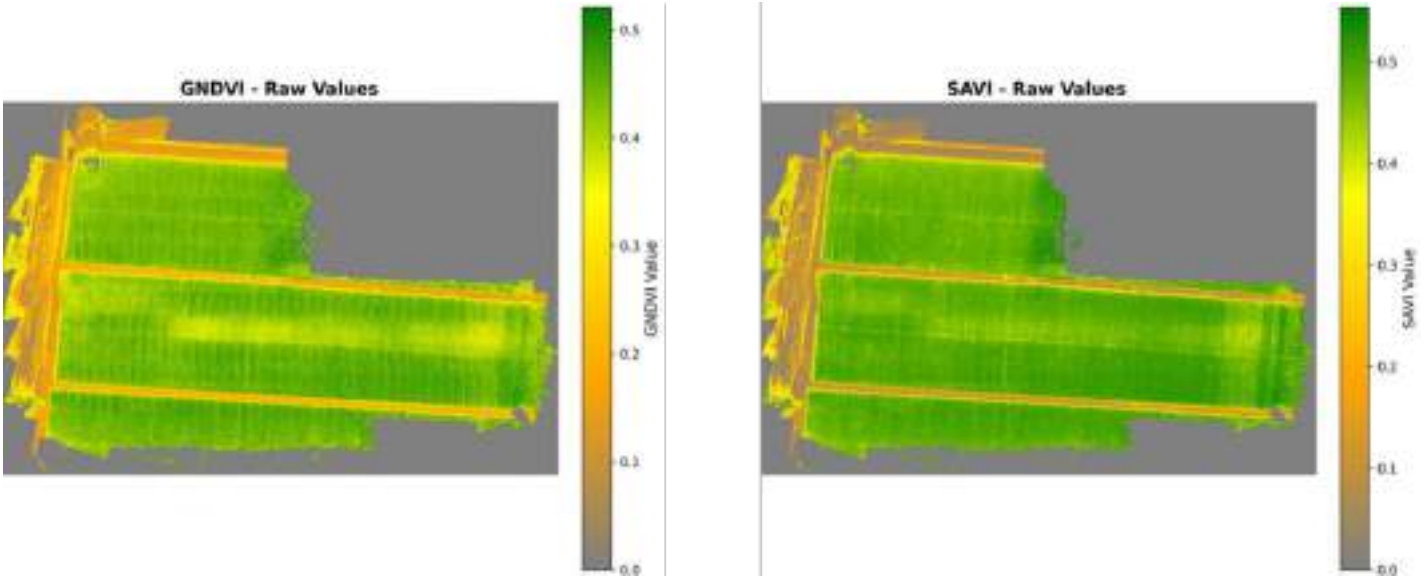

Figure 36: Visualization of GNDVI (at the left) and SAVI (at the right) over a field with cherry tomatoes. The growth stage of cherry tomato is maturity

Also a second analysis was carried out using a dataset of images captured from a UAV equipped with a multispectral camera, containing 5 channels, instead of the 3 channels of the aforementioned dataset [7]. The aim of this dataset was to monitor Maize across its different phenological stages and it was also selected as Maize is one of the available crops of the NESTLER mobile app for pest recognition. Having the RGB channels and also the Near-Infrared and the Red-Edge multispectral channels of an image, lets us compute a bigger variation of vegetation indices (VI) that reveal the level of biotic stress of a crop. Vegetation indices such as NDVI, GNDVI, NDRE, CIG (Chlorophyll Index Green Channel), CIR (Chlorophyll Index Red Edge Channel) are also useful for distinguishing the healthy from the stressed part of the crop and generally over a field. Proper biotic stress thresholds are set for each indicator in order to classify the pixels into stressed areas, healthy and non-vegetation areas. Pixel of the VIs with values in between these thresholds indicate that it is highly possible that a crop is stressed by pests or other abiotic factors such as drought or flood. Users (farmers or agronomists) can conduct an on-field inspection of the crop using the NESTLER pest recognition mobile application to check if pests are present on a crop and infestating it.

The dataset contains one multispectral raster image (raster images are high spatial resolution georeferenced images containing multiple spectral bands) for each of the six phenological stages of Spring Maize, that is, trefoil stage, jointing stage, tassel stage, silking stage, milk stage and maturity stage. Each image has a resolution of 12965 (width) x 10531 (height).

In order to monitor changes in Maize crops that possibly hinder pest infestation, different VIs were extracted from the relevant multispectral bands. The VIs used are NDVI (Normalized Difference Vegetation Index), GNDVI (Green Normalized Difference Vegetation Index), NDRE (Normalized Difference Red Edge Index), CIG (Chlorophyll Index Green Channel), CIR (Chlorophyll Index Red Edge Channel).

- $NDVI = (NIR - RED)/(NIR + RED)$:

  It is sensitive to the crop's chlorophyll content and biomass, thus, it measures the greenness and the overall vegetation health. One of its common uses is for identifying healthy vegetation and distinguishing it from stressed vegetation or bare soil [7]. The typical thresholds which help decide about the crop's vegetation health are the following:

  - § -1 < NDVI < 0.2: No vegetation
  - § 0.2 < NDVI < 0.4: Severely stressed
  - § 0.4 < NDVI < 0.6: Moderately stressed
  - § 0.6 < NDVI < 1: Healthy

- $GNDVI = (NIR - GREEN)/(NIR + GREEN)$:

  In contrast to NDVI, it is more sensitive to early-stage crop stress because it focuses on the green reflectance band to better assess chlorophyll concentration making it more responsive to subtle changes in plant health [9], [3]. It is suitable for monitoring crop vigor during the growing season,

as is the case of the dataset used. The typical thresholds which help decide about the crop's vegetation health are the following:

§ -1 < GNDVI < 0.2: No vegetation

§ 0.2 < GNDVI < 0.4: Severely stressed

§ 0.4 < GNDVI < 0.6: Moderately stressed

§ 0.6 < GNDVI < 1: Healthy

- $NDRE = -(NIR + RED\_EDGE)$:

It is sensitive to subtle changes in chlorophyll content and stress because it exploits the red-edge reflectance band which allows for better assessment of dense vegetation compared to NDVI [11]. It is suitable for monitoring crop stress caused by drought, pests, or diseases. The typical thresholds which help decide about the crop's vegetation health are the following:

§ -1 < NDRE < 0.1: No vegetation

§ 0.1 < NDRE < 0.2: Severely stressed

§ 0.2 < NDRE < 0.4: Moderately stressed

§ 0.4 < NDRE < 1: Healthy

- $CIG = -GREEN - 1$:

It measures the chlorophyll concentration using the green band and is less affected by soil background reflectance compared to NDVI [12]. The typical thresholds which help decide about the crop's vegetation health are the following:

§ -1 < CIG < 1.0: No vegetation

§ 1.0 < CIG < 2.5: Severely stressed

§ 2.5 < CIG < 3.5: Moderately stressed

§ 3.5 < CIG < 10: Healthy

- $CIR = -RED\_EDGE - 1$:

It focuses on the red edge band, which is strongly absorbed by chlorophyll concentration, thus it is effective for quantifying high chlorophyll content [13]. The typical thresholds which help decide about the crop's vegetation health are the following:

§ -1 < CIR < 2.0: No vegetation

§ 2.0 < CIR < 3.0: Severely stressed

§ 3.0 < CIR < 5.0: Moderately stressed

§ 5.0 < CIR < 15: Healthy

After the extraction of each VI, the resulting image is quantized to four values based on the four vegetation status of the aforementioned typical thresholds that indicate areas with a healthy plantation, a moderately stressed plantation, a severely stressed plantation or areas with bare soil and no vegetation at all. This is useful in order to better visually distinguish areas of different vegetation health status.

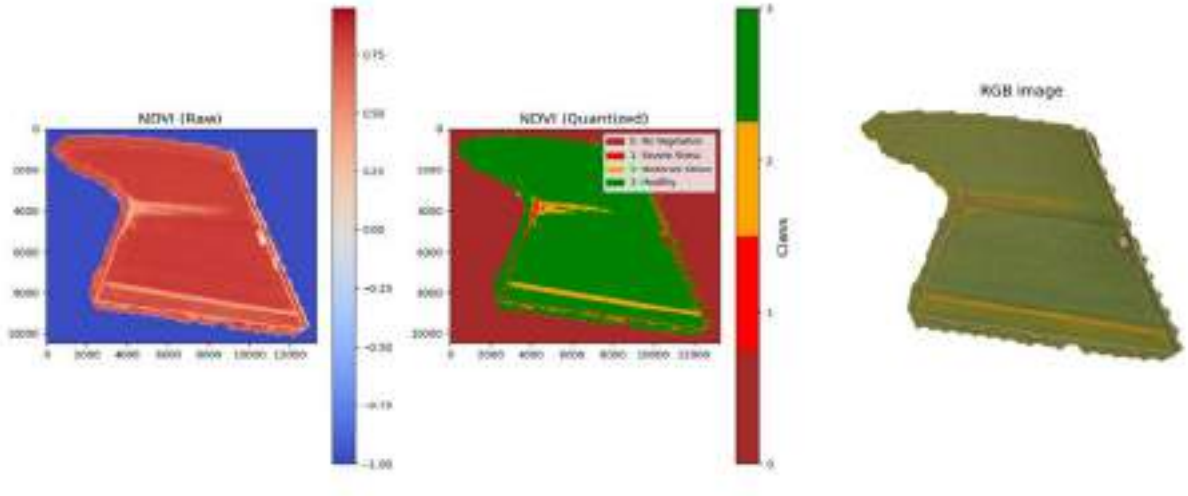

Figure 37: NDVI Maize Field Visualization

Figure 37 shows the overview of the field using RGB channels (at the right), the NDVI visualization mapping of the field (at the left), and a 4-level classification of the vegetation (at the center). The four vegetation healthiness levels of the central figure are 'No Vegetation', 'Severe Stress', 'Moderate Stress', 'Healthy'.

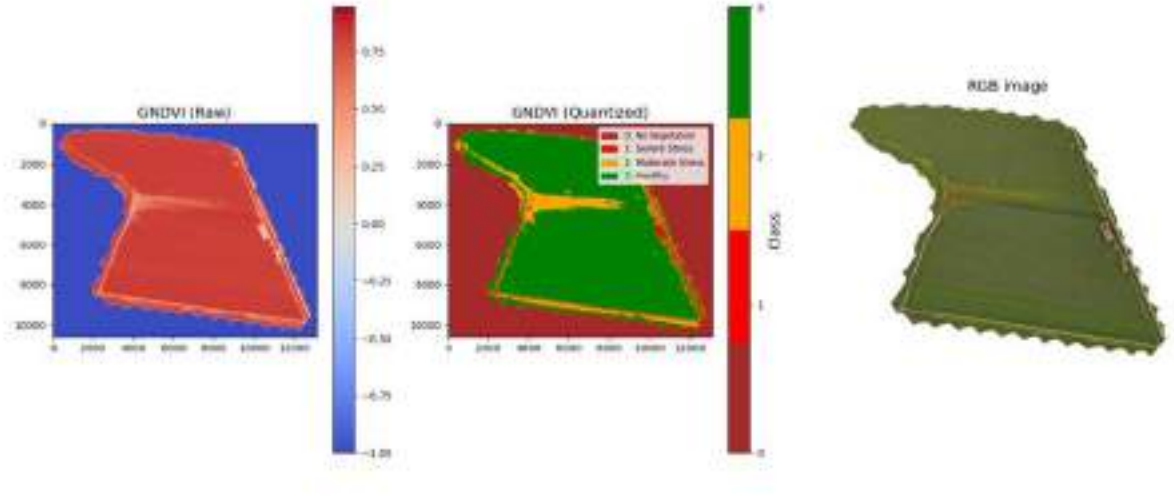

Figure 38: GNDVI Maize Field Visualizations

Figure 38 shows the overview of the field using RGB channels (at the right), the GNDVI visualization mapping of the field (at the left), and a 4-level classification of the vegetation (at the center). The four vegetation healthiness levels of the central figure are 'No Vegetation', 'Severe Stress', 'Moderate Stress', 'Healthy'.

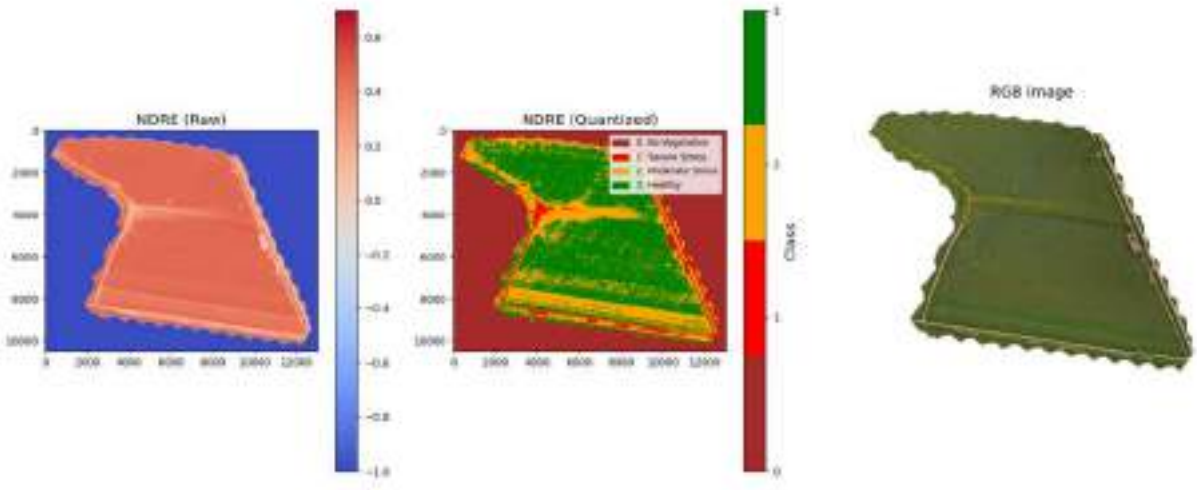

Figure 39: NDRE Maize Field Visualizations

Figure 39 shows the overview of the field using RGB channels (at the right), the NDRE visualization mapping of the field (at the left), and a 4-level classification of the vegetation (at the center). The four vegetation healthiness levels of the central figure are 'No Vegetation', 'Severe Stress', 'Moderate Stress', 'Healthy'.

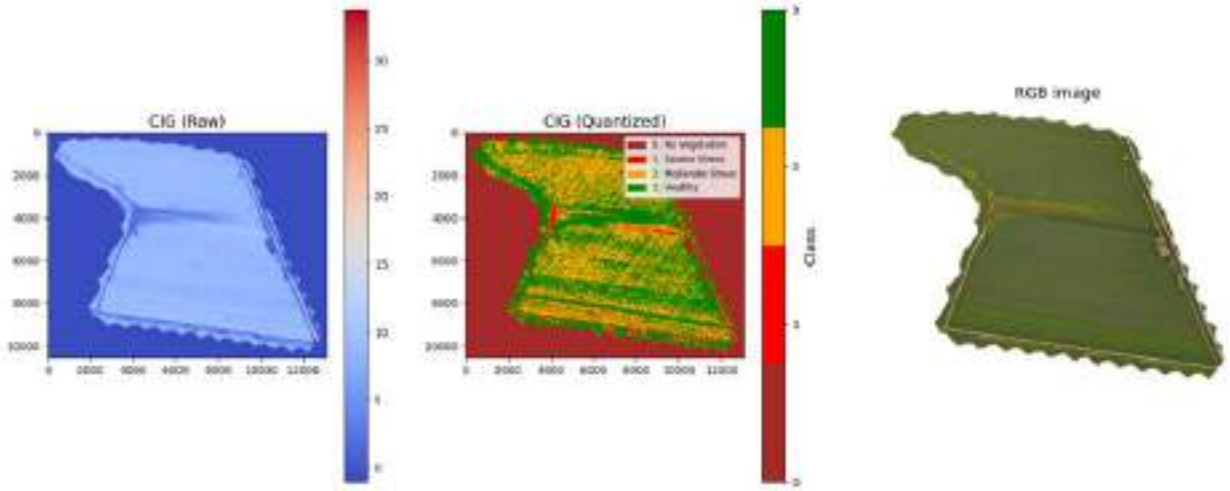

Figure 40: CIG Maize Field Visualizations

Figure 40 shows the overview of the field using RGB channels (at the right), the CIG visualization mapping of the field (at the left), and a 4-level classification of the vegetation (at the center). The four vegetation healthiness levels of the central figure are 'No Vegetation', 'Severe Stress', 'Moderate Stress', 'Healthy'.

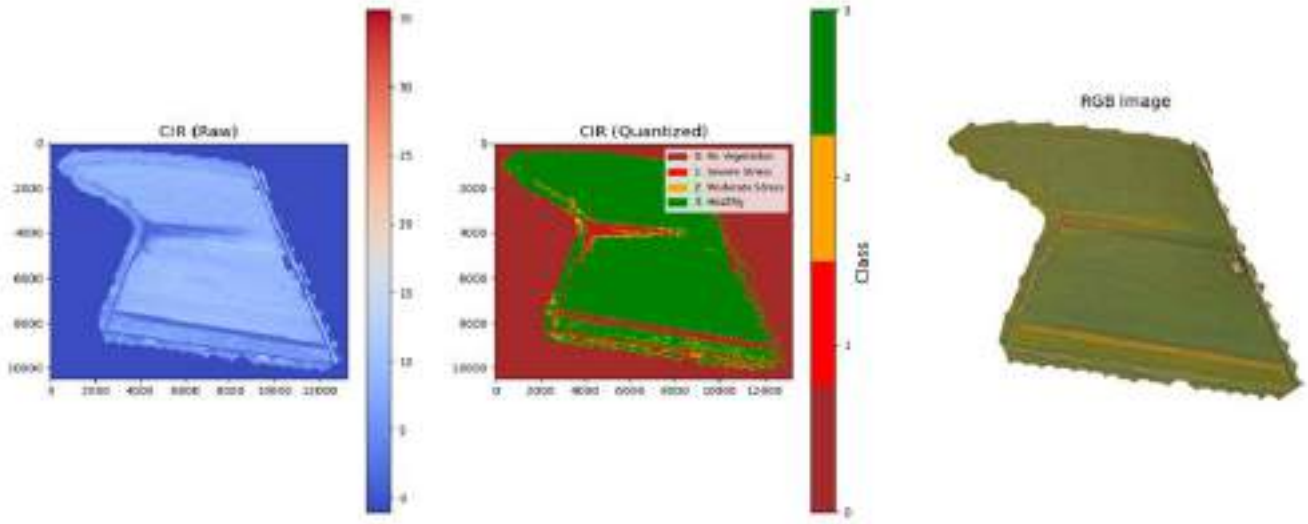

Figure 41: CIR Maize Field Visualizations

Figure 41 shows the Overview of the field using RGB channels (at the right), the CIR visualization mapping of the field (at the left), and a 4-level classification of the vegetation (at the center). The four vegetation healthiness levels of the central figure are 'No Vegetation', 'Severe Stress', 'Moderate Stress', 'Healthy'.

It can be noticed from the above visualizations, that a classification to different crop healthiness levels needs to defining the appropriate thresholds taking into consideration the type of the crop, the growth stage of the crop and also the climate conditions. Here, we used the thresholds that are typically used in similar works and this is the reason that the healthiness classification figures are not successfully depicting the vegetation differences in every VI. However, the healthiness classification figure is not essential; inspecting the appropriate VI figure and detecting even subtle differences in vegetation health using these georeferenced images can give useful insights for specific stressed areas of a field.

Each VI (or a combination of them) can be useful to detect vegetation changes at different crop growth stages. NDVI is typically used as a general vegetation health indicator, while GNDVI is better for early stage stress detection and NDRE is more suited for revealing subtle stress changes. CIR would be a good choice for changes during photosynthetic plant stages and CIG can measure the chlorophyll concentration of a crop, therefore, these VIs might not be ideal for detecting changes at the first crop growth stages.

The combination of the aforementioned VIs and the proper choice of them for each crop growth stage is crucial; not all of these VIs are suitable for every case: NDVI and GNDVI are better at the first to the mid growth stages [14] and NDRE is better for mid to late growth stages [15], while CIG and CIR would help as stress indicators at the later growth stages of the crop [16].

Such a remote-sensing monitoring system for early-stage pest identification would warn farmers that it is highly possible that pests are infesting crops of a field and in that case farmers would inspect the crops with NESTLER mobile application to verify the presence of pests.

An example of the NESTLER mobile application utility is shown at Figure 42 where a farmer captures an image of possible pest infestation on tomatoes. The image is processed by the NESTLER mobile application and if the presence of a pest is verified, then its name is displayed along with some treatment-related information.

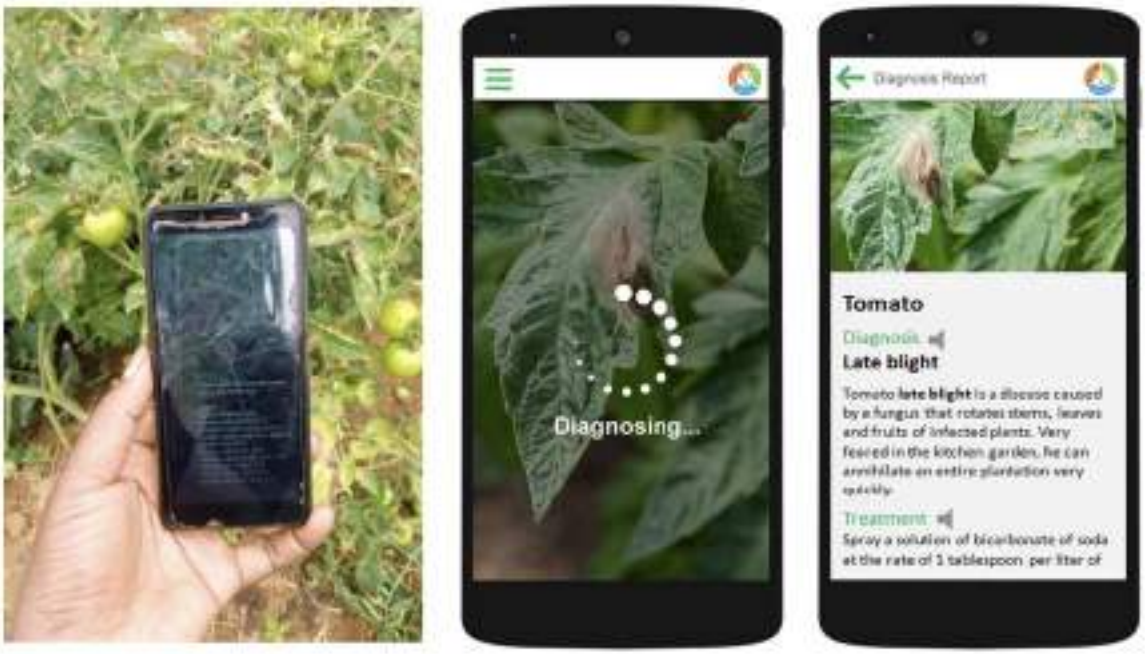

Figure 42: An example of the NESTLER mobile application utility

5.1.2. Cocoa Pest Identification

Some African countries (Ivory Coast, Ghana, Nigeria and Cameroon) currently provide more than 70% of the worldwide cocoa production [17], [18]. Hence, these countries' income depends on cocoa production. The most serious threat of cocoa production in Africa is the strong presence of diseases and pests [19]. Pest insects are one of the biggest threats facing cocoa farming in Africa. Especially Mirids are the most-detrimental cocoa pests to global cocoa production, causing 30% to 40% of cocoa production damage [20].

The identification and also localization of the infested cocoa plant area is the aim of this solution. Specifically, if pest infestation is present on a cocoa plant, then the algorithm produces an oriented bounding box around the detected pest area. We treated the problem as an object detection task fine-tuning a YoloV8 detection model.

To fine-tune the YoloV8 detector, a publicly available dataset was used [21]. The dataset includes 4 classes, 3 of them are pest classes, namely Blackpod, Frostyrot, Mirid and there is one no-pest class the Healthy class. The dataset consists of 1385 train images, 404 validation images and 202 test images. Of course, none of the test images is processed by the model during training. At Figure 43 there is shown the number of instances per class among training, validation and test parts. Since mirids are the most damaging pests of cocoa plants, reasonably mirid class images are the majority among the pest classes of the dataset.

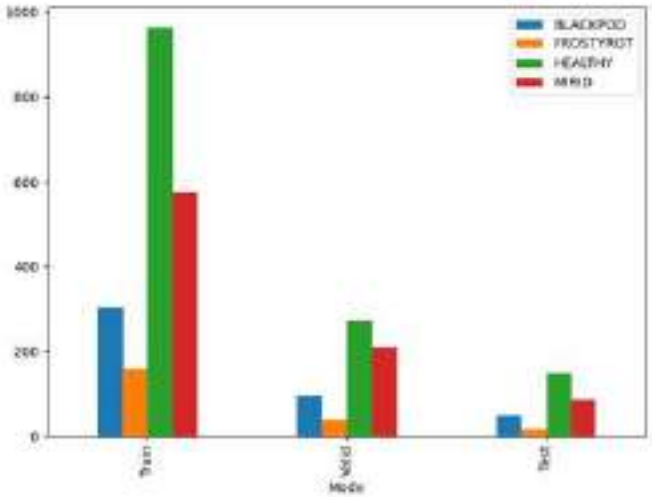

Figure 43: Number of instances per class

YoloV10 detection model was set to be fine-tuned for 400 epochs. The best training epoch (in terms of validation metrics) was 324. mAP50 and mAP50-95 as the most representative metrics used to evaluate an object detection model were explained at deliverable D3.1 (8.3.4.4, page 102) of NESTLER project. Training and validation statistics are presented at Figure 44.

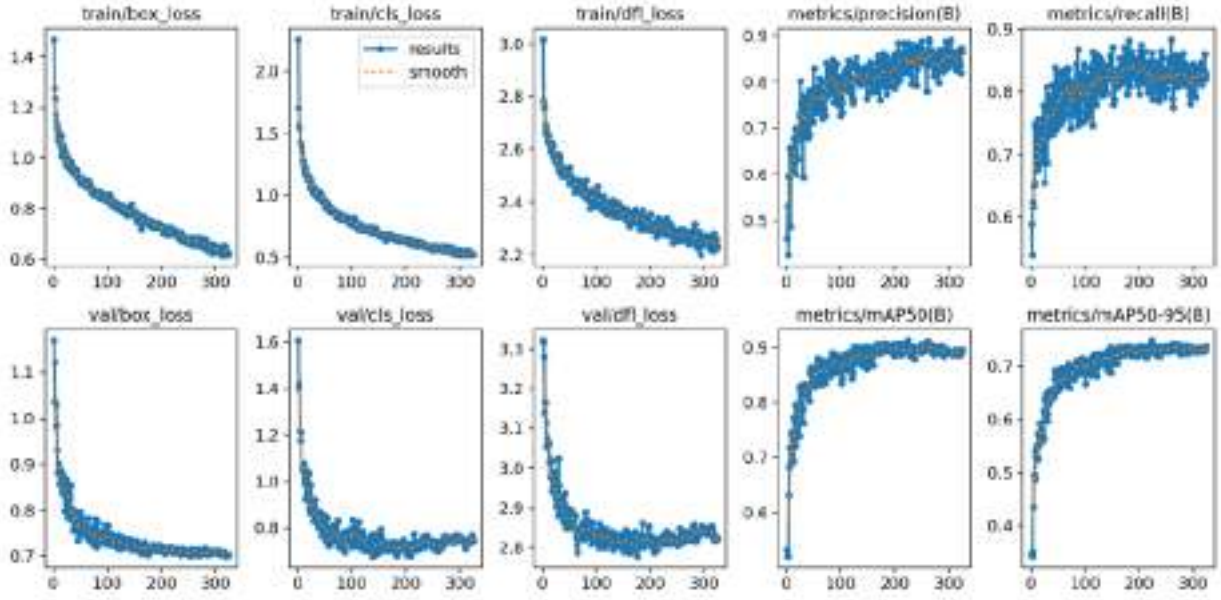

Figure 44: Training and validation loss and performance metrics (precision,recall,mAP50,mAP50-95)

At Table 1, Cocoa Detection results are shown.

Table 1: Test Cocoa Detection results. The first row shows the results for all classes and the next rows show the results per each class

Class	Images	Instances	Precision	Recall	mAP50	mAP50-95
All	202	300	0.772	0.848	0.869	0.71
Blackpod	202	48	0.886	0.75	0.837	0.659
Frostyrot	202	18	0.666	0.889	0.88	0.732
Healthy	202	148	0.795	0.899	0.906	0.767
Mirid	202	86	0.821	0.853	0.854	0.683

Considering Table 1 results, we can claim that our Cocoa Pest Detection model has a very good performance. The lower values of the rightmost column results, that is mAP50-95 column, are not discouraging, since this metric is very sensitive even to small (in terms of number of pixels) differences between the predicted and the ground truth bounding boxes. For a more intuitive evaluation, some test image results are displayed at Figure 45. A visual inspection of the results by a human is often needed and useful depending on the data. For each test image both the predicted and the ground truth labels are displayed.

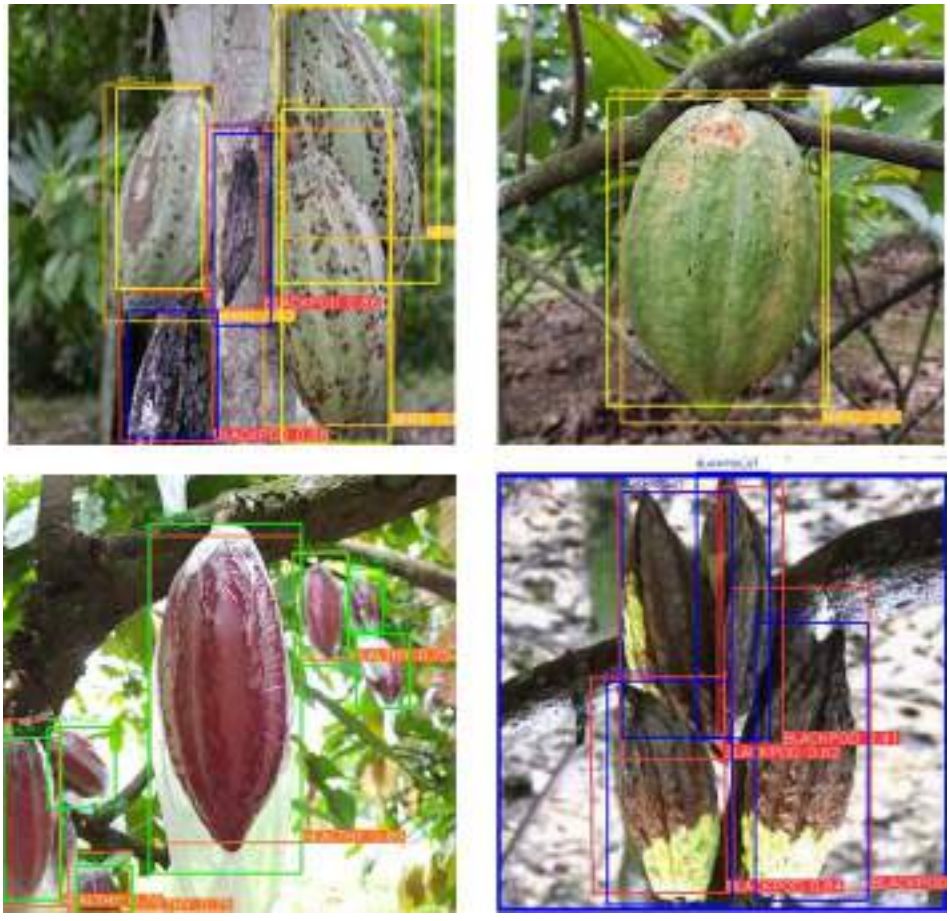

Figure 45: Sample test results. Blue and yellow bounding boxes denote the ground truth labels whereas red and orange are the predictions

5.1.3. Mango Pest Identification

The production of mango is usually severely affected by pests that attack the fruit, stem, root or mango leaf. Mango trees may suffer from many pests, whose symptoms may look alike so mango pest identification is a challenging solution.

The solved task here is an image classification problem where we performed transfer learning on a pretrained CNN model, MobilenetV3. On top of MobilenetV3 we added a two-layer fully connected network with 16 outputs, as the number of pest classes. MobilenetV3 backbone model parameters remained frozen and the trainable parameters were set to be those of the two fully connected layers on top of the backbone MobilenetV3.

Given an input image of a mango plantation, the CNN outputs the name of the pest class or a Healthy class if there is not pest infestation. The dataset used for transfer learning is publicly available [22] and includes totally 16 classes (15 pest classes and one Healthy class). Specifically, the pest classes are the following: *"Apoderus Javanicus", "Aulacaspis Tubercularis", "Ceroplastes Rubens", "Cisaberoptus Kenyae", "Dappula Tertia", "Dialeuropora Decempuncta", "Erosomyia SP", "Icerya Seychellarum", "Ischnaspis Longirostris", "Mictis Longicornis", "Neomelicharia Sparsa", "Normal", "Orthaga Euadrusalis", "Procontarinia Matteiana", "Procontarinia Rubus", "Valanga Nigricornis".*

As can be noticed from the Table 2 Number of instances per class before and after augmentation, the amount of images per class is small. Initially the dataset was already weak since it contained few images per class and also some classes were visually similar. Learning on a neural model with such a few images would probably result in overfitting. To avoid this, we performed data augmentation on the images. There were three augmentation techniques, flipping both horizontally and vertically, rotating at 30, 45, 60 and 90 degrees and also Gaussian Blurring with sigma between 0.5 to 1.5, resulting in 7 augmentations per image.

Table 2: Number of instances per pest class before and after augmentation

Pest Name	Number of Images Before Augmentation	Number of Images After Augmentation
Apoderus Javanicus	63	441
Aulacaspis Tubercularis	13	91
Ceroplastes Rubens	11	79
Cisaberoptus Kenyae	19	133
Dappula Tertia	38	266
Dialeuropora Decempuncta	30	210
Erosomyia SP	13	91
Icerya Seychellarum	27	189
Ischnaspis Longirostris	7	49
Mictis Longicornis	86	602
Neomelicharia Sparsa	36	252

Normal	36	252
Orthaga Euadrusalis	22	153
Procontarinia Matteiana	27	189
Procontarinia Rubus	26	182
Valanga Nigricornis	56	392

The dataset was firstly splitted in train, validation and test parts at a ratio of 80%/10%/10%. Then, we performed data augmentation on training and validation parts. Considering the amount of images after data augmentation (Table 3), the model is expected to have a better convergence. Of course, none of the test images are processed by the model during training (or validation).

Table 3: Number of instances before and after augmentation

	Before data augmentation	After Data augmentation
Train set	408	3192
Validation set	49	344
Test set	68	68

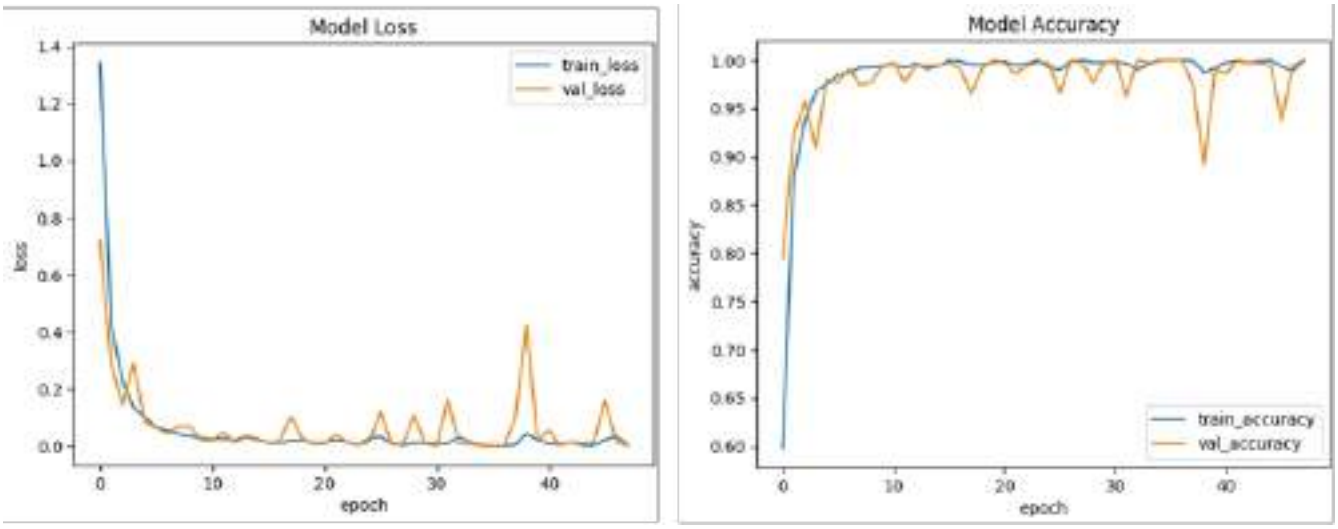

Figure 46: Training and validation loss/accuracy results

At the left part of Figure 46, there is shown the training and validation loss and at the right part there is the training and validation accuracy. Despite the spikes that occur at the validation loss and accuracy, which is reasonably caused by the limited diversity of the dataset even though we performed augmentation, we can notice that the validation curve follows the training curve, implying a satisfying training procedure.

It is also helpful to evaluate the results by visually inspecting them. Some correctly predicted images are shown in Figure 47. At the up-left corner of each image is also displayed the name of the class along with the class probability.

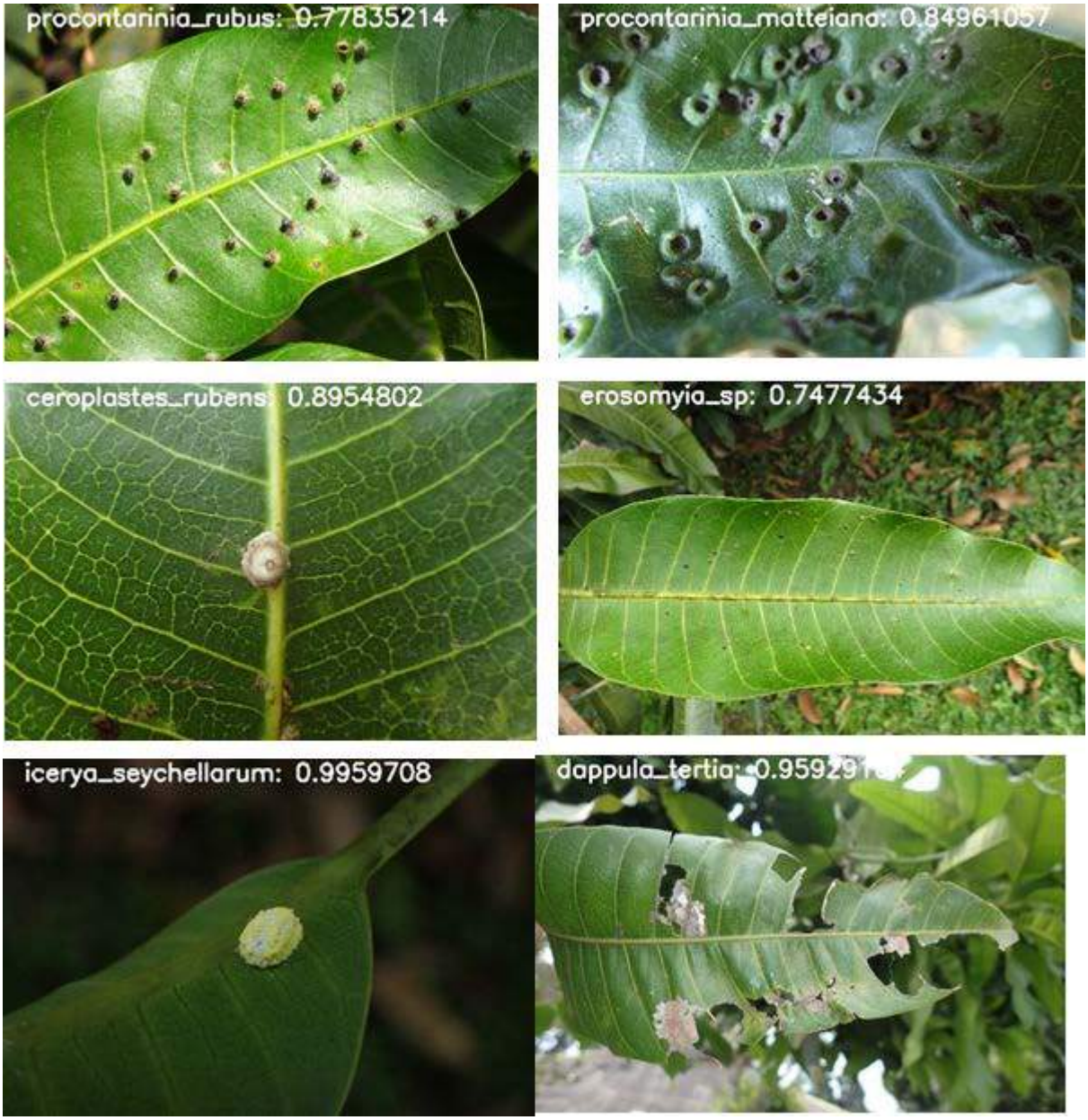

Figure 47: At the up-left corner is displayed the name of the (correctly predicted pest) class along with its probability

The classification results can be better evaluated by their metrics at Table 4. Accuracy as overall correctly predicted results is not a sufficient metric in case of imbalanced datasets. Precision and recall show the ability of the model to minimize false alarms and the ability of the model to correctly predict positive instances respectively. F1-Score as the harmonic mean of Precision and Recall is a better interpretation of the classification results.

Table 4: Mango Pest Classification Test results

Test Results	Accuracy	F1-Score	Precision	Recall
All Classes	0.8382	0.85071	0.8636	0.8382

5.1.4. Maize and Coffee Pest Identification

Maize and coffee are two of the most important crops in Africa. Maize is a staple crop for many African countries, providing food for humans and livestock, while coffee is a major cash crop, generating significant revenue for farmers and governments. Pest infestations pose a major threat to the production of these crops, resulting in substantial yield losses and economic hardship for farmers. Timely and accurate identification of pests is crucial for effective pest management. However, it can be challenging due to the resemblance of some species and the similarity of symptoms they cause on crops.

We developed a deep learning model leveraging a pre-trained model such as mobileNet V3. On top of MobilenetV3 we added a Maxpooling layer to reduce spatial dimensions and extract dominant features, then we added a three-layer fully connected network with 5 outputs, as the number of pest classes.

Given an input image, the model outputs the name of a pest or "Not a pest"if there is no pest infestation. The dataset used for transfer learning is publicly available [23]. We carefully selected in this dataset the four classes that contain images of maize and coffee pests: beetle, aphids, armyworms and corn bores.

Table 5: Number of pest images per class

Pest Name	Number of images
Beetle	112
Aphids	88
Armyworm	96
Corn bores	115
Other_insect	120

The dataset was firstly split in train, validation and test parts at a ratio of 68%/12%/20%.

Table 6: Number of pest images per set

	Number of images
Train set	361
Validation set	64
Test set	106

Figure 48 displays a few of the predictions on test images. The predicted class name and the actual class name are also shown on the top every image.

Figure 48: On the top of each image is displayed the name of the predicted class along with the actual class name

Table 7 provides metrics to more accurately assess the model performance.

Table 7: Maize and coffee Pest Classification Test results

Test Results	Accuracy	Specificity	Precision	Recall
All Classes	0.94	0.91	0.90	0.89

The developed classification model demonstrated excellent performance in distinguishing between key maize and coffee pests (Beetle, Aphids, Armyworm, Corn borers) and non-target insects. With an overall accuracy of 94%, the model correctly identifies the vast majority of insects in the test set. More importantly, the high specificity (91%) confirms its strong ability to correctly rule out non-pests (Other_insects), minimizing false alarms that could lead to unnecessary interventions. Furthermore, the balanced and high scores for both precision (90%) and recall (89%) indicate a robust and reliable model: it successfully finds most relevant pests (high recall) while ensuring that what it classifies as a pest is highly likely to be correct (high precision). This balance is crucial for building trust in an automated system designed to support effective and targeted pest management decisions.

5.2. Pest Recognition Implementation

The implementation of Pest Recognition consists of two parts; the development of the AI algorithms and the development of the Mobile Application. Part of the pest recognition implementation is already described in D3.1.

The NESTLER system identifies possible pest infested crops through visual information from the images acquired by the Mobile Application.

5.2.1. Cocoa Pest Detection Implementation

Here, we performed Cocoa Pest Detection to find the type of the pest and also its location. We utilized Ultralytics YoloV8 Detector (version 8.2.15) [24] and fine-tuned it on the 4 classes of the aforementioned Cocoa Pest detection dataset. We made use of the lightest (among Ultralytics Yolo versions) Nano version of YoloV8 since the model is destined to run in the mobile app.

We set the model to be fine-tuned for 400 epochs but considering the early stopping module, the training process took 324 epochs. For the optimizer we left the default choice which is 'auto'. It is not clear from its documentation, however Ultralytics Yolo seems to use AdamW for the first 10,000 iterations of training, and after that, it switches to SGD for the remaining process. This switching of optimizers is done based on the observation that using AdamW initially can help with faster convergence, especially during the early stages of training. However, after a certain number of iterations (in this case, 10,000), switching to SGD can provide better fine-tuning and overall performance.

Having trained and evaluated the performance of the model, we convert it and extract it in .tflite format in order to be integrated into the mobile app.

5.2.2. Mango Pest Classification Implementation

Here, we performed Mango Pest Classification to find the type of the pest in the image. We used TensorFlow (version 2.13.1[25]) to fine-tune a MobileNetV3 small CNN model at the aforementioned augmented mango pest dataset which contains 16 classes. We made use of the small version of the MobileNetV3 model because it was going to be integrated in the mobile app so there was a need for lightweight sources.

We set the (trainable part of the) model to be trained for 200 epochs but considering the early stopping module, the training process took 120 epochs. For the optimization of the model parameters, we used Adam optimizer with an initial learning rate of 10^{-3} with a decay ratio of 0.15 every 2500 training steps.

After the training and the evaluation phases, the CNN model is converted and extracted in .tflite format to be integrated to the mobile app.

5.2.3. Maize and Coffee Pest Classification Implementation

Here, we performed Maize and Coffee Pest Classification to find the type of the pest in the image. We used TensorFlow to fine-tune a MobileNetV3 model at the aforementioned Maize and Coffee Pest dataset which contains 5 classes.

We set the model to be trained for 5 epochs. For the optimization of the model parameters, we used Adam optimizer with an initial learning rate of $2x10^{-3}$.

After the training and the evaluation phases, the CNN model is converted and extracted in .tflite format to be integrated to the mobile app.

5.3. Prediction of Locust Activity Based on Environmental and Meteorological Features

The study involves evaluating the performance of predictive models under various configurations of locust classification. A binary classification approach was chosen to simplify the analysis, categorizing outcomes into two classes: "locust presence" and "no locust presence."

Due to the limited availability of relevant features in open-source datasets, meta-features were derived and utilized. These meta-features include:

- **Average temperature** over the past 62 days.
- **Total precipitation** over the past 62 days.
- **Number of rainy days** in the same period.
- **Average wind speed** for the past 62 days. These features are hypothesized to provide proxy indicators for environmental conditions conducive to locust outbreaks.

Algorithm Development

A machine learning-based binary classification model was developed and trained using historical data. The aim was to predict locust activity based on environmental and meteorological features.

Conducting the research involves analysing the performance of predictive models under different configurations of locust classification. For simplicity and clarity, a binary classification approach was chosen, where predictions are categorized as either "locust presence" or "no locust presence." Due to the limited availability of specific features in open-source datasets, meta-features were derived and utilized to improve model performance. These meta-features include the average temperature over the past 62 days, total precipitation for the same period, the number of rainy days within those 62 days, and the average wind speed over that timeframe. These features are selected based on their potential to serve as indicators of environmental conditions favourable for locust activity.

F1-score of the model is 0.86.

Model quality metrics:

Accuracy - 0.8605;

Precision - 0.8614;

Recall - 0.8613.

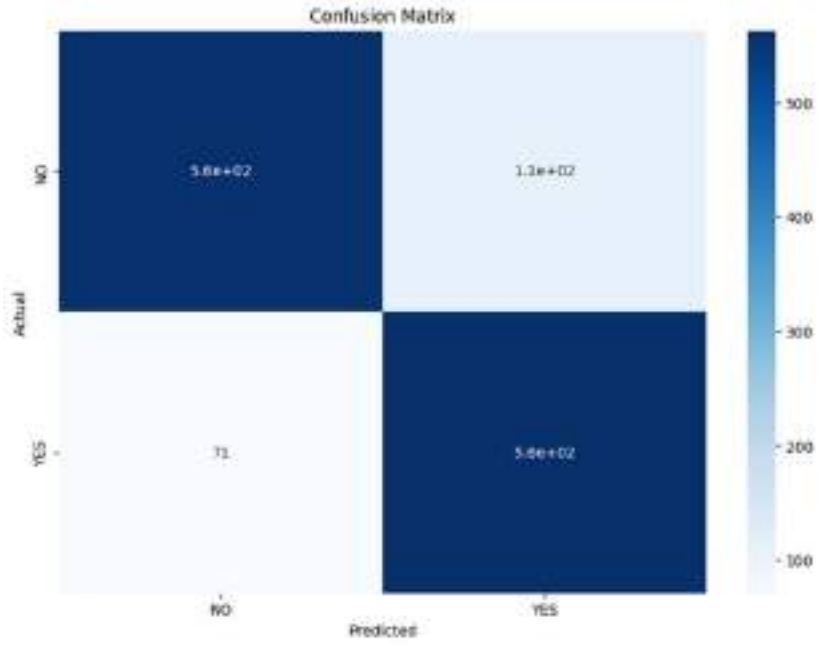

Figure 49: Confusion Matrix

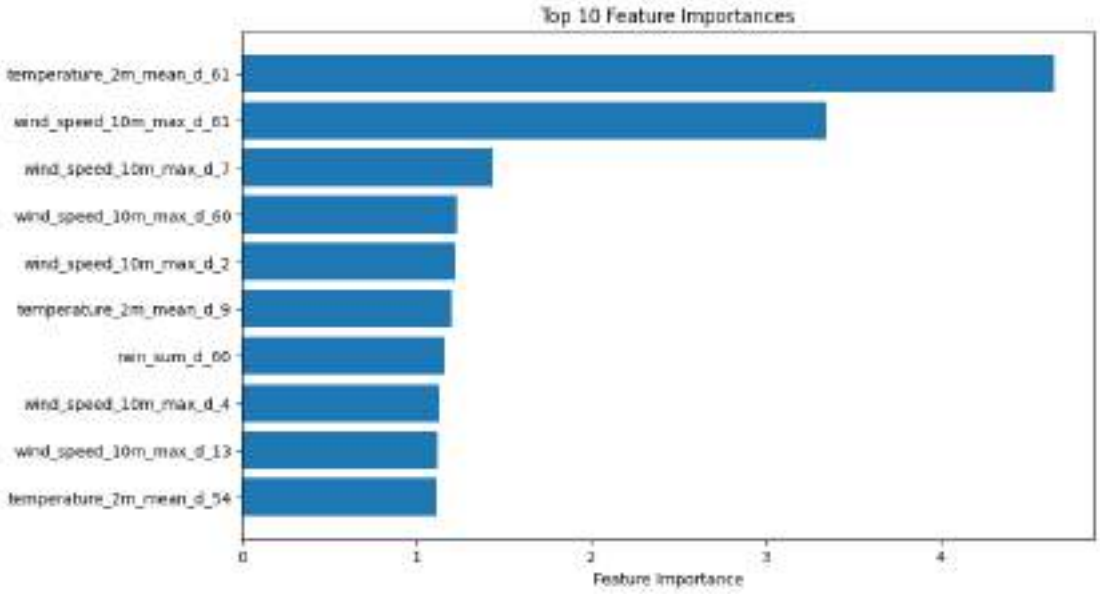

Figure 50: Important Features

Algorithm development focused on training a binary classification model using historical environmental and meteorological data. Additionally, a service was developed to facilitate the inference process. This service uses a geospatial grid system, dividing the African continent into 100 by 100-kilometer tiles. The coordinates at the intersections of these tiles serve as spatial reference points. When the service is invoked, weather data for these coordinates is retrieved, covering historical data for the preceding 46 days and forecasted data for the next 16 days. The retrieved weather data is processed into feature sets, which are then passed through the binary classification model to predict the likelihood of locust presence for the upcoming 16 days. These predictions are systematically stored in a database for further analysis and decision-making. This comprehensive approach integrates advanced machine learning techniques, geospatial data analysis, and predictive modelling to support locust management efforts.

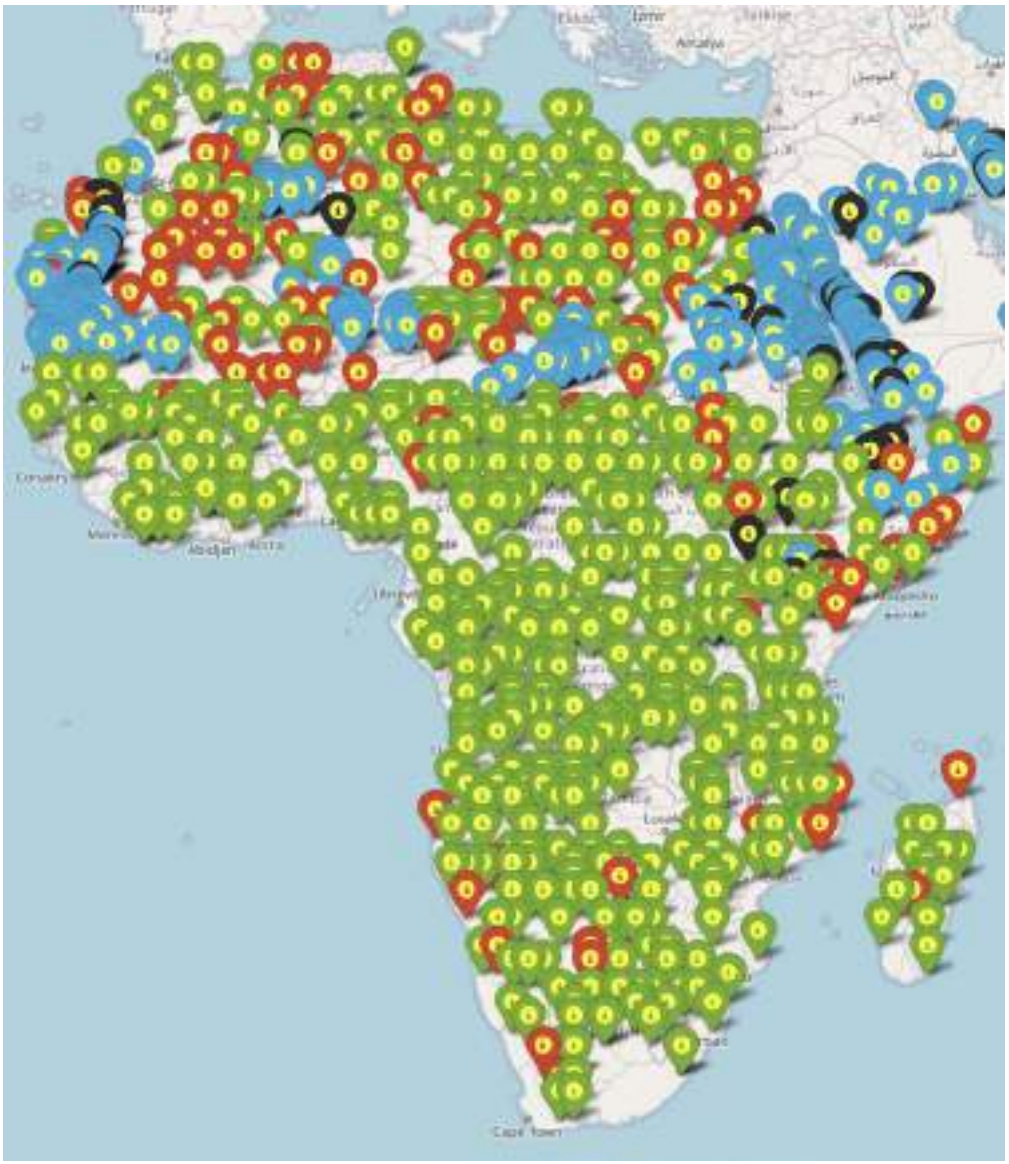

Figure 51: Map with the Markers

The following color-coded markers are used to interpret and visualize the model's prediction results:

- **GREEN markers**: Indicate instances where there are no locusts at a given point, and the model correctly predicts their absence. This represents a true negative outcome.
- **BLUE markers:** Indicate instances where locusts are present at a given point, and the model correctly predicts their presence. This represents a true positive outcome.
- **RED markers:** Indicate instances where the model predicts the presence of locusts at a given point, but actually, locusts are not present. This represents a false positive outcome.
- **BLACK markers:** Indicate instances where the model predicts the absence of locusts at a given point, but locusts are actually present. This represents a false negative outcome.

6. Insect Traps Network Subsystem Deployment

Many zoonotic diseases are driven by complex ecological interactions, often exacerbated by climate change, habitat loss, and increased human-wildlife contact. Especially in Africa, deforestation and agricultural expansion can bring humans closer to wildlife reservoirs, facilitating the spillover of diseases such as Ebola and SARS-CoV-2. The risks of cross-species viral transmission are predicted to increase with climate change, as warming temperatures alter species' habitats and behaviours, increasing opportunities for pathogens to jump between species. Moreover, there is a growing recognition that zoonotic disease management requires a multidisciplinary approach involving on one hand state of the art technology and on the other scientists, ranging from veterinarians, ecologists, technological experts to public health experts, and policymakers.

This chapter describes technological solutions for addressing interspecies interactions, zoonotic disease outbreaks and providing epidemiology reports.

6.1. Network of insects' traps to capture and analyse wild insects (mosquitoes, flies)

The project aimed to deploy a network of insect traps to identify epidemic corridors associated with zoonotic diseases. Target species included major vectors such as mosquitoes and flies, and the corresponding traps were placed in hotspots to trace geographic routes, historical epidemic pathways, and wildlife feeding patterns that facilitate disease spread.

In the second project phase, commercially available traps were selected and integrated with the NESTLER platform. Attractants were tailored to target species; for mosquitoes, host-related cues such as LED lights, CO_2, sweat mimics, and octenol were used. Trap autonomy was improved by adding photovoltaic shells and rechargeable batteries. These mosquito traps are shown in Figure 52.

Figure 52: Photos of mosquito traps

A network of 36 fly traps was deployed at locations chosen through historical data analysis, wildlife route mapping, and terrain inspections. Initial deployment took place in Kenya, followed by relocation to Rwanda to account for mosquito seasonality. Strategic placement optimised operational costs and data coverage. An example of these traps is shown in Figure 53.

Specifically for flies, traps were deployed in Coastal Kenya, at Shimba Hill area (NZI, Monoconical, biconical) to increase the catch of diverse vectors as they have different trap design preference.

The traps were deployed along national park, grazing land and home steads to map the spatial distribution of the vectors. Tsetse flies and tabanus were concentrated around the park, but stomoxys where widespread all the way to the home stead.

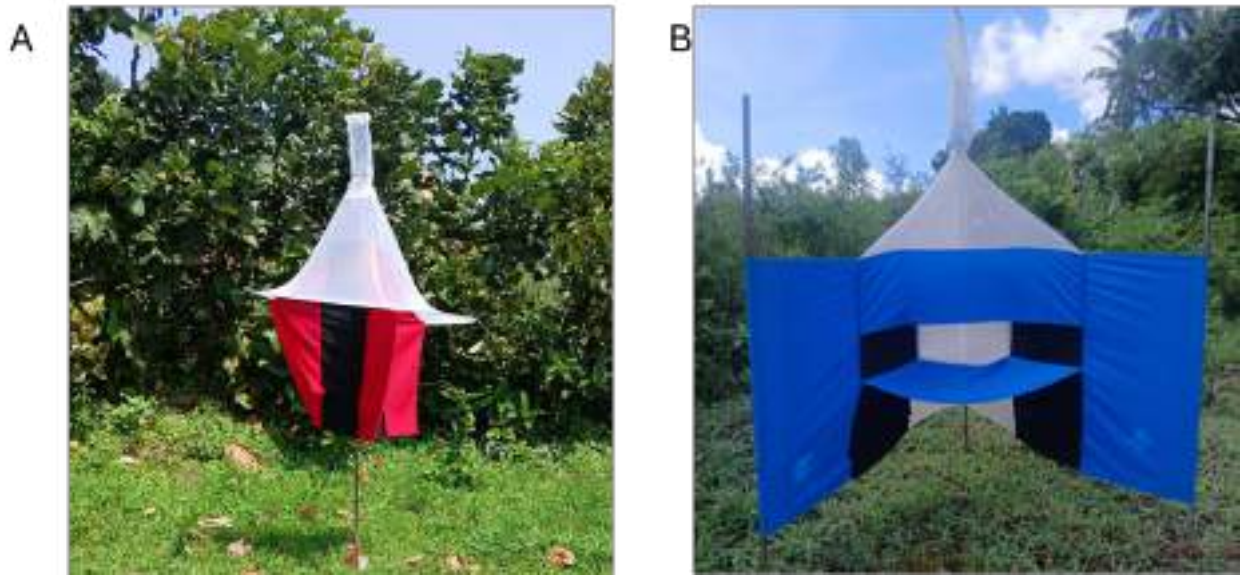

Figure 53: Photo showing biting Flies trap deployed at field sites(A)Red monoconical (B) bi-level Nzi trap

There were captured 2947 biting flies that belong to 12 species as indicated in Figure 54. The flies were identified based on morphology, where we need clarity mainly pangonia and small stomoxys we extracted the cytochrome c oxidase subunit I (COI) gene sequence for molecular confirmation. These biting flies have feeding range of wild, and domestic animals including human and associated with the transmission of dynamics of various pathogens including zoonotic. The pathogen analysis of selected vectors, which previously not characterized mainly *Haematopota pruvialis*, *Pangonia spp* and *Stomoxys s*pp is ongoing using molecular technique.

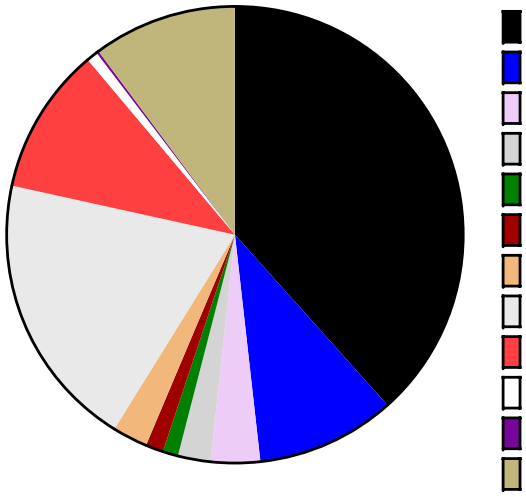

Figure 54: Pie chart showing the species diversity and their relative abundance in Shimba Hill, coastal Kenya

Similarly, the same traps diversity was deployed in Uganda to survey the vectors diversity. Specifically the two areas that were selected for the traps installation are Queen Elizabeth National Park and Bwindi. Only *Glossina pallidipes* and various Stomoxys species were captured. In Queen Elizabethe 92 tsetse flies (*G.pallidpes*) and 300 Stomoxys spp were captured, while in Bwindi 840 Stomoxys were captured. From pathogen analysis there were detected various pathogens that vary between localities and vectors. G.pallidipes were harbouring trypanosomes and Theileria (Figure 55). However, stomoxys species harbouredmore pathoges including trypanosomes, Coxiella, anaplasma, theileria and Ehlichia (Figure 56).

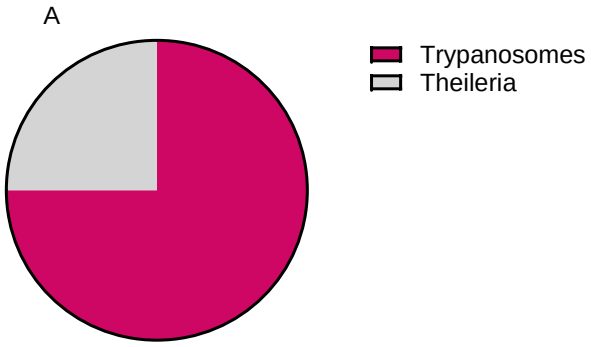

Figure 55: Pathogens diversity in vectors collected from Queen Elizabetha National Park (A)

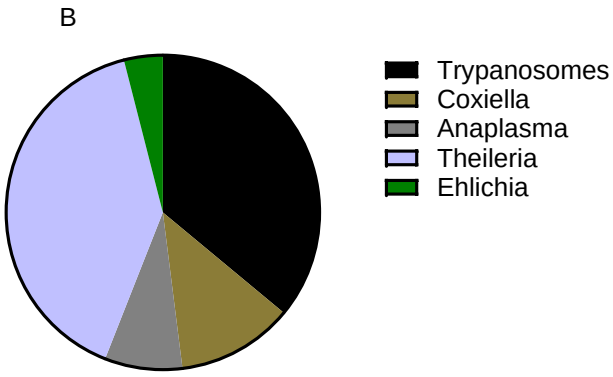

Figure 56: Pathogens diversity and prevalence in field caught G.pallidipes (B) Stomoxys species.

Mosquito traps were installed at NESTLER livestock pilot sites, slaughterhouses, and other high-risk locations across Kenya, Rwanda, and Uganda. Collected mosquito specimens were morphologically identified, processed, and stored at −70 °C for laboratory analysis.

6.2. Pathogen analysis

Pathogen detection was performed using gene extraction, pathogen testing, Nested PCR, real-time RT-PCR, standard PCR, and sequencing in accordance with manufacturer protocols.

Table 8: Various primers used for pathogens detection

Primer	Target gene	Primer sequence (5' – 3')	Product size (bp)
LCO1490 HCO2198	CO1	GGTCAACAAATCATAAAGATATTGG TAAACTTCAGGGTGACCAAAAAATCA	710
AnaplasmaJV F AnaplasmaJV R	*Anaplasma* 16S rRNA	CGGTGGAGCATGTGGTTTAATTC CGRCGTTGCAACCTATTGTAGTC	300
EHR 16SD pH1492	*Anaplasma*/*Ehrlichia* 16S rRNA	GGTACCYACAGAAGAAGTCC GGTTACCTTGTTACGACTT	1030
Ehrlichia16S F Ehrlichia16S R	*Ehrlichia* 16S rRNA	CGTAAAGGGCACGTAGGTGGACTA CACCTCAGTGTCAGTATCGAACCA	200
PER1 PER2	*Ehrlichia* 16S rRNA	TTTATCGCTATTAGATGAGCCTATG CTCTACACTAGGAATTCCGCTAT	451
Rick_F Rick_R	*Rickettsia* 16S rRNA	GAACGCTATCGGTATGCTTAACACA CATCACTCACTCGGTATTGCTGGA	364
ompB 120-2788 ompB 120-3599	*Rickettsia ompB*	AAACAATAATCAAGGTACTGT TACTTCCGGTTACAGCAAAGT	836
Trans1 Trans2	*Coxiella* IS1111	TGGTATTCTTGCCGATGAC GATCGTAACTGCTTAATAAACCG	687
RLB F RLB R	*Theileria*/*Babesia* 18S rRNA	GAGGTAGTGACAAGAAATAACAATA TCTTCGATCCCCTAACTTTC	500
ITS1_CF ITS1_BR	*Trypanosoma* sp.	CCGGAAGTTCACCGATATTG TTGCTGCGTTCTTCAACGAA	250 – 710

Molecular identification pathogens in biting flies

DNA extraction from flies

In the initial stages of DNA pre-extraction, the flies were subjected to a 1% sodium hydroxide immersion for one minute to eliminate any exogenous material on their bodies. Subsequently, they underwent a one-minute rinsing procedure with 1 × phosphate-buffered saline (pH = 7.4). Each fly was mechanically homogenized in sterilized 1.5 mL microfuge tubes containing 750 mg of 2.0-mm yttria-stabilised zirconium (YSZ) oxide beads (Glen Mills, Clifton, NJ, USA) and 80 µL of 1 × PBS using a Mini-Beadbeater-16 (BioSpec, Bartlesville, OK, USA) for one minute. Genomic DNA extraction was done using a DNeasy blood and tissue kit (Qiagen, Hilden, Germany) following the manufacturer's protocol to obtain DNA from flies for molecular analysis. The quality of the DNA obtained was assessed using a Nanodrop spectrophotometer (Thermo Scientific, Wilmington, DE, United States) by comparing absorbance at 260 and 280 nm and later stored at −20°C for molecular work.

6.3. Pathogens diversity

From pathogen analysis we detected various pathogens that varies between localities and vectors. *G.pallidipes* were harbouring Trypanosomes and Theileria (Figure 57A). However, stomoxys species harboured more pathogens including trypanosomes, Coxiella, anaplasma, theileria and Ehlichia (Fig 57B and 58).

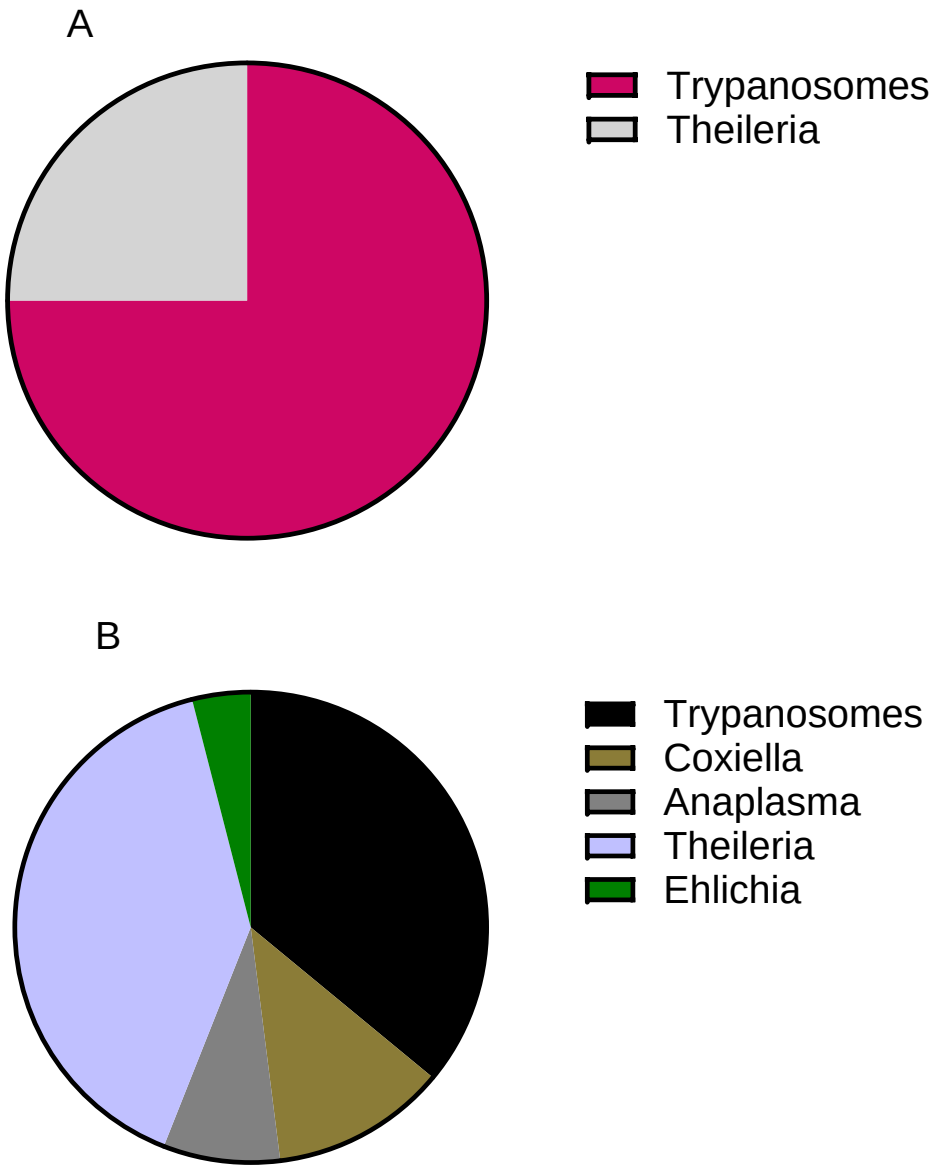

Figure 57: Pie chart showing pathogens diversity in vectors collected from Queen Elizabetha National Park (A) pathogens diversity and prevalence in field caught G.pallidipes (B) Stomoxys species

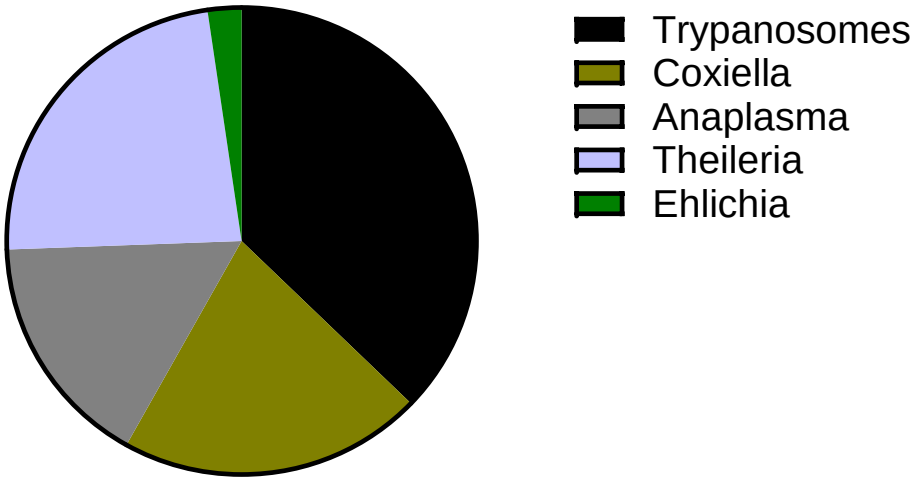

Figure 58: Pathogens prevalence in field trapped Stomoxys spp. from Bwindi area, Uganda. Trypanosomes species detected

At Queen Elizabeth, out of 24 *G.pallidipes* infected with Trypanosome species, 21 were identified as *Trypanosome congolense* and 3 as *T. brucei*. Concerning nine Stomoxys infected with trypanosomes, five and four were infected with *T. congolense* and *T. brucei*, respectively. In Bwindi, out of 32 stomoxys infected with trypanosomes, 29 were *T. congolense* and 3 were *T. brucei*.

Note: The *T. brucei* may be zoonotic pathogens responsible for human sleeping sickness, however further validation is required.

Note: Blood meal analysis and detailed pathogen analysis and identifications on going.

6.4. Traps to capture wild insects (mosquitoes) attracted by edible insects' larvae feeding

After hatching, edible insect larvae such as Black Soldier Fly Larvae (BSFL) fed on decomposing organic matter, including food waste, manure, and plant residues. This stage lasted approximately 14–18 days, depending on temperature and feed availability. During growth, the larvae progressed through multiple instars, increasing from about 1 mm to 25 mm in length and consuming large volumes of organic material, which they converted into nutrient-rich waste (FRASS).

Observation revealed that feeding and growing infrastructure, including feed storage sites, lacked adequate isolation or protection. As a result, the larvae and their feed attracted various wild, predatory, or social insects – such as domestic mosquitoes, flies, tsetse flies, and lice – that are significant carriers of vector-borne diseases, with a higher tendency to feed on livestock than humans. In regions where BSFL farming is widespread in the EU, other species, such as fruit flies and olive tree flies, were also attracted.

In the second phase of NESTLER, insect traps were deployed in and around BSFL farming and feed storage sites to study how micro-livestock and feedstock farming activities influence the presence of

harmful wild insects. The monitoring focused on assessing whether BSF and BSFL activity could contribute to the emergence of new zoonotic hotspots and epidemic corridors.

Findings will be shared with EU policy regulators to inform guidelines and biosecurity measures for edible insect farming.

6.5. NESTLER platform for Big-data visualisation for interactive GIS presentation of NESTLER results and epidemical reports

The process of implementing the interactive GIS visualization of platform outcomes and epidemiological risk assessment adheres to the following sequence.

Initially, the platform collects via the NESTLER restful API and stores all relevant data in the database, including geographical regions, traps' captures, IoT device readings (from SynField and cassava handheld tools), as well as information on weather, soil and water conditions, wildlife, animals and aquaculture well-being data, weather, floods and drought forecast, and other environmental factors. Based on this raw data, zoonotic disease outbreaks are then calculated and the resulting insights are also stored in the database.

The aforementioned data are available in the NESTLER platform services (e.g. dashboard) via the published layers in the geospatial server cluster and the NESTLER restful API. The below figures depict indicative layers that have been published in the geospatial server cluster.

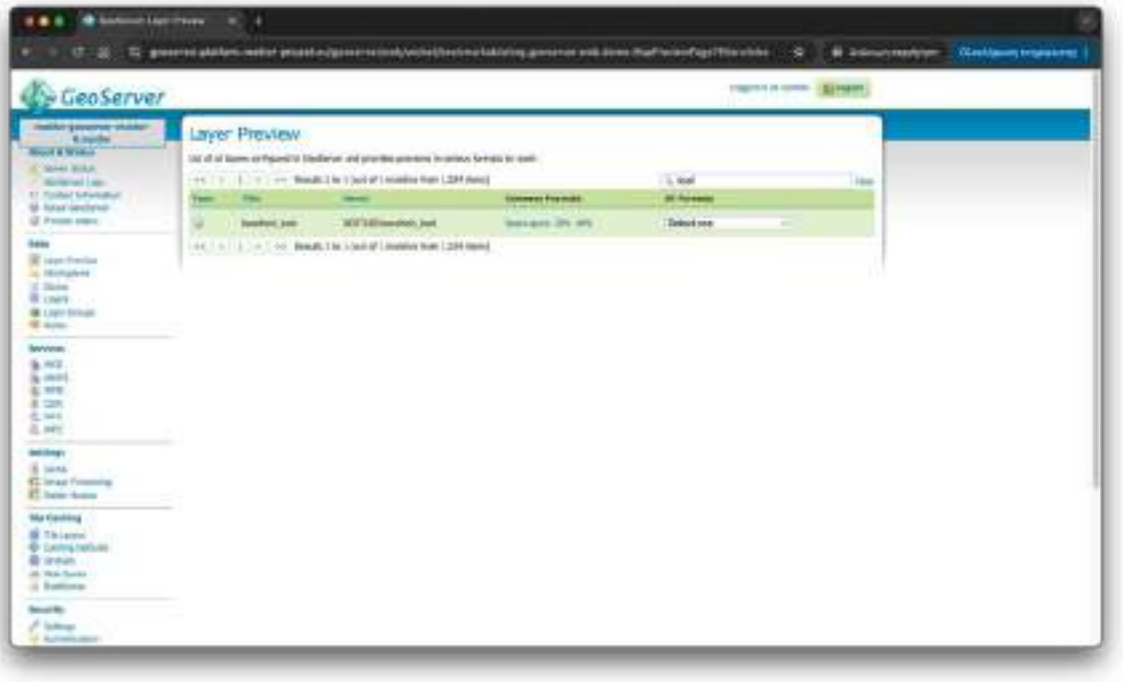

Figure 59: Published WFS layer for the measurements of the handheld devices

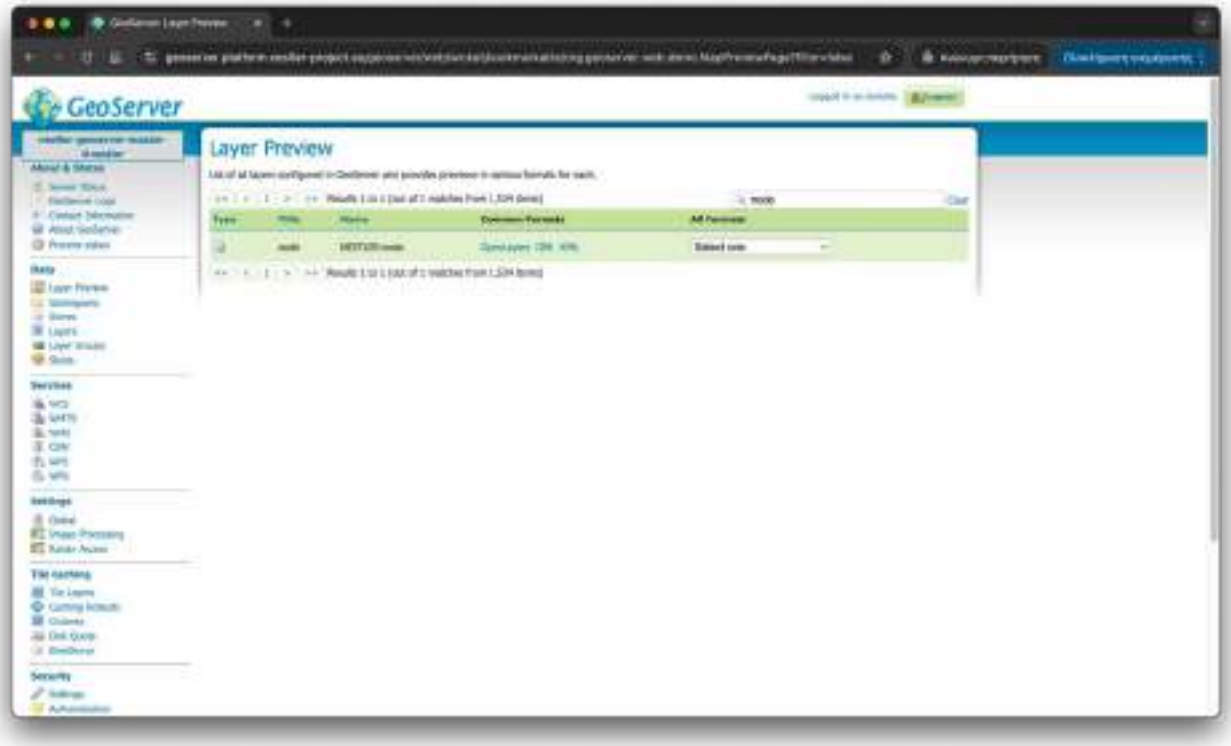

Figure 60: Published WFS layer for the measurements of the SynField devices

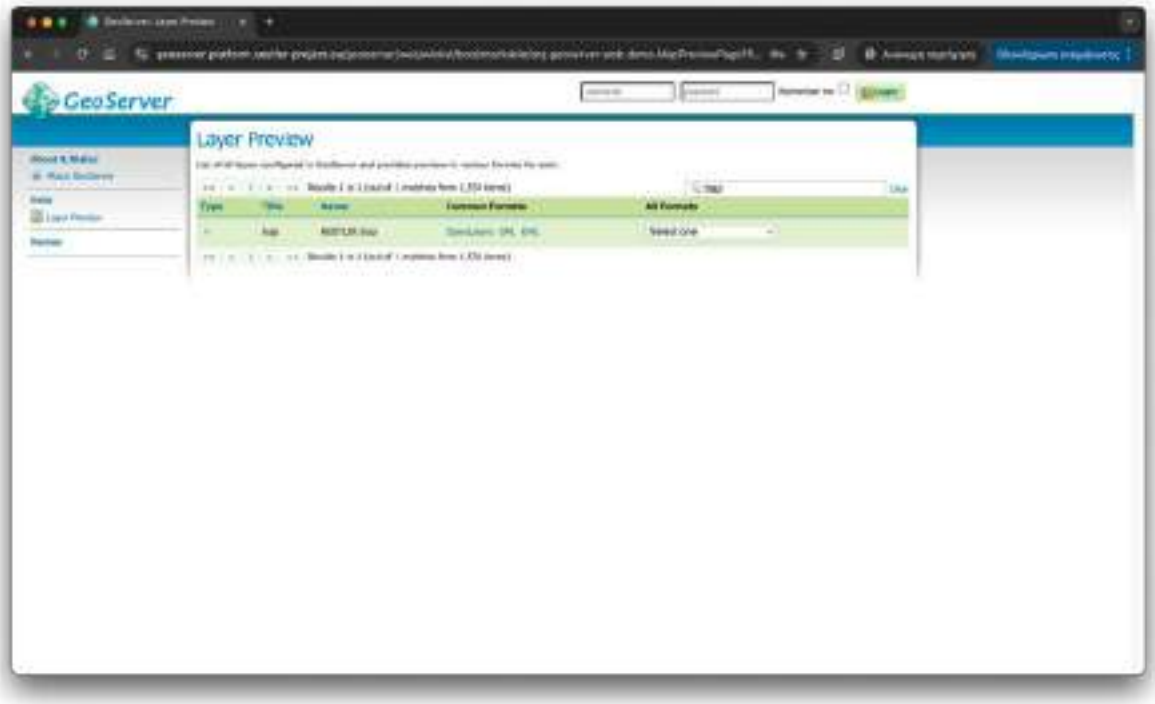

Figure 61: Published WFS layer for the captures of the traps

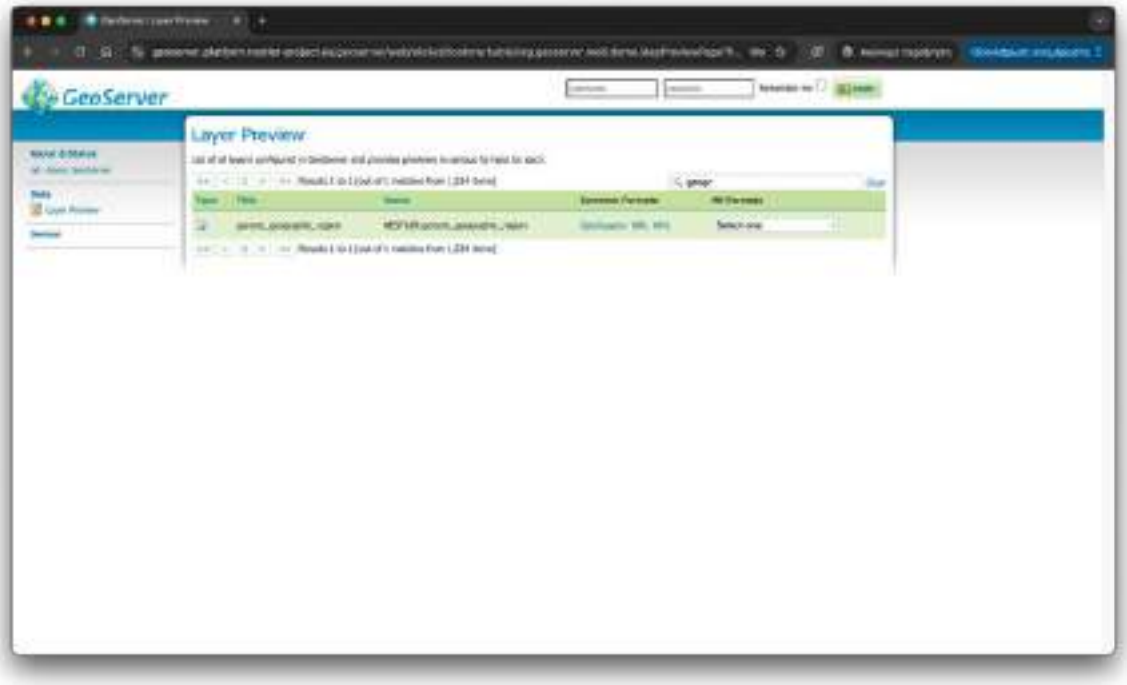

Figure 62: Published WFS/WMS layer for the geographic regions in pilot countries

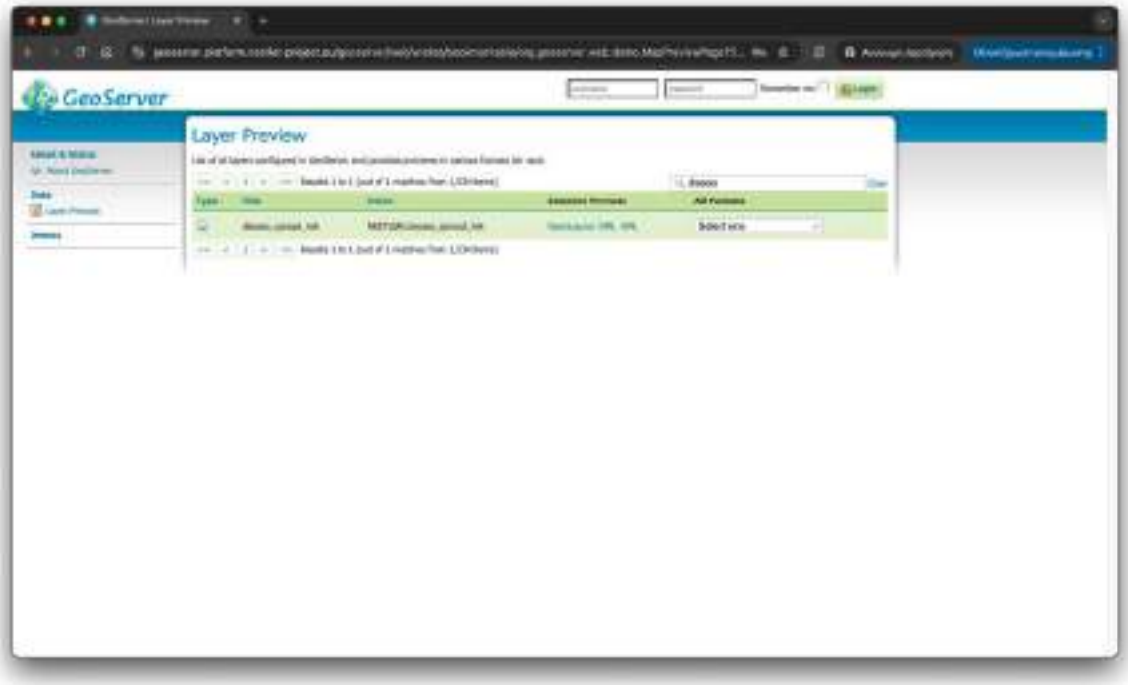

Figure 63: Published WMS layer for the disease spreading risk in pilot countries

Geospatial server cluster exposes OWS interfaces such as WMS and WFS. To fetch the first 50000 entries of a layer (*layer_name*), the below service could be invoked:

```
GET https://geoserver-api.platform.NESTLER-project.eu/geoserver/NESTLER/ows?service=WFS&version=1.0.0&request=GetFeature&typeName=NESTLER&{layer_name}&maxFeatures=50000&outputFormat=application/json
```

To fetch the representation of a WMS layer (*layer_name*) in specific BBOX as an PNG image, the below service could be invoked:

```
GET http://geoserver-api.platform.NESTLER-project.eu/geoserver/NESTLER/wms?service=WMS&version=1.1.0&request=GetMap&layers={layer_name}&bbox=-180.0,-90.0,180.0,90.0&width=768&height=384&srs=EPSG:4326&styles={style}&format=image/png
```

Both WMS and WFS layers are consumed in the NESTLER dashboard allowing end-users to view and interact with the installed traps and devices, their measurements and other types of data. The following figure depicts an initial snapshot of the installed traps, SynField devices and cassava handheld devices and the geographic regions in six pilot countries.

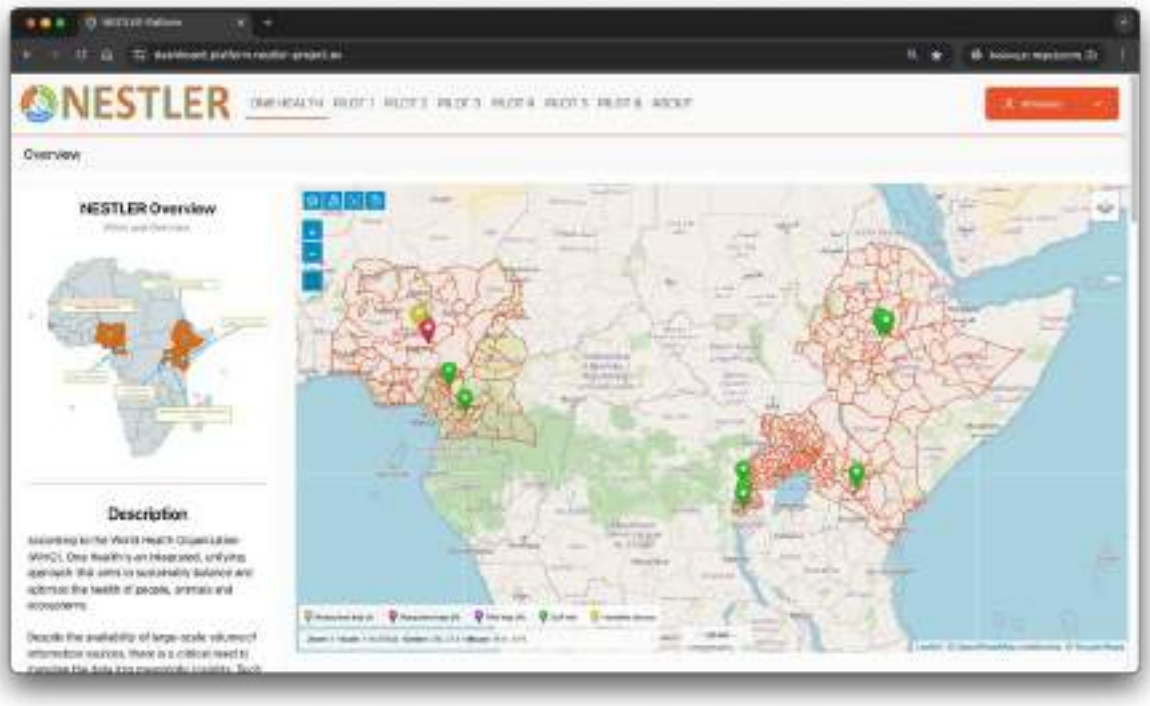

Figure 64: Interactive GIS that presents the various layers in the landing page of the dashboard

7. Last Mile Wireless Communication For Data Transmission

This chapter discusses the significance of last-mile wireless communication technologies in the context of smart agriculture, with particular emphasis on their application in the EU NESTLER project. By employing innovative solutions such as the RapidNet mesh topology, wireless transmission protocols, and terrestrial data transfer protocols, smart agriculture initiatives enhance data collection, communication, and decision-making processes.

7.1. Overview of Last Mile Wireless Communication

Last-mile wireless communication technologies are pivotal for connecting remote, data-rich environments with centralized decision-making systems. In smart agriculture, where farmlands are often located in regions with sparse communication infrastructure, innovative solutions are required to bridge this gap and ensure reliable real-time data collection and transmission.

Task 3.5 of the NESTLER project addresses this challenge by implementing a last-mile communication platform using UAV-based mesh networks. The Mesh-in-the-Sky architecture, developed in collaboration with RINIS and eBOS, enables robust, energy-efficient, and scalable communication for IoT sensors deployed across agricultural landscapes.

7.2. Mesh Topology of RapidNet (Mesh in the Sky) Rinicom

MESH network is a further application of mobile ad-hoc networks in the field of drones. Different from the common mobile AD hoc network, network nodes in drone mesh networks are not affected by terrain during movement, and their speed is generally much faster than that of traditional mobile self-organizing networks.

Its network structure is mostly distributed. The advantage is that routing selection is completed by a small number of nodes in the network. This not only reduces the network information exchange between nodes but also overcomes the disadvantage of over-centralized routing control.

The network structure of UAV swarm MESH networks can be divided into planar structure and clustered structure[1].

In the planar structure, the network has high robustness and security, but weak scalability, which is suitable for small-scale self-organizing networks.

[1] https://www.iwavecomms.com/news/3-network-structures-of-micro-drone-swarms-mesh-radio/

In the clustered structure, the network has strong scalability and is more suitable for large-scale drone swarm ad-hoc networking.

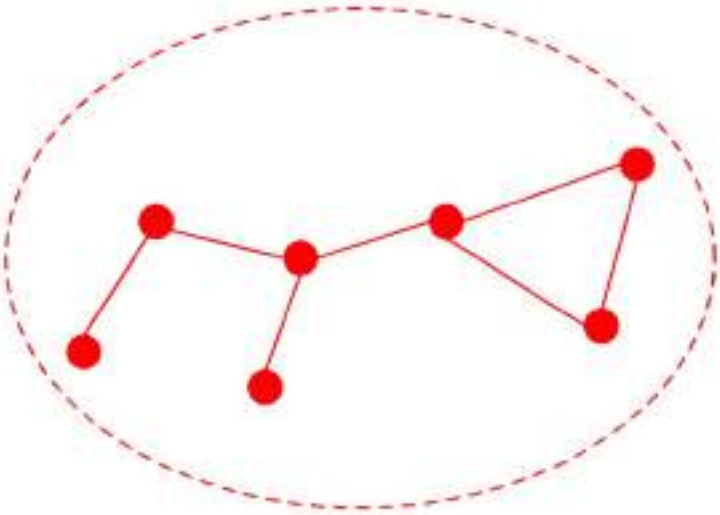

Figure 65: Planar Structure

The planar structure is also called a peer-to-peer structure. In this structure, each node is the same in terms of energy distribution, network structure, and routing selection.

Due to the limited number of drone nodes and simple distribution, the network has strong robustness and high security, and the interference between channels is small.

However, as the number of nodes increases, the routing table and task information stored in each node increases, the network load increases, and the system control overhead increases sharply, making the system difficult to control and prone to collapse.

Therefore, the planar structure cannot have a large number of nodes at the same time, resulting in poor scalability and is only suitable for small-scale MESH networks.

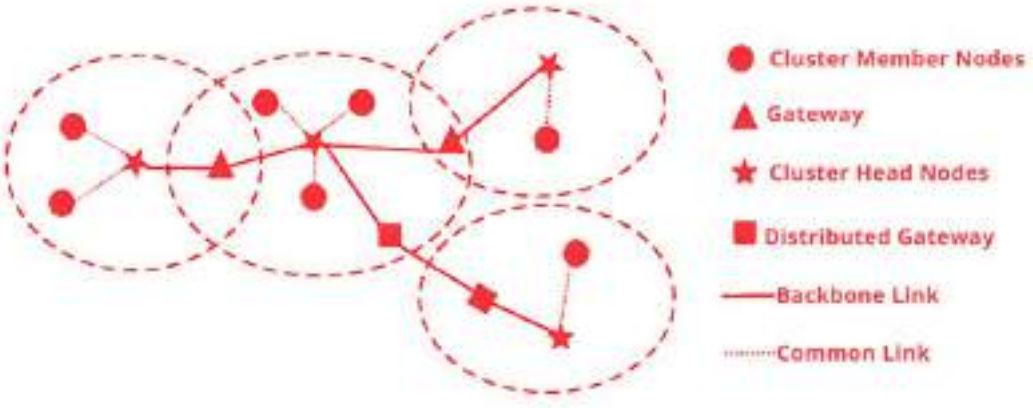

Figure 66: Clustered Structure

RapidNet's "Mesh in the Sky" architecture uses a planar network structure, providing flexibility and reliability for last-mile communications in smart agriculture. Its decentralized and dynamic design makes it particularly suitable for large-scale agricultural operations and projects such as NESTLER.

Applications in Smart Agriculture:

1. **Field Sensor Networks**: Sensors monitoring soil moisture, temperature, and crop health can connect via the RapidNet mesh topology. The decentralized system ensures continuous data collection even if some nodes fail due to harsh weather or equipment malfunction.
2. **UAV Integration**: Drones equipped with RapidNet-compatible nodes can relay real-time data from remote fields to central servers, supporting tasks such as crop mapping and pest monitoring.
3. **Scalability for Large Farms**: As farms expand, additional sensors or devices can be seamlessly integrated into the network without requiring extensive reconfiguration.

NESTLER Project Implementation:

The NESTLER project aims to enhance agricultural productivity through real-time data-driven interventions. RapidNet could be deployed to create a resilient communication network across diverse terrains and regions:

- **Node Placement**: Strategic placement of nodes ensures data flow across vast agricultural plots.
- **Integration with Iota Devices**: The mesh supports Iota devices monitoring crop conditions, water usage, and greenhouse environments.
- **Disaster Recovery**: In case of network disruptions due to storms or equipment failure, RapidNet's self-healing capability ensures continuity in data transmission.

7.3. Wireless Transmission Protocol Overview

Wireless transmission protocols underpin the seamless operation of smart agriculture technologies, enabling the transfer of vast amounts of data from sensors, drones, and other devices to decision-making systems.

Applications in Smart Agriculture:

1. **Wi-Fi (802.11):** Localized data transfer in greenhouses or warehouses where high-speed communication is essential.
2. **Zigbee:** Low-power communication for battery-operated sensors monitoring parameters like soil pH and humidity.
3. **LoRaWAN:** Ensures long-range communication for sensors located across vast farmlands, particularly useful for crop fields and pastures.

4. **5G NR:** High-speed, low-latency communication enables real-time video feeds from drones or autonomous vehicles.

NESTLER Project Implementation:

The project's focus on real-time agricultural insights can benefit from these protocols:

1. **LoRaWAN for Field Data:** Long-range communication between field sensors and gateways allows efficient monitoring of crops in remote locations.
2. **5G for Autonomous Systems:** High-speed 5G networks facilitate the operation of autonomous farming equipment, such as tractors or drones, which require instantaneous communication.
3. **Data Aggregation:** Centralized hubs within the NESTLER framework can use Zigbee for localized data collection and Wi-Fi for high-speed data uploads to the cloud.

7.4. Terrestrial Data Transfer Protocol

Terrestrial data transfer protocols address the challenges of connecting agricultural fields to centralized data centers or cloud platforms. They ensure reliable communication even in environments with limited infrastructure or high variability in connectivity.

Applications in Smart Agriculture:

1. **TCP/IP (Tactical Variant):** Facilitates reliable data transfer over inconsistent networks, ideal for remote farms where connectivity fluctuates.
2. **DTN (Delay-Tolerant Networking):** Supports periodic data uploads from sensors in areas with intermittent connectivity. For instance, mobile devices or drones can collect data and upload it when within range of a base station.
3. **MPLS:** Efficiently manages data prioritization, ensuring that critical information like pest outbreak alerts is transmitted first.

NESTLER Project Implementation:

The NESTLER project can integrate terrestrial data transfer protocols to ensure consistent and prioritized communication:

1. **Field-to-Cloud Data Transmission**: DTN can be used in areas with weak terrestrial infrastructure, allowing devices to store and forward data when connectivity is available.
2. **Prioritized Data Management**: MPLS ensures that time-sensitive data, such as irrigation needs or disease outbreak warnings, is transmitted without delay.
3. **Hybrid Communication Models**: Combine terrestrial protocols with wireless systems to maintain robust communication networks across NESTLER project regions.

7.5. System Architecture and Methodology

The Mesh-in-the-Sky system architecture (Figure 67) integrates Unmanned Aerial Vehicles (UAVs) equipped with RiniMesh Software-Defined Radios (SDRs) to create a self-healing, multi-hop mesh network. This architecture addresses connectivity issues in regions lacking cellular or long-range terrestrial networks. The system is designed to aggregate data from ground-deployed IoT sensors and relay it to data processing centers, enabling seamless monitoring of agricultural environments.

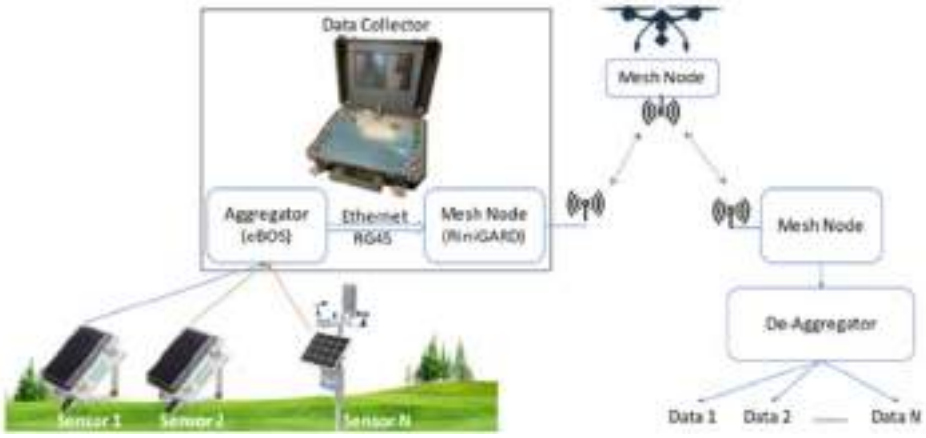

Figure 67: Mesh-in-the-Sky UAV-based Communication System

The UAV-based mesh network utilizes SDR nodes that dynamically form an ad-hoc communication infrastructure. The mesh topology adheres to a planar structure, ensuring a balance of robustness and reliability for small- to medium-scale deployments. Each UAV node autonomously adjusts its routing configuration, optimizing energy usage and data transmission pathways. To maintain seamless communication, critical factors such as node placement, signal strength, and power consumption were optimized.

A key innovation of the system lies in the integration of environmental IoT sensors deployed in agricultural fields. These sensors continuously monitor parameters such as soil moisture, temperature, and crop health, generating critical insights for agronomic decision-making. Data from these sensors is collected and aggregated using a Data Aggregator equipped with LoRa and BLE modules. The aggregated data, formatted in JSON, is relayed to the cloud through MQTT protocols for visualization on advanced dashboards.

7.5.1. Sensors

The sensors are designed to continuously collect a range of environmental data, including soil moisture, temperature, humidity, light intensity, and factors affecting crop health [26], [27], as well as crop quality at the end of the production cycle providing critical insights for agronomic decision-making [30]. This

aggregated data provides a real-time, detailed view of environmental conditions, enabling predictive assessments of crop quality and enabling tailored agronomic interventions [28].

The field sensors utilize various communication interfaces, including cellular or LoRa coverage when available [28], [31]. However, to represent diverse agroecological conditions in pilot regions, these sensors are often deployed in areas with limited or no cellular or LoRa coverage [32]. For instance, one NESTLER pilot in Nigeria aims to model cassava yield across six distinct agro-ecological zones, spanning regions from the Atlantic coast to the Sahel [33]. In such remote sites with limited network coverage, the proposed Mesh-in-the-Sky ensures seamless integration and connectivity with all deployed sensors, maintaining reliable data aggregation and communication.

7.5.2. Ground Station Case

Seamless integration with deployed sensors is achieved through the proposed Data Collector (DC) or Ground Station (GS), specifically designed for installation in areas with limited or no communication infrastructure. The GS is responsible for aggregating data from the sensors and serves as a host for a mesh node or Software Defined Radio (SDR) device known as RiniGARD, along with a Data Aggregator and a laptop for verifying internet connectivity across the regions. Additionally, the ground station can interface with any Internet Protocol (IP) system, such as IEEE802.11xx or LoRa, thereby simplifying integration processes and enhancing the reliability of communication.

7.5.3. Data Aggregator

The Data aggregator is a device specifically designed to support the complete operating cycle of the mesh radio architecture (Figure 64). It serves as a critical component for receiving and transmitting data to the cloud [34]. At its receiving end, the device features two communication protocols: a Long-Range Radio Module (LoRa) and a Bluetooth Low Energy Module (BLE), which are embedded in the Infineon CYBLE-416045-02EZ-BLE Microcontroller Unit (MCU).

The LoRa and BLE communication modules retrieve data from a network of sensors and store it in the MCU memory. In addition to data storage, the MCU processes and prepares batches of data for cloud transmission [35]. The final step of the Data Aggregator involves transmitting the aggregated data from the aggregator to the cloud via the Mesh in the Sky network. The Data Aggregator is configured to send data in JSON format to an MQTT broker via the Message Queuing Telemetry Transport (MQTT) protocol. Once transmitted, the data is represented on a dashboard using data visualization tools.

Figure 68: Data Aggregator PCB

7.5.4. Mesh Nodes - Software Defined Radio

The Rinimesh Software Defined Radio (SDR), as the main component of the concept of operations (CONOPS) architecture, is a device that manages radio communication and signals via software. Its software capabilities handles both the modulation and demodulation of radio signals, enabling seamless data transmission and reception using predefined communication protocols, including IEEE 802.11xx.

The SDR offers, in a single device, a database of waveforms to meet different customers' needs across a wide range of wireless applications and uses.

Additionally, the SDRs can be connected on an ad-hoc basis to form a network that allows each radio to automatically connect to other nodes and establish a self-healing, mobile, and dynamic IP mesh network. Each node automatically routes data around the wireless network and can be easily configured to operate without user intervention. This makes the system ideal for harsh environments and rapid deployment scenarios.

Figure 69: NESTLER Mesh in the Sky Radio Node

7.5.5. Mesh in the Sky

The Mesh-in-the-Sky is an IP based communication system designed in accordance with the NATO IST 118 standard [36]. This standard is specifically developed for mesh communication in disadvantaged networks where traditional ground infrastructure is either limited or not available. The system operates as a broadband mesh network, capable of supporting speeds up to 100 Mb/s (depending upon the range), with guaranteed connectivity of 20 Mb/s for UAVs operating at ranges of up to 20 km from the Ground Station (GS). Its flexible architecture allows for the deployment of multiple ground stations distributed upon the area of interest.

The system supports multiple live High Definition (HD) video streams from drones, providing real-time situational awareness and video surveillance. These capabilities are invaluable for analytical applications, such as early fire detection, fire size estimation and the integrations of other IoT sensors. In addition, the system transmits critical flight related data, including GPS coordinates, control signals and telemetry.

The Mesh-in-the-Sky system architecture allows the installation of various IoT sensors either directly connected on the Drone or indirectly via a Ground Station. Sensors integrated directly into the Mesh-in-the-Sky, significantly simplify the overall networking architecture enabling real time transmission of sensory data over vast surveillance areas. In cases where direct integration is not feasible, sensors can be connected to the nearest Ground Station, from where the aggregated traffic will be transmitted to any control centre via Mesh-in-the-Sky.

7.6. Field Validation and Real-World Trials

The system underwent rigorous testing in controlled laboratory environments and real-world agricultural settings.

The Mesh-in-the-Sky infrastructure was tested and verified in the field transferring data from field-deployed IoT sensors. IoT communication was integrated with the Wireless Mesh and connected to the Internet via a 5G router, enabling Internet access for the sensors. The wireless mesh reliably transported images and HD videos from the field.

The demonstration had two stages. In stage one, sensors and one SDR on Station A, and Ground Station B shown in Figure 66, were deployed at a distance where the two SDRs could not communicate. This was confirmed via the open source device management platform as in Figure 70. Field trials demonstrated the ability of the Mesh-in-the-Sky system to achieve seamless connectivity over distances of up to 20 kilometers. The system reliably transported environmental sensor data, HD video streams, and telemetry from UAV nodes to central data hubs.

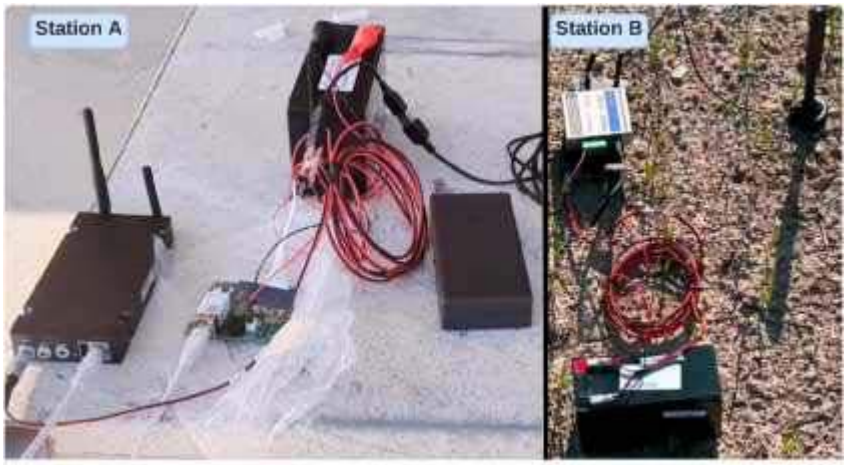

Figure 70: Field-trial - Aggregator/Sensors side

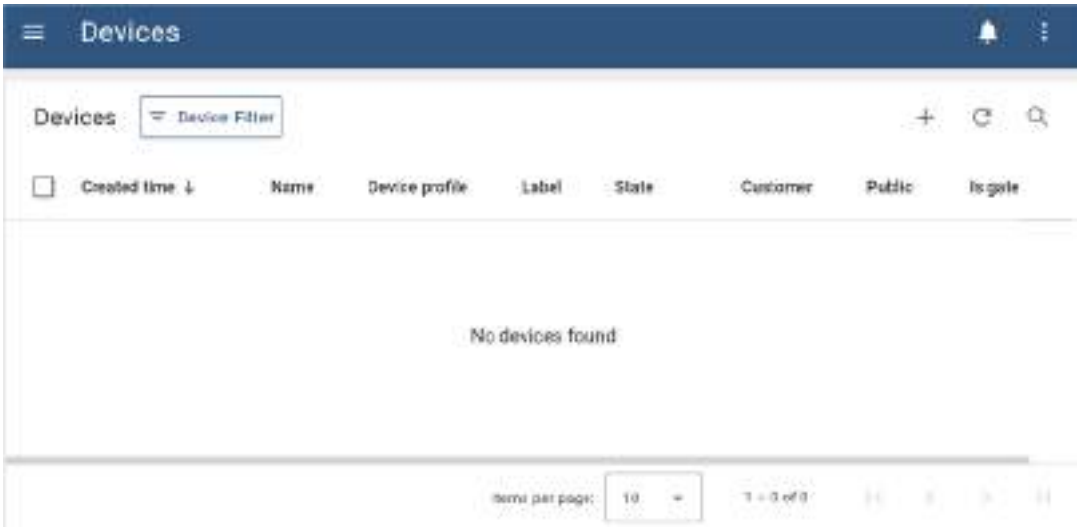

Figure 71: Device Management Platform - No device found

Proceeding to the Mesh-in-the-Sky part of the field trials, and after acknowledging that there was no communication between the two stations, a UAV incorporating an SDR, as shown in Figure 72, was launched to establish a connection between the two stations.

Figure 72: Field-trial - Node on UAV

As shown in Figure 73, during the drone's flight, a link was successfully established between the two stations, as confirmed by the reception of data on the open-source device management platform.

Figure 73: Device Management Platform - Generated data

Field trials demonstrated the ability of the Mesh-in-the-Sky system to achieve seamless connectivity over distances of up to 20 kilometers. The system reliably transported environmental sensor data, HD video streams, and telemetry from UAV nodes to central data hubs.

During the trials, zero packet loss was observed for IoT sensor data transmission, even under varying environmental conditions such as wind interference and terrain obstructions. The network's self-healing capabilities ensured uninterrupted communication when individual UAV nodes were repositioned or temporarily unavailable.

The advancements made in Task 3.5 of the NESTLER project demonstrate the transformative potential of UAV-based wireless communication systems for smart agriculture. By combining a self-healing mesh

network, adaptive wireless protocols, and efficient data aggregation mechanisms, the system provides a reliable, scalable, and energy-efficient solution for last-mile communication challenges.

The integration of these advanced communication technologies within the EU NESTLER project can significantly enhance the efficiency and resilience of smart agriculture systems. By leveraging RapidNet's mesh topology, robust wireless protocols, and adaptable terrestrial protocols, the project can overcome traditional limitations in data transmission, ensuring precise and timely agricultural interventions.

8. Knowledge extraction from GIS and remote sensing services

8.1. Satellite-based Crop Yield Estimation Algorithm

Crop production is essential for livelihood and food security in smallholder farming systems [37]. However, climate change, drought, land degradation, and soil infertility cause significant yield variability, leading to food insecurity [38]. Traditional yield estimation methods in sub-Saharan Africa are labor-intensive and often inaccurate for small fields (≤1ha) [39]. Satellite Earth Observation (EO) data offers a more efficient solution. With advancements in satellite technology, images have higher resolution, and decreased processing costs, improving crop yield estimation accuracy [38]. This suggests that satellite-based yield estimation can play a substantial role in measuring and understanding agricultural productivity [40].

A dedicated crop yield estimation algorithm was developed to support agricultural practices in Uganda, specifically targeting coffee plantations. The algorithm was tailored to address the unique challenges and requirements identified in the use case for additional services under the NESTLER project. By integrating high-resolution remote sensing data and advanced geospatial analysis techniques, the solution delivers estimations for actionable insights into crop health and productivity. The focus on coffee, one of the most popular plantation product in Uganda, was driven by the project's goal to enhance decision-making processes for local farmers and stakeholders, improving yield predictions and supporting sustainable agricultural practices in the region.

8.1.1. Datasets and Technologies Used

By selecting the appropriate index related to different crop properties, satellite-based yield measures can explain as much or more variation in yields as the gold-standard full-plot crop cuts [40]. The Copernicus Global Land Monitoring Service products, such as the Fraction of Absorbed Photosynthetically Active Radiation (FAPAR) and Land Surface Temperature (LST), provide valuable insights into vegetation health and productivity [41]. FAPAR quantifies the fraction of sunlight absorbed by plants for photosynthesis, indicating plant health and vigor, while LST measures, as its name suggests, the temperature at the Earth’s surface, encompassing trees, buildings, and all other surface features. These indices are crucial for assessing crop conditions and predicting yields, especially in fragmented and diverse agricultural landscapes. By incorporating LST and FAPAR data, yield estimation models can achieve good accuracy and reliability, supporting better agricultural planning and food security efforts in smallholder farming systems [42] [43] [44].

Another feature that is incorporated into the algorithm is the elevation. Elevation plays a crucial role in accurately estimating crop yields, particularly for coffee plantations, where altitude significantly influences growth and productivity [45] [46]. Research such as Hanan et al. (2024) highlights the importance of altitude, showing that Arabica coffee yields vary across different harvest seasons and altitudes in the Gayo Highlands, Aceh. Similar patterns are observed in Uganda, where elevation impacts microclimate conditions such as temperature, humidity, and rainfall, which are critical for coffee plant development [47]. By incorporating this feature, the algorithm improves the accuracy of yield predictions, aligning closely with local agricultural conditions.

To develop a crop yield estimation algorithm for Uganda's coffee plantations, the following Copernicus Global Land Monitoring Service datasets were incorporated: FAPAR, Land Surface Temperature (LST), and the Copernicus Global Land Cover Layer. The latter was used as a crop mask, to define the agricultural areas of the entire country of Uganda, and thus to extract meaningful analytics. The - static - dataset of elevation was also ingested into the input parameters for both the training and validation processes. The training and validation dataset of the generated model was the 2017 Spatially-Disaggregated Crop Production Statistics Data in Sub-Saharan Africa, generated and provided by the International Food Policy and Research Institute [48]. This dataset offers essential crop production features such as area, production, and yield for 42 crops, presented in spatially disaggregated 10 km grids available in CSV/DBF and GeoTIFF formats.

The following table summarizes the datasets used as input in the crop yield estimation algorithm.

Table 9: Datasets used as input in the satellite-based crop yield estimation algorithm

Dataset	Provider	Data type	Usage in the Algorithm	Spatial Resolution
Land Surface Temperature (LST)	Copernicus Land Monitoring Service	Raster	Model parameter with monthly aggregated values	10km
Fraction of Absorbed Photosynthetically Active Radiation (FAPAR)	Copernicus Land Monitoring Service	Raster	Model parameter with monthly aggregated values	300m
Elevation	ASTER GDEM	Raster	Model parameter	30m
Global Land Cover	Copernicus Land Monitoring Service	Raster	Cropland areas mask	100m
Uganda boundaries	Food and Agriculture Organization	Vector	Area of interest	N/A
Spatially-Disaggregated Crop Production Statistics Data in Sub-Saharan Africa	International Food Policy and Research Institute	Raster	Train/Val dataset with crop yield values	10km

The developed crop yield estimation algorithm leverages a robust suite of Python libraries to ensure not only efficient geospatial data handling and advanced modelling, but also scalability. Key libraries used include:

- **osteon** (**gal**, **ogre**, **or**, **gdalconst**): Core tools for geospatial data operations, including raster reprojection, vector data analysis, and geospatial metadata handling. These libraries are critical for preparing elevation data and satellite imagery for modelling.
- **pandas**: Enables effective data wrangling and tabular data manipulation, essential for organizing and integrating diverse datasets used in model training.
- **scikit-learn**: Powers the machine learning components of the algorithm, specifically employing the *RandomForestRegressor* for predictive modelling, *train_test_split* for data partitioning, and *mean_squared_error* for model performance assessment.
- **numpy**: Facilitates efficient array computations, enabling matrix operations and numerical preprocessing required for input data preparation.
- **datetime** and **timedelta**: Enable precise temporal data handling, crucial for aligning satellite imagery with appropriate time frames.
- **requests**: Provides robust HTTP requests for downloading remote sensing data and related datasets from APIs or online repositories.

8.1.2. Methodology and Algorithm Main Components

The crop yield quality estimation method is twofold: firstly, the machine learning model is generated using the time series of the aforementioned Copernicus datasets for 2017, and secondly, the model, when run, predicts yield values for the specific crop type over the selected area of interest according to the latest Copernicus data.

The methodology involved in this study includes several key steps aimed at accurate crop yield estimation using satellite data and machine learning techniques. The steps followed were:

1. Clipping and aligning datasets to the area of interest,

2. Creating time series and generating monthly statistics for LST and FAPAR,

3. Creating a Random Forests classifier model for yield estimations, and

4. Applying the model to predict crop yield.

Initially, all available LST and FAPAR datasets for the year 2017 and elevation were reprojected to the same coordinate system (WGS84/EPSG:4326), clipped, and aligned, ensuring focus on the geographical boundaries of Uganda, and preventing any miscalculations between the rasters during the next steps. Subsequently, time series were generated to capture monthly variations in LST and FAPAR. These features were namely the minimum, maximum, and average values per month. In this way, a normalization of the different datasets was achieved. As a next step, twelve different Random Forests classifier models were generated to predict crop yield depending on the base month, leveraging the yield data from the training dataset, and the relationships identified between input variables (LST, FAPAR, elevation) for the respective time periods.

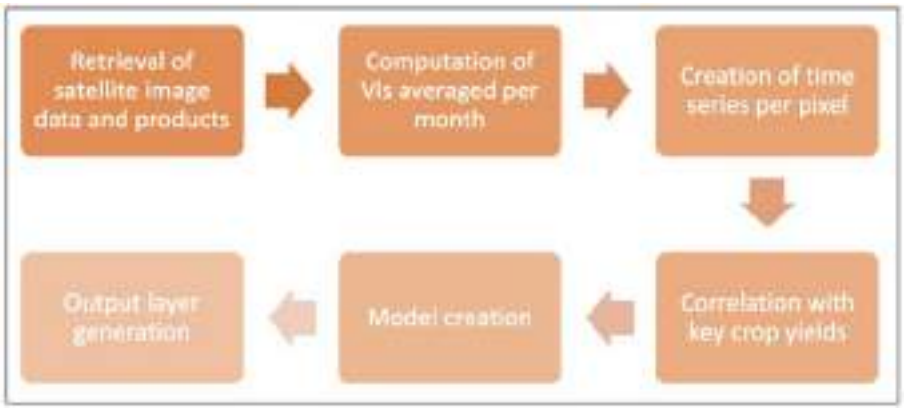

Figure 74: The followed methodology for the creation of the Random Forests models for yield estimation based on the 2017 datasets

To determine the within-season crop yield quality for coffee plantations in Uganda for each year, the model needs to run each month to predict the yield values taking into consideration all available data since January 1st of the same year. Again, all available LST and FAPAR datasets are downloaded, and reprojected to the same coordinate system (WGS84/EPSG:4326), clipped, and aligned to the geographical boundaries of Uganda. Time series are generated per pixel to capture the same monthly variations as in the previous process, in LST and FAPAR. The final step is the fitting of the respective model to the time series dataset, based on the current month. For instance, to forecast the 2024 yield in May 2024, all Copernicus Global Land Monitoring Service datasets from January 2024 until April are automatically downloaded, transformed into time series - together with the elevation dataset, and utilized to generate the corresponding crop yield estimation layer for the year 2024 based on the Random Forests model for April (*random_forest_model_4*, see next table).

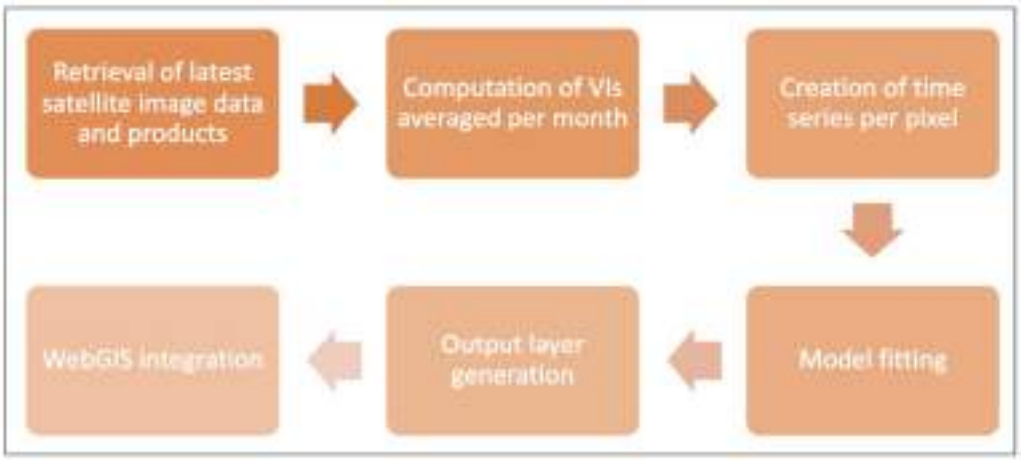

Figure 75: The followed methodology for the generation of the within-season crop yield quality estimation layer

The core components of the algorithm include downloading the CLMS latest data, processing data homogenization functions to ensure smooth ingestion into the Random Forests model fitting, and modelling the Random Forests processes.

Specifically:

- the ***downloader*** module handles the latest data acquisition, ensuring seamless access to the relevant CLMS satellite products,
- processing and preprocessing operations are managed through the ***processing*** module, which includes functions such as *modelCreation*, *applyModel*, and *elevationPrep*, designed to prepare input data, train predictive models, and integrate the elevation data.

8.1.3. Output and Results

The final outputs of the algorithm are twelve Random Forests models based on the 2017 dataset that predict the yield quality for coffee plantations. Each model takes as input the previous month's LST and FAPAR datasets when the estimation for the current year needs to be performed. For instance, if the algorithm runs in June, it will automatically utilize *random_forest_model_5*, as complete data for the previous month (May) will be available by then. All models were validated against the 20% of the samples extracted from the training-validation dataset. The achieved accuracies are shown in the table below.

Table 10: The developed Random Forest models for crop yield estimation, including the dataset months they reference, and the performance metrics achieved (overall accuracy)

Model name	Months included	Overall Accuracy
random_forest_model_1	January	0.805
random_forest_model_2	January and February	0.792
random_forest_model_3	January to March	0.804
random_forest_model_4	January to April	0.808
random_forest_model_5	January to May	0.837
random_forest_model_6	January to June	0.827
random_forest_model_7	January to July	0.827
random_forest_model_8	January to August	0.825
random_forest_model_9	January to September	0.822
random_forest_model_10	January to October	0.818
random_forest_model_11	January to November	0.787
random_forest_model_12	January to December	0.754

An example of the raster crop yield estimation layer is shown in the following figure. The output values are: “Low quality”, “Medium quality”, and “Good quality”. It is delivered at a spatial resolution of 300m, and its reference system is the EPSG:4326 - WGS 84.

Figure 76: Example raster output of the satellite-based crop yield estimation algorithm

8.2. Knowledge Extraction from External Services

The NESTLER project incorporates knowledge extraction from external data sources to enhance the visualization capabilities of its platform. By integrating meteorological datasets and satellite observations, NESTLER will be able to support advanced insights for its pilot activities across Africa and Europe. These external services provide a range of environmental data tailored to the unique needs of each pilot project, enabling improved decision-making and operational outcomes.

8.2.1. Meteorological Measurements and Forecasts

Meteorological data plays a crucial role in the NESTLER project, offering valuable insights into weather and climate dynamics that influence agricultural and environmental systems. Using the Windy tool, users can access a rich array of ready-to-use meteorological data layers, providing both historical measurements and forecasted conditions.

Key data layers include temperature, precipitation, wind speed, atmospheric pressure, and humidity, derived from renowned meteorological models such as ECMWF, GFS, and ICON. These datasets offer high spatial and temporal resolution, allowing detailed analysis of climatic patterns and their effects on the regions of interest. Additional layers, such as storm tracking and radar imagery, provide essential information for monitoring extreme weather events and their potential impacts.

This meteorological knowledge adds significant value by contextualizing satellite observations with real-time and forecasted weather information. For example, understanding precipitation patterns or temperature forecasts contributes to the decision-making of the end users. Windy’s ability to visualize these parameters in a dynamic, multi-layered format enables users to identify trends, predict risks, and develop informed strategies for managing natural resources and agricultural activities. The integration of these diverse meteorological insights ensures that NESTLER delivers to its end-users a holistic understanding of environmental conditions across its pilots.

8.2.2. Satellite-derived Data Layers for Land Conditions Monitoring

Satellite-based measurements are a crucial component of the NESTLER knowledge extraction framework, providing accurate and actionable insights. These image acquisitions must be global in scope to cover all NESTLER pilot regions and near real-time, delivering updated data within a day to ensure timely and relevant information.

To meet these requirements, the NESTLER project can leverage NASA's Global Imagery Browse Services (GIBS), which provides near real-time satellite imagery and a wide range of environmental data layers. GIBS offers timely access to global datasets, including true color composites of the current status of the Earth's surface, vegetation indices, land surface temperatures, and atmospheric conditions, which is essential knowledge for monitoring land health, crop conditions, and other critical environmental factors across the pilot regions. With its high spatial and temporal resolution, GIBS ensures that NESTLER has access to accurate, up-to-date data that supports informed decision-making and enhances the project's ability to address environmental challenges effectively.

The GIBS layers identified as providing value to the project are listed in the table that follows[2].

Table 11: NASA's Global Imagery Browse Services layers as ancillary knowledge for land conditions monitoring

Thematic Layers	Title / Name	Description	Temporal Resolution	Spatial Resolution
Corrected Reflectance (True Color)	MODIS_Aqua_CorrectedReflectance_TrueColor	True-color imagery from MODIS Aqua, providing realistic views of Earth's surface for land cover and vegetation monitoring.	Daily	250m
Soil Moisture	SMAP_Sentinel-1_L2_Active_Passive_Soil_Moisture	Combines Soil Moisture Active Passive (SMAP) and Copernicus Sentinel-1 data to measure soil moisture, vital for assessing water availability and soil conditions.	Daily	2km
Soil Temperature	SMAP_L4_Soil_Temperature_Layer_1	Soil temperature data from SMAP, important for monitoring soil health and crop growth conditions.	Daily	2km
Land Surface Temperature	MODIS_Terra_Land_Surface_Temp_Day	Daytime land surface temperature data from MODIS Terra, useful for assessing thermal conditions impacting vegetation and agriculture.	Daily	1km

[2] Source: https://nasa-gibs.github.io/gibs-api-docs/available-visualizations/#visualization-product-catalog

Air Surface Temperature	AIRS_L3_Surface_Air_Temperature_Daily_Day	Daily surface air temperature data from Atmospheric Infrared Sounder (AIRS), helping monitor temperature variations and their effects on crops.	Daily	2km
Normalized Difference Vegetation Index (NDVI) (rolling 8-day)	MODIS_Terra_NDVI_8Day	8-day NDVI composite from Terra, an indicator of vegetation health and land cover changes.	Daily	250m

9. Conclusions

This report outlines the role of IoT sensors, devices, and remote sensing techniques in agricultural monitoring within the NESTLER project. It highlights their significance in improving efficiency and sustainability.

The project has developed IoT-enabled sensors that are central to this ecosystem, collecting real-time data on key parameters such as soil moisture, temperature, humidity, atmospheric conditions, and water quality. These sensors are designed to be reliable, solar-powered, and adaptable to diverse conditions, enabling precision farming through tailored interventions. This targeted approach reduces resource overuse - such as water, fertilizers, and pesticides - while supporting real-time decision-making to address emerging challenges like disease outbreaks and pest infestations.

The AI technologies integrated into the project, leveraging video stream analysis and machine learning algorithms, play a pivotal role. Tools like YOLO and convolutional neural networks (CNNs) detect and classify objects, identify pests, monitor livestock, and analyse crop health. Advanced models such as DinoV2 detect subtle physical anomalies in animals, while recurrent neural networks (RNNs) analyse time-series data to recognize dynamic behaviours in poultry and fish. These AI-driven tools enhance early detection and enable proactive measures for pest control, disease prevention, and stress mitigation, significantly improving operational efficiency and reducing reliance on manual intervention.

Remote sensing technologies used in the project provide comprehensive insights into ecological and agricultural conditions. Unmanned aerial vehicles (UAVs) equipped with multispectral cameras capture images that are processed to calculate vegetation indices, including NDVI, GNDVI, and NDRE. These indices detect biotic and abiotic stressors in crops, guiding interventions that minimize chemical use and enhance resilience. Additionally, a method for synthesizing data from Sentinel satellites enables large-scale crop monitoring and yield estimation, integrating weather and soil data to identify long-term trends.

Pest monitoring and management are key components of the project. Advanced AI models, fine-tuned for specific crops and pests such as cocoa mirids and mango stem borers, enable precise identification and classification. Drone-mounted visualization systems and a project-modified Mesh communication network provide rapid pest detection and density estimation, reducing the need for extensive pesticide applications. Integration with mobile apps further supports farmers by offering real-time pest alerts and targeted recommendations, promoting sustainable pest management practices.

The implications of these technologies for agriculture and environmental monitoring are profound. By combining real-time monitoring with predictive analytics, NESTLER empowers stakeholders to make informed decisions that enhance productivity and minimize environmental impact. Early stage detection of stressors and proactive intervention reduce resource waste and increase resilience to challenges such as climate change, pest outbreaks, and diseases. The scalability and adaptability of these solutions make them suitable for diverse agricultural settings, from small farms to large enterprises.

10. References

[1] M. Carvajal-Yepes, K. Cardwell, A. Nelson, K. A. Garrett, B. Giovani, D. G. Saunders, S. Kamoun, J. P. Legg, V. Verdier and J. Lessel, "A global surveillance system for crop diseases," Science, vol. 364, no. American Association for the Advancement of Science, pp. 1237-1239, 2019.

[2] M. Taddese, K. Dibaba, W. Bayissa, D. Hunde, E. Mendesil, M. Kassie, C. Mutungi and T. Tefera, "Assessment of quantitative and qualitative losses of stored grains due to insect infestation in Ethiopia," Journal of Stored Products Research, vol. 89, p. 101689, 2020.

[3] S. T. Narenderan, S. N. Meyyanathan and B. Babu, "Review of pesticide residue analysis in fruits and vegetables. Pre-treatment, extraction and detection techniques," Food Research International, vol. 133, no. Elsevier, p. 109141, 2020.

[4] T. T. Høye, J. Ärje, K. Bjerge, O. L. P. Hansen, A. Iosifidis, F. Leese, H. M. R. Mann, K. Meissner, C. Melvad and J. Raitoharju, "Deep learning and computer vision will transform entomology," in Proceedings of the National Academy of Sciences, U.S.A, 2021.

[5] D. Xia, P. Chen, B. Wang, J. Zhang and C. Xie, "Insect detection and classification based on an improved convolutional neural network," Sensors, mdpi, vol. 18, no. 12, p. 4269, 2018.

[6] Chavez-Martinez, Osiris; Monjardin-Armenta, Sergio Alberto; Rangel-Peraza, Jesus Gabriel et al. (2024). Dataset of aerial photographs acquired with UAV using a multispectral (Green, Red and Near-infrared) camera for cherry tomato (Solanum lycopersicum var. cerasiforme) monitoring [Dataset]. Dryad. https://doi.org/10.5061/dryad.63xsj3vbd

[7] yujiaxin. Raw data from monitoring spring maize using a multispectral drone. And hand-measured plant height data.[DS/OL]. V1. Science Data Bank, 2024[2025-09-30]. https://doi.org/10.57760/sciencedb.16192. DOI:10.57760/sciencedb.16192.

[8] yujiaxin, Raw data from monitoring spring maize using a multispectral drone. And hand-measured plant height data, Science Data Bank, 2024.

[9] J. Rouse, R. H. Haas, S. J. A. and D. W. Deering, "Monitoring vegetation systems in the Great Plains with ERTS.," Third Earth Resources Technology Satellite-1 Symposium, NASA sp-351, vol. 1, p. 309–317, 1973.

[10] A. Gitelson and M. M. N., "Remote sensing of chlorophyll concentration in higher plant leaves," Advances in Space Research, vol. 22, pp. 689-692, 1998.

[11] E. Barnes, T. Clarke, S. Richards, P. Colaizzi, J. Haberland, M. Kostrzewski, P. Waller, C. Choi, E. Riley and T. Thompson, "Coincident detection of crop water stress, nitrogen status, and canopy density using ground based multispectral data," 01 2000.

[12] A. Gitelson, Y. J. Kaufman and M. N. Merzylak, "Use of a green channel in remote sensing of global vegetation from EOS-MODIS," Remote Sensing of Environment, vol. 58, no. https://doi.org/10.1016/S0034-4257(96)00072-7, pp. 289-298, 1996.

[13] Gitelson, A. Vina, T. Arkebauer, D. Rundquist, G. Keydan, B. Leavitt and G. Keydan, "Remote estimation of leaf area index and green leaf biomass in maize canopies," Geophysical Research Letters, vol. 30, no. 10.1029/2002GL016450, 2003.

[14] J. Tucker, "Red and photographic infrared linear combinations for monitoring vegetation," Remote Sensing of Environment, vol. 8, no. https://doi.org/10.1016/0034-4257(79)90013-0, pp. 127-150, 1979.

[15] Boiarskii and H. Hasegawa, "Comparison of NDVI and NDRE Indices to Detect Differences in Vegetation and Chlorophyll Content," JOURNAL OF MECHANICS OF CONTINUA AND MATHEMATICAL SCIENCES, vol. spl1, 2019.

[16] T. O. C. Barboza, M. Ardigueri, G. F. C. Souza, M. A. J. Ferraz, J. R. F. Gaudencio and A. F. d. Santos, "Use of Multispectral Airborne Images to Improve In-Season Nitrogen Management, Predict Grain Yield and Estimate Economic Return of Maize in Irrigated High Yielding Environments," AgriEngineering, vol. 5, no. https://www.mdpi.com/2624-7402/5/2/52, pp. 840--854, 2023.

[17] Organization, Icco quarterly bulletin of cocoa statistics., The International Cocoa Organization XLII, 2016.

[18] D. Ngounou Ntoukam, J. C. Kamgang, V. C. Kamla, Y. Muala, I. Tchappa, S. Galland and Y. S. Emvudu Wono, "Agent-Based Model of Cocoa Mirids at the Scale of a Cocoa Farm," in The 4th International Workshop on Agent-based Modeling and Applications with SARL, 2020.

[19] M. P. Squicciarini (ed.) and J. Swinnen (ed.), The Economics of Chocolate, Oxford University Press, https://doi.org/10.1093/acprof:oso/9780198726449.001.0001,, 2016.

[21] R. Babin, C. Djieto-Lordon, C. Cilas, L. Dibog, R. Mahob and C. Bilong, "True Bug (Heteroptera) Impact on Cocoa Fruit Mortality," Journal of Economic Entomology, pp. 1285-1292, 2012.

[21] "https://universe.roboflow.com/major-project-ju11j/blackpod-cocoa/dataset/1," [Online].

[22] Kusrini, S. Suputa, A. Setyanto, I. M. A. Agastya, H. Priantoro, K. Chandramouli and E. Izquierdo, Dataset for pest classification in Mango farms from Indonesia, Mendeley Data, V1, doi: 10.17632/94jf97jzc8.1, 2020.

[23] https://www.kaggle.com/datasets/tarundalal/dangerous-insects-dataset

[24] "Ultralytics YoloV8," [Online]. Available: https://github.com/ultralytics/ultralytics/tree/v8.2.15. [Accessed 8 5 2024].

[25] "Tensorflow v2.13," [Online]. Available: https://www.tensorflow.org/versions/r2.13/api_docs/python/tf. [Accessed 8 5 2024].

[26] Issa, A., Odedeyi, T., & Darwazeh, I. (2024). Iot-driven precision agriculture using communication technologies for crop quality and real-time environmental monitoring. 30th IEEE International Conference on Telecommunication (ICT).

[27] Sophocleous, M., Karkotis, A., Papasavva, A., Goldberger, M., Vasiliou, L., Ros-Lis, J., . . . Georgiou, J. (2024). A stand alone, in situ, soil quality sensing system for precision agriculture. IEEE Transactions on AgriFood Electronics, vol. 2, no. 1, pp. 43–50.

[28] Odedeyi, T., Poole, C., Liu, X., Kassem, A., Oyebode, G., Ismail, R., & Darwazeh, I. (2020). A low-cost instrument for estimating the starch content of cassava roots based on the measurement of rf return loss. 2020 IEEE International Symposium on Circuits and Systems (ISCAS).

[29] Odedeyi, T., Issa, A., Poole, C., & Darwazeh, I. (2024). High-throughput starch content estimation using rf return loss: Theory, analysis and test instrument design. 2024 IEEE International Symposium on Circuits and Systems (ISCAS).

[30] NESTLER Official Website. (2025, 01 13). Retrieved from https://NESTLER-project.eu/index.php/pilots/

[31] Bala, A. (2025, 01 13). Description of cropping systems, climate, and soils in Nigeria. Retrieved from Global Yield Gap Atlas: https://www.yieldgap.org/Nigeria#:%E2%88%BC:text=The%20country%20has%20six%20distinct,savanna%20and%20Sahel%20savanna%20zones

[32] He, T., Gu, L., Luo, L., Yan, T., Stankovic, J., & Son, S. (2006). An overview of data aggregation architecture for real-time tracking with sensor networks. Proceedings 20th IEEE International Parallel & Distributed Processing Symposium, (p. 8).

[33] Khade, G., & Mini, S. (2017). Identification of data aggregators in wireless sensor network. 1979-1983.

[34] Markarian, G., & Staniforth, A. (2021). Countermeasures for Aerial Drones. ARTECH House.

[35] Burke, and D. B. Lobell, “Satellite-based assessment of yield variation and its determinants in smallholder African systems,” Proc Natl Acad Sci U S A, vol. 114, no. 9, pp. 2189-2194, February 2017.

[36] T. Meshesha, and M. Abeje, “Developing crop yield forecasting models for four major Ethiopian agricultural commodities,” Remote Sensing Applications: Society and Environment, vol. 11, pp. 83-93, 2018.

[37] D. B. Lobell, “The use of satellite data for crop yield gap analysis,” Field Crops Research, vol. 143, pp. 56-64, 2013.

[38] Mitchell Roznik, Milton Boyd, Lysa Porth, “Improving crop yield estimation by applying higher resolution satellite NDVI imagery and high-resolution cropland masks”, Remote Sensing Applications:

Society and Environment, Volume 25, 2022, 100693, ISSN 2352-9385, https://doi.org/10.1016/j.rsase.2022.100693.

[39] D. B. Lobell, G. Azzari, M. Burke, S. Gourlay, Z. Jin, T. Kilic, and S. Murray, “Eyes in the Sky, Boots on the Ground: Assessing Satellite- and Ground-Based Approaches to Crop Yield Measurement and Analysis”, American Journal of Agricultural Economics, August 2019, p. 1-18.

[40] Jumi, N. K. Newlands, Z. Mehrabi, N. C. Coops, and N. Ramankutty, “Assessing the Performance of Satellite-Based Models for Crop Yield Estimation in the Canadian Prairies.” Canadian Journal of Remote Sensing 49 (1), 2023. doi:10.1080/07038992.2023.2252926.

[41] V. Sergio, R. Martínez-Peña, and D. Castrillo, "Beyond Vegetation: A Review Unveiling Additional Insights into Agriculture and Forestry through the Application of Vegetation Indices" J 6, no. 3: 421-436, 2023. https://doi.org/10.3390/j6030028

[42] T. S. Abdul-Jabbar et al 2023 IOP Conf. Ser.: Earth Environ. Sci. 1129 012004

[43]T. Pede, G. Mountrakis, St. B. Shaw, “Improving corn yield prediction across the US Corn Belt by replacing air temperature with daily MODIS land surface temperature”, Agricultural and Forest Meteorology, Volumes 276–277, 2019, 107615, ISSN 0168-1923, https://doi.org/10.1016/j.agrformet.2019.107615.

[44] Cammalleri, N. McCormick, and A. Toreti, “Analysis of the relationship between yield in cereals and remotely sensed fAPAR in the framework of monitoring drought impacts in Europe”, Nat. Hazards Earth Syst. Sci., 22, 3737–3750, https://doi.org/10.5194/nhess-22-3737-2022, 2022.

[45] Hanan, A & Anhar, A & Abubakar, Y & Karim, A. (2024). Arabica coffee yields at various harvest seasons and altitudes in the Gayo Highlands, Aceh. IOP Conference Series: Earth and Environmental Science. 1297. 012001. 10.1088/1755-1315/1297/1/012001.

[46] Kumhálová, Jitka & Kumhála, F. & Kroulik, M. & Matějková, Štěpánka. (2011). The impact of topography on soil properties and yield and the effects of weather conditions. Precision Agriculture. 12. 813-830. 10.1007/s11119-011-9221-x.

[47] Abigaba, D., Chemura, A., Gornott, C. et al. The potential of agroforestry to buffer climate change impacts on suitability of coffee and banana in Uganda. Agroforest Syst 98, 1555–1577 (2024). https://doi.org/10.1007/s10457-024-01025-3

[48] International Food Policy Research Institute (IFPRI), 2020, "Spatially-Disaggregated Crop Production Statistics Data in Africa South of the Sahara for 2017", https://doi.org/10.7910/DVN/FSSKBW, Harvard Dataverse, V3.